Understanding the role of regulatory T cells in pregnancy mediated protection from multiple sclerosis

Dissertation

**zur Erlangung des Grades einer Doktorin der Naturwissenschaften
der Fakultät für Mathematik, Informatik und Naturwissenschaften,
Fachbereich Biologie,
der Universität Hamburg**

vorgelegt von

Nina Felicitas Heckmann

aus Duisburg

Hamburg 2019

Conducted at

Institut für Neuroimmunologie und Multiple Sklerose (INIMS),

Zentrum für molekulare Neurobiologie Hamburg (ZMNH),

Universitätsklinikum Hamburg-Eppendorf (UKE)

Doctorate supervisor and referee: Prof. Dr. Manuel A. Friese

Referee: Prof. Dr. Tim Gilberger

Date of disputation: 07.06.2019

Stephanie Snelson (M.A., PG Dip Clin Psyc)

New Zealand

03.03.2019

Bestätigung zur Korrektheit der englischen Sprache

Confirmation of correctness of the English language

Hiermit bestätige ich, dass die Dissertation von Nina Felicitas Heckmann in korrekter englischer Sprache verfasst ist.

I hereby certify that the Doctoral Thesis of Nina Felicitas Heckmann is written in correct English.

Stephanie Snelson

Contents

I. List of Figures

II. List of Tables

III. Abbreviations

Abbreviation	Long version
aa	Amino acid
ACC1	Acetyl-CoA carboxylase 1
ADP	Adenosine diphosphate
AML-1	Acute myeloid leukemia-1
AMP	Adenosine monophosphate
APC	- Antigen presenting cell (cell type) - Allophcocyanin (dye, antibody-coupled)
ATP	Adenosine triphosphate
bp	Base pair
BrdU	Bromodeoxyuridine
BV510	Brilliant Violet 510 (dye, antibody- coupled)
cDNA	Complementary deoxyribonucleic acid
CD3	Cluster of differentiation 3
CD4	Cluster of differentiation 4
CD8	Cluster of differentiation 8
CD25	Cluster of differentiation 25
CD28	Cluster of differentiation 28
CD52	Cluster of differentiation 52
CD90.2	Cluster of differentiation 90 (Thy1) isoform 2
CDR3	Complementary determining region 3
CFA	Complete Freunds' Adjuvant
CNS	Central nervous system
CNS-1	Conserved non-coding sequence-1
CO_2	Carbon dioxide
CSF	Cerebrospinal fluid
Day E	Embryonic day
DC	Dendritic cell
ddH_2O	Double distilled water
DNA	Deoxyribonucleic acid
dNTP	Desoxyribonucleoside triphosphate
EAE	Experimental autoimmune encephalomyelitis
EBV	Epstein-Barr Virus
ECAR	Extracellular acidification rate
EDTA	Ethylenediaminetetraacetic acid
eGFP	Enhanced green fluorescent protein
ETC	Electron transport chain
FAO	Fatty acid oxidation
Fc region	Fragment crystallizable region (tail region of an antibody)
FCCP	Carbonyl cyanide-*4*-(trifluoromethoxy)phenylhydrazone
FITC	Fluorescein (dye, antibody-coupled)
Foxp3	Forkhead box P3 (protein)
FOXP3-E2	Foxp3 splicing variant containing exon 2
FSC-A	Foreward Scatter - Area
FSC-H	Foreward Scatter - Height
fw	Foreward
g	Standard gravity
GAPDH	glyceraldehyde 3-phosphate dehydrogenase

Abbreviation	Long version
GM-CSF	Granulocyte-macrophage colony-stimulating factor
Gy	Gray (unit)
h	Hour(s)
HAT	Histone acetyl transferase
HBSS	Hank's Balanced Salt Solution
HDAC	Histone deacetyl transferase
HHV	Human Herpes Virus
HLA	Human Leukocyte Antigen
HPLC-water	High performance liquid chromatography-pure water
H+	Protons
IFN-γ	Interferon gamma
IL-2	Interleukin 2
IL-7	Interleukin 7
i.v.	Intravenous
MBP	Myelin basic protein
MHC	Mayor histocompatibility complex
min	Minute(s)
ml	Milli liter
mM	Milli Molar
MOG	Myelin oligodendrocyte protein
MS	Multiple sclerosis
mtDNA	Mitochondrial DNA
NADH	Nicotinamide adenine dinucleotide (reduced form)
NAD^+	Nicotinamide adenine dinucleotide (oxidized form)
NFAT	Nuclear factor of activated T cells
nt	Nucleotide
OCR	O_2 consumption rate
OXPHOS	Oxidative phosphorylation
O_2	Oxygen
PB	Pacific Blue (dye, antibody-coupled)
PBMCs	Peripheral Blood Mononuclear Cells
PBS	Phosphate Buffered Saline
PCR	Polymerase chain reaction
PE	Phycoerythrin (dye, antibody-coupled)
PLP	Proteolipid protein
PML	Progressive multifocal leukoencephalopathy
PPMS	Primary progressive multiple sclerosis
rev	Reverse
RNA	Ribonucleic acid
rpm	Revolutions per minute
RPMI 1640 medium	Roswell Park Memorial Institute-1640 medium
RRMS	Relapsing-remitting multiple sclerosis
RT	Room temperature
RT-PCR	Real time-polymerase chain reaction
Runx1	Runt-related transcription factor 1
s.c.	Subcutaneous
sec	Seconds
SEM	Standard error of mean
SNP	Single nucleotide polymorphisms
SPMS	Secondary progressive multiple sclerosis
SRC	Spare respiratory capacity

Abbreviation	Long version
SSC-A	Sideward Scatter - Area
SSC-H	Sideward Scatter - Height
TCA	Tricarboxylic acid
Tcon	Conventional T cell
TCR	T cell receptor
TdT	Terminaldeoxyribonucleotidyl transferase
TGF-β	Transforming growth factor-β
Th1	CD4+ T helper 1 cell
Th17	CD4+ T helper 17 cell
Treg	Regulatory T cell
µl	Micro liter
µM	Micro Molar
µm	Micro meter
VCAM-1	Vascular cell adhesion molecule-1
VLA-4	Very late antigen-4
2D	Two-dimensional

1. Introduction

1.1 Context

Multiple sclerosis (MS) is the most frequent inflammatory disease of the central nervous system (CNS) and affects around 2.5 million people worldwide. Women are more often affected than men. MS is characterized by neurological dysfunction, which can involve decline of vision, motor, sensory and cognitive abilities. Its pathogenesis is attributed to a breakdown of immune tolerance towards CNS autoantigens, leading to infiltration of autoreactive conventional T cells (Tcon), which trigger local inflammation, demyelination and neuroaxonal degeneration [1]. Remarkably, pregnancy is a bold suppressor of disease activity in MS [2] and its animal model experimental autoimmune encephalomyelitis (EAE) [3,4] leading to a reduction of approximately 80% of the MS relapse rates in the third trimester of pregnancy [5]. This phenomenon bears the potential of understanding mechanisms underlying the disease and of utilizing the knowledge for the development of MS therapeutics. However, the identity and relative contribution of involved mechanisms is still incompletely understood [6].

In addition to MS, also pregnancy is a complex process with many changes in the endocrine system and the immune system. Several aspects of how autoimmunity could interfere with pregnancy have been proposed [6] and parts could recently be attributed to changes in regulatory T cells (Treg) [3].

Treg have various functions. They are effective suppressors of autoreactive Tcon [7] and further, Treg are necessary to regulate maternal immune responses against the semi-allogenic fetus during pregnancy [8–12]. Preservation of the fetus during gestation is acquired by a local expansion of the Treg in the reproductive tract [13] and uterus draining lymph nodes. This is to some extend rendered by a selection of hormone-resistant Treg over hormone-sensitive Tcon [3]. This leads to the question whether these Treg are not only increased in numbers, but also enhance their functionality and become more potent in fulfilling these functions. Besides a hormone dependent Treg increase during pregnancy, Treg expansion has also been shown to be mainly fetal antigen-specific in the first place [14,15]. However, it has been shown that these cells are also able to suppress T cell responses to unrelated antigens [14], leading to the question to which extent the protective phenomenon is driven by antigen-specific versus non-specific triggers.

As a consequence of the raised questions in this work the three most important functionalities of Treg in pregnancy and EAE diseased state are investigated. These are:

- Suppressive capacity of Treg in counteracting effector Tcon actions
- Metabolism of Treg and
- Specificity of the T cell receptor (TCR) β repertoire

In the following a more detailed overview is provided on the etiology and pathophysiology of MS, on its animal model EAE, on relevant processes of pregnancy and pregnancy protection from autoimmunity, on the branch of Treg as well as on their three most important functionalities: suppressive capacity, immunometabolism and TCR specificity.

1.2 Multiple Sclerosis

The French pathologist Jean-Martin Charcot was the first to broadly characterize MS in 1868 as one disease entity. He systematically described the histological examination of sclerotic central nervous system (CNS) lesions in patients with neurological malfunction, naming it "la sclérose en plaques disséminées", the disease that we today call multiple sclerosis [16].

Today, MS affects around 2.5 million individuals worldwide [1,17] with women being two to three times more often affected than men [18]. MS can be diagnosed at all ages, however the main age of onset is usually childbearing, young adulthood at approximate 30 years of age [1,17]. MS is a very heterogeneous disease. However, efforts to categorize patients by similar disease patterns have lead to the following subtypes:

In about 85% of MS patients, the disease presents as relapsing-remitting MS (RRMS), characterized by isolated attacks of disease activity with complete or incomplete remission between the attacks. With on-going disease the extent of remission in between the relapses becomes incomplete. 80% of the RRMS patients develop a progressive form of MS over time (secondary progressive MS, SPMS). Here phases of remission are absent [1,17]. Only about 10% of the patients present with such a progressive disease type right from the beginning (primary progressive MS, PPMS) [17]. Most common MS symptoms are different types of sensory or motor functional disturbances like optic neuritis, limb weakness or paraesthesia, gait ataxia, bladder, bowl and sexual dysfunction as well as fatigue, depression and also mild cognitive impairment [19,20].

The overall risk of developing MS is determined by a combination of genetic susceptibility and environmental factors, which is similar to other autoimmune diseases [1,17]. IummunoChip genotyping arrays have identified that genetic variation accounts for approximately 30% of the overall MS disease risk [21]. Genome wide association studies (GWASs) have identified over 100 genetic regions to be associated with MS. Many different so-called single nucleotide polymorphisms (SNPs) have been identified, which show essential variability in the human population. SNP comparisons of MS patients and healthy controls have lead to the identification of genetic differences in genes associated with immune cell function, like T cell activation or differentiation [1]. A very strong association has been shown for the human leukocyte antigen (HLA) locus variant HLA-DRB1*15:01, as a main risk factor for MS development. However HLA-A*02:01 has been shown to be protective [22–24]. Further genetic risk factors are connected to cytokine signaling involving variants in the genes encoding the α chains of the receptors for interleukin 2 (IL-2) and interleukin 7 (IL-7). Both are involved in the formation of adequate T cell responses [25–28]. However, most associated genetic variants are non-coding regions. They might co-localize with gene enhancers or repressors in immune cells, but more detailed investigations of their function are needed. Overall a multiple sclerosis predisposition may be implemented via changes to central tolerance mechanisms and via peripheral differences in effector T cell function mediated via changes in responsiveness to cytokines, cytokine production and homeostatic proliferation [1].

Non-genetic factors have a proportionately larger contribution than genetic factors. However, rather little is known about them. There is a strong MS prevalence in westernized countries like northern Europe, North America and Australia with about 100 cases per 1 million individuals. In contrast there is a much

lower MS prevalence in rather equatorial regions of about 20 patients per 1 million persons [17]. The exact environmental factors underlying this observation are still unclear, but differences in vitamin D levels, caused by differences in sunlight exposure are discussed as a reason [29,30]. This prevalence correlates with growing up in an MS risk region, however moving to a low MS risk region before adolescence leads to adapting the risk of the new home country and vice versa [31,32]. Another important factor are previous infections. A significant association has been exhibited for MS and a previous infection with Epstein Barr virus (EBV) [33] or human herpes viruses 6 (HHV6) [34]. It has been hypothesized that inadequate regulation of the virus can lead to a reactivation in the CNS [1,35]. Furthermore it has been suspected that these infectious agents convey risk by molecular mimicry of CNS auto-antigens [36]. A formerly assumed association of MS with cytomegalovirus (CMV) infection has been disproven [37]. Other environmental risk factors for MS involve gender [18,38,39], smoking [40], and the bacterial microbiome, influenced by the diet [41-43].

In order to treat MS a number of disease-modifying drugs have been developed. However, currently there is no medication available that can cure MS. The existing drugs interfere with the immune system in different ways, however not for all drugs the exact working mechanisms are fully understood. In RRMS as a first line of medication outside acute relapses but depending on disease course different drugs are available and recommended. For highly active disease courses these are Alemtuzumab, Fingolimod, Natalizumab, Ocrelizumab and Mitoxantron. For milder disease courses recommended drugs are Dimethyl fumarate, Glatirameracetate, different forms of Interferon beta and Teriflunomide [44].

Alemtuzumab is a monoclonal anti-CD52 antibody and depletes CD52+ B and T cells and monocytes in peripheral blood. Its application leads to a long lasting removal of these lymphocytes from the blood [45]. Fingolimod is a sphingosine-1-phosphate receptor modulator. It interferes with lymphocyte migration, captures lymphocytes in the lymph nodes and keeps them away from performing their usual function [46]. Natalizumab is a humanized monoclonal antibody that is directed against very late antigen-4 (VLA-4) on immune cells, which mediates binding to vascular cell adhesion molecule-1 (VCAM-1) on endothelial cells. Via the antibody blockade of this interaction, activated T cells cannot adhere to CNS endothelium to cross the blood brain barrier (BBB) and cause inflammatory lesions [47]. Ocrelizumab is a humanized and monoclonal antibody against CD20 on B lymphocytes and thus eliminates the CD20+ B cells from the circulation [48]. Mitoxantron is an anti-neoplastic agent, hampering lymphocyte proliferation and antigen presentation [49]. It became recently known that Dimethyl fumarate and its metabolite, monomethyl fumarate, inactivate the glycolytic enzyme glyceraldehyde 3-phosphate dehydrogenase (GAPDH). Therefore aerobic glycolysis is down-regulated in myeloid and lymphoid cells, which results in down-modulated immune responses, as inflammatory immune cell subsets require aerobic glycolysis. This primarily affects activated immune cells such as effector and memory T cells [50]. Furthermore Dimethyl fumarate dampens pathogenic B cell functions, by abrogating their APC function and by reducing the production of proinflammatory cytokines [51]. The working mechanism of Dimethyl fumarate had for a longtime only been partially understood even though derivates of fumaric acid had been used as a treatment for psoriasis since decades [44,52]. Glatirameracetate is an amino acid copolymer and has multiple effects in the innate as well as in the adaptive immune system that together shift the balance from pro-inflammatory to anti-inflammatory signaling pathways [53]. The exact working mechanism of Interferon beta is not understood in detail. It has been shown that it down regulates the expression of MHC class II on the surface of monocytes and macrophages as well as on microglia and that it prevents the restimulation of autoreactive cells [54]. Teriflunomide is used in combination with drugs like Interferon beta or Glatirameracetate. Teriflunomide inhibits the mitochondrial enzyme dihydro-orotate dehydrogenase

and therefore inhibits the *de novo* synthesis of pyrimidine and hampers immune cell proliferation e.g. T cells [55].

Upon relapses drugs like Methylprednisolone are the first choice of medication [44]. Methylprednisolone is a synthetic glucocorticoid, which suppresses proliferation and improving the apoptosis pathways of T cells. Furthermore it increases IgG synthesis, has an anti-inflammatory effect, suppresses inflammatory cell invasion into the CNS and inhibits the production of pro-inflammatory cytokines [56–59].

In summary, gaining more detailed mechanistic insights that can be translated to new treatment strategies will still require substantial efforts in human MS research and the study of MS mouse models.

1.3 Immunopathology of MS

It is still an open question whether MS is triggered in the periphery or in the CNS of an effected individual. Therefore two opposing hypothesis exist on the development of MS:

In the peripheral hypothesis auto-reactive T cells are activated outside the CNS. This could happen via molecular mimicry: an innocuous virus mimicking self-antigen in order to escape from detection by the host. Peripheral activation could also happen via bystander activation, which is activation of unspecific cells due to nearby activity of antigen-specific cells that secret activating factors, leading to activation of uninvolved cells. Yet another possibility for peripheral activation is the co-expression of TCRs with different specificities on the same cell. In all cases the activated T cells travel to the CNS along with activated B cells and monocytes, which finally attack the CNS or attract more cells that attack the CNS cells [1]. B cells are also lymphocytes of the adaptive immune system. They work by generating and secreting antibodies and thereby tag cells for destruction or they neutralize the microbe by themselves. Additionally, B cells present antigen as professional antigen presenting cells (APCs) to activate antigen-specific T cells [60]. Monocytes are leukocytes, which can differentiate into macrophages or myeloid dendritic cells (DCs) in their target tissue. Macrophages engulf and digest cellular debris, recruit other immune cells and can also present antigen to T cells and thereby activate them. DCs are antigen-presenting cells, mainly presenting antigen to T cells and thereby activating the T cells [60]. These immune cells are created for targeted degradation of harmful cells, cellular residues or microbes, which need to be removed for a healthy condition. However, if the clearing mechanisms are activated under false circumstances they can be harmful to its host. This peripheral hypothesis of MS development is congruent with the pathology of the MS mouse model EAE, which is used to mimic the disease and to examine and understand its pathology.

In the second hypothesis, the CNS model, CNS-intrinsic events induce the disease development. Here infiltration of auto-reactive lymphocytes might take place as a secondary phenomenon. Until now it remains unclear what these CNS-intrinsic events could be. There are speculations about so far unknown CNS viral infections or other processes leading to neurodegeneration similar to e.g. Alzheimer disease [1].

Ultimately, the MS pathology is attributed to a breakdown of immune tolerance towards CNS

auto-antigens, leading to infiltration of auto-reactive T cells (mainly CD4+ T helper 1 (Th1) and CD4+ T helper 17 (Th17) cells) and other lymphocytes [1]. CD4+ T cells can be activated via presentation of 'their' peptide antigen on their TCR - via the mayor histocompatibility complex (MHC) class II molecule sitting on the surface of APCs. Activated CD4+ cells can then assist B cells and cytotoxic T cells in maturation and fulfillment of their tasks of antibody production and elimination of pathogen infected cells [60]. Myelin directed auto-antigens have been proposed as disease mediating but have been shown to be present in healthy controls as well [61,62]. The CNS infiltrating lymphocytes trigger local inflammatory processes and finally lead to continuous demyelination in areas of grey and white matter of the brain and spinal cord. Affected areas are called plaques or lesions. In these lesions a loss of the myelin sheath and oligodendrocytes is happening, which usually give support and insulation to axons of the CNS. The subjacent axons and neurons are preserved in early MS. Partly the demyelinated areas can be repaired by remyelination. However, disease progression finally leads to neuroaxonal degeneration, which is correlating with patient disability. The lesions are the pathological hallmark of MS. Further, astrocytes form glial scars in the white matter lesions [1,20]. Astrocytes are glial cells supporting endothelial cells and building the BBB, a highly selective semipermeable barrier between the circulating blood and the extracellular fluid of the CNS [63]. The BBB becomes leaky in the affected areas. Through these gaps even more peripheral immune cells like macrophages, CD8+ T cells, lower numbers of CD4+ T cells, B cells and plasma cells invade and boost inflammation, demyelination, neuroaxonal degeneration and finally disable neuronal signaling. This results in atrophy of the grey and white matter and as a consequence leads to enlarged ventricles [1,20]. CD8+ T cells are known as cytotoxic T cells and usually kill virus infected or tumor cells. They recognize their targets in an antigen-specific way, presented to them via the MHC class I molecule sitting on the surface of APCs. Plasma cells originate from B cells, but have begun to secret antibodies, which can target the detected antigen [60]. Usually the mechanisms of the immune system act very precise and effectively, when necessary. However, if these mechanisms are activated under wrong circumstances the mechanisms of the immune system cannot work properly with sometimes fatal effects.

1.4 Experimental autoimmune encephalomyelitis (EAE) as MS mouse model

In 1885 Louis Pasteur was the first to apply rabies infected, dried spinal cord extracts from rabbits as a first rabies vaccine. However, an intended refinement of the method lead to the development of severe complications such as pain and muscle paralysis that were ascending from lower to upper extremities and resulted in a mortality of up to 30%. This illness was characterized by lymphoid infiltrates and demyelination around blood vessels in the CNS, but not by any rabies typical symptoms like abnormal nerve cells, scattered lymphocytes, swelling and gliosis. It was found that repeated injections of healthy human spinal cord into rabbits occasionally also resulted in the described paralysis. Finally, this lead to the discovery that brain-specific antigens delivered together with attenuated *Mycobacterium tuberculosis* and paraffin oil resulted in an autoimmune encephalomyelitis, nowadays called experimental autoimmune encephalomyelitis (EAE). EAE can be induced in many different species, resulting in species-specific varying disease patterns. The analogy to human demyelinating diseases, like MS, was quickly detected [62-64].

Today, EAE is a widely used animal model and furthermore one of the most intensively studied models of humane autoimmune disease [66,67]. It is commonly induced in several different laboratory animal inbreed stains like e.g. C57/BL6 mice, SJL mice or Lewis rats. Crucial is the MHC haplotype (e.g. H2-A^u, H2-B) to which the inbreed stain is restricted, as well as the origin of the myelin peptide used for induction. Typically used peptides are myelin basic protein (MBP), proteolipid protein (PLP) and myelin oligodendrocyte glycoprotein (MOG). Working combinations of animal stains, myelin protein and the particularly crucial protein sequences are publically available today [68].

EAE played a major role in the identification and characterization of processes in immune surveillance, inflammation and immune mediated tissue-injury. Many currently used MS drugs have been developed, tested or validated on the basis of EAE studies, like Glatiramer acetate, Mitoxantrone and Natalizumab. On the other hand the EAE model has been criticized a lot for leading to the development of potential therapeutics that later on failed to prove their efficacy in the clinic or even lead to clinical complications (e.g. progressive multifocal leukoencephalopathy (PML) with Natalizumab) [66,69]. The model is under constant debate, also as it does not cover the entire spectrum of the clinical, pathological and immunological features of the MS disease. The current EAE model and its variations are mainly based on inflammation induced by auto-reactive CD4+ T cells. This reflects important aspects of MS, however, there is a lot of data indicating that CD8+ T cells and B cells play an important role in disseminating MS inflammation and tissue damage as well [70]. Despite various attempts no better model could be developed yet.

In particular, in C57BL/6 mice EAE is commonly induced by active immunization with myelin oligodendrocyte glycoprotein peptide 35-55 (MOG_{35-55}) administered together in a mixture with Complete Freunds' Adjuvant (CFA), an oily mixture with heat inactivated *Mycobacterium tuberculosis*. EAE induction gives rise to pathogenic Th1 cells and Th17 cells in the draining lymph nodes. These cells enter the circulation, cross the BBB or the blood-cerebrospinal fluid (CSF) barrier and eventually perform their effector functions in the CNS [1]. There they secrete cytokines to promote inflammation (via Granulocyte-macrophage colony-stimulating factor (GM-CSF) and Interferon gamma (IFNγ)) [71] or to attract other immune cells e.g. macrophages and CD8+ cells which can perform direct killing. There are also adoptive transfer models of EAE in which myelin reactive T cells are transferred into host mice to trigger disease [72]. The symptoms of EAE usually start with a weakness of the tail and progress to a paralysis of the hind limbs.

1.5 Pregnancy and reproductive immunology

Reproduction is crucial to the maintenance and evolution of all species. Mammals like humans belong to the strain of placentalia [73] and reproduce via a pregnancy of the female. Reproduction inside the body protects and sustains the fetus steadily with nutrients, but imposes problems to the immunological tolerance of the mother [74], which is no problem in egg lying species [73]. Usually the immune system tightly patrols the organism and fights all foreign pathogens e.g. bacteria and viruses (detected as foreign antigens), but tolerates self-tissue (self-antigens) e.g. from brain or skin. Under normal circumstances a sensitive balance between immune cells like the conventional effector T cells and Treg is mediating such a healthy immune surveillance [75]. However, the differentiation between foreign and self becomes more

complicated with pregnancy. The immune system of the mother has to tolerate the semi-allogenic fetal tissue. It is half self to her, as it contains her genetic information, but it is also half foreign to her, as it also contains genetic information from the father [76,77].

Today it is known that the immune system of pregnant women is tuned in a specific way to tolerate the fetus. Strong mechanisms of immune evasion and immune regulation mediate a successful pregnancy [77,78]. Over the course of pregnancy the levels of circulating hormones such as estrogens, glucocorticoids or progesterone are increased (Fig. 1.1) [79–81]. In early pregnancy, they ensure that the blastocyst adheres and implants into the remodeling uterine endometrial lining and that the blastocyst is nourished and differentiates into the embryo [74,82]. In later pregnancy, increasing hormone levels sustain the pregnancy progression.

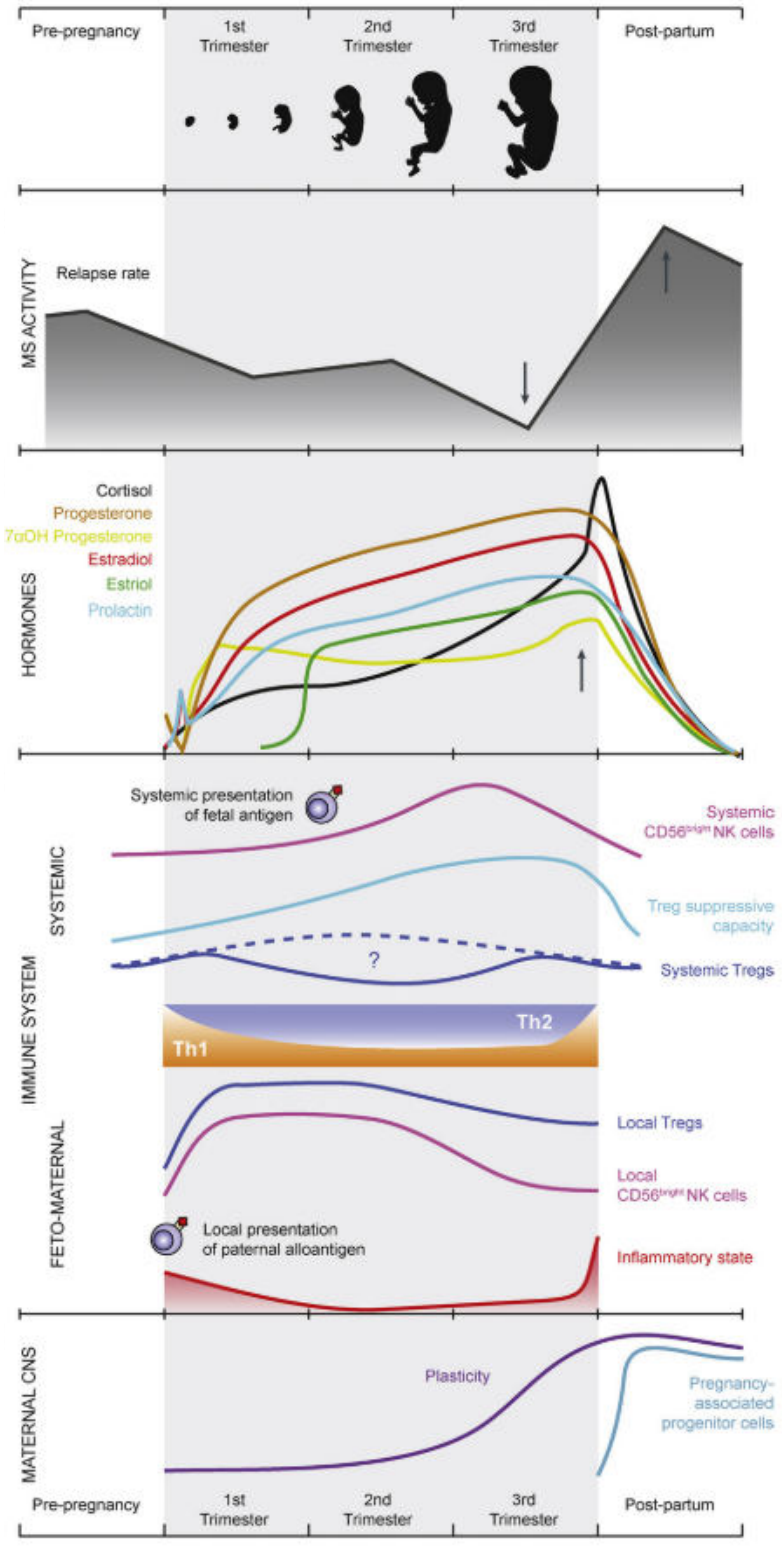

Figure 1. 1 Changes during MS and simultaneous pregnancy

Human gestational stages, MS activity rate over course of pregnancy, changing hormone levels during pregnancy and systemic changes, changes to immune system and feto-maternal changes. Figure taken from Patas et al., 2013, 141 [6].

For a long time detailed mechanisms to prevent fetus-directed immune responses were not very well known. Until today it has been clarified that changing levels of pregnancy hormones also have immune-modulatory properties [79,83]. Fetal antigens directly interact with the maternal immune system, which results in specific immunomodulation like fetal-antigen dependent induction of Treg [84–86].

During pregnancy complex pathways occur at the fetomaternal interface, such as the formation of a functional synapse, which forms between invading fetal trophoblast cells. Also various maternal immune cell subsets are involved as well as epigenetically modified decidual stromal cells. Precisely regulated feto-maternal immune cross-talk enables a successful pregnancy [74]. Moreover, changes in cytokine production are induced, adhesion molecule expression and antigen-presentation are decreased [79,80].

Expanding numbers of natural killer (NK) cells in the decidua secrete cytokines (Fig. 1.1), which are inhibitory to macrophages and therefore prevent macrophage-mediated destruction. Furthermore, NK cell secreted cytokines induce tolerogenic DCs (tDCs), which allow for the induction of increasing numbers of Treg. Elevated levels of Treg numbers exert increased regulatory function in counteracting effector T cells. Further, NK cells and decidual stromal cells also promote apoptosis of activated T cells and thereby protect the fetus from being attacked [74,87]. Furthermore, DCs in the decidua are prevented from migrating to the local lymph nodes to prime local T cells with fetal antigen [88]. Peripheral T cells are kept from entering the decidua, as the chemokines responsible for their attraction are epigenetically silenced in decidual stromal cells [89]. Also CD8+ regulatory T cells contribute to fetal tolerance and are found to increase with later gestation [9,74]. They may dampen antibody production by B cells. Generally B cell numbers are minimized in the decidua [90].

Essentially, all immune adaptations during pregnancy are precisely fine tuned, well timed and contribute distinctly to pregnancy success or failure [91,92].

The pregnancy-mediated protection from MS is not a consequence of general immunosuppression during pregnancy but most probably occurs in an antigen-specific fashion as part of feto-maternal tolerance [6].

1.6 Autoimmune disease amelioration during pregnancy

Pregnancy is one of the strongest known suppressors of inflammatory activity in several autoimmune diseases including MS [2], rheumatoid arthritis [93], autoimmune hepatitis [94], uveitis [95] and also psoriasis [96]. However, other autoimmune diseases like systemic lupus erythematosus [97] and type I diabetes [98] experience increased activity. The mechanisms behind the disease ameliorations or exacerbations during pregnancy are incompletely understood.

In MS during pregnancy the relapse activity is reduced by approximately 80% in the third trimester [2,5]. This phenomenon surmounts the disease modifying effects of most available disease-modifying drugs. The beneficial effect however is limited to the gestational period and is followed by a postpartum rebound phase of disease activity [2,5,20] (Fig. 1.2 A). Altogether pregnant MS patients are described to return to pre-pregnancy levels after the initial increase in relapses [5].

Similar to pregnant human MS patients, pregnant mice are protected from the inflammatory disease activity of EAE [1,3,4]. Likewise, the beneficial effect is limited to the gestational period and is followed by a vigorous postpartum rebound phase of disease activity (Fig. 1.2 B) [3]. Despite the potential therapeutic implications of this phenomenon, the identity and relative contribution of the involved mechanisms are still incompletely understood [6].

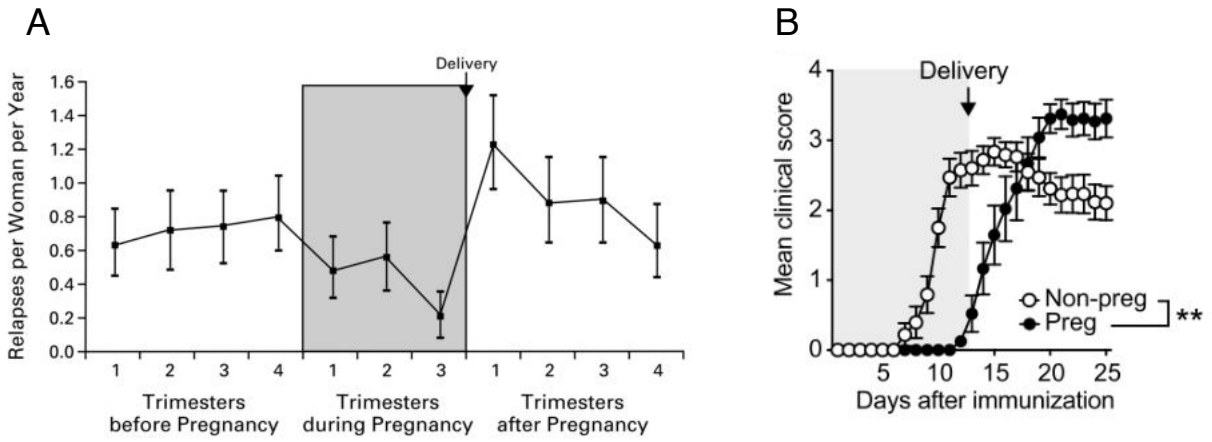

Figure 1. 2 Pregnancy temporarily reduces MS and EAE disease

(**A**) In human pregnancy the MS relapse rate is reduced by approximately 80%. After pregnancy patients experience increased diseased activity, shown in n = 227 MS pregnancies. Grey area marks the pregnancy period. Figure taken from Confavreux et al., 1998, 289 [2]. (**B**) Pregnancy also protects from EAE disease. Non-pregnant EAE animals develop an unusual clinical score with a disease onset around seven days after immunization. Pregnant animals are protected from EAE until delivery. Grey area marks the pregnancy period. Then they develop an overshooting EAE disease similar to the human situation. Figure taken from Engler et al., 2017, E186 [3].

For a long time the focus in investigating the MS disease amelioration was rather set on global modulators such as circulating hormones like estrogen, glucocorticoids or progesterone or other global shifts in maternal immunity [99,100]. These hormones show peak levels in the third pregnancy trimester (Fig. 1.1) [6], which coincides with the disease amelioration phase. Administered as a disease treatment pregnancy hormones and other sex hormones (e.g. estriol, testosterone) have been shown to have some therapeutic potential, via anti-inflammatory and neuroprotective effects, in MS [101] and in EAE [102]. However, it has been difficult to fully replicate the protective effect of pregnancy in MS by using these rather global modulators [101,103].

Along with progress made in understanding the mechanisms of feto-maternal immune cross-talk and the understanding that fetal tolerance is partly achieved via antigen-specific modulation of lymphocytes [14,74], the focus in investigating MS disease amelioration during pregnancy was set onto lymphocyte subsets like Treg, Th17 and NK cells. In particular the involvement of Treg has received increasing attention [3,6,9,85,86,104].

1.7 Regulatory T cells

Since the introduction and consolidation of the concept of regulatory T cells (Treg) with suppressor function many aspects on Treg have been elucidated. However still many open questions remain. The biochemical nature of the suppressor mechanisms is not entirely understood, or further it remains unclear whether all concepts from *in vitro* studies can be applied to *in vivo* function [75,105,106].

Studies in human and mice have repeatedly shown a crucial role of Treg in feto-maternal tolerance [8,9,74] and in autoimmunity [78,107].

In the context of pregnancy, Treg were observed to expand in mice, while their depletion resulted in fetal loss [10,14,15]. Adoptive transfer of Treg into abortion-prone or Treg depleted mice prevented fetal rejection [12,108]. In humans Treg were also observed to expand with highest amounts found in the second trimester in the peripheral blood (Fig. 1.1) [109–111].

Two Treg subsets can be distinguished, which are pTreg and tTreg. During pregnancy Treg can be induced peripherally from naïve Tcon and are therefore called pTreg [11,14]. Within the maternal body fetal antigen are released continuously [104]. In the periphery naïve Tcon recognize these peptides presented to them on the MHC molecules and induce and maintain a population of 'fetal-specific' Treg [11]. This occurs after TCR engagement without strong co-stimulation and in the presence of transforming growth factor-β (TGF-β). Further it depends on expression of the enhancer element of forkhead box P3 (Foxp3) conserved non-coding sequence-1 (CNS-1). Consequently, disruption of CNS-1 mediated pTreg induction provokes fetal loss [112,113]. However Foxp3 was found to be less stable in the population of pTreg [114]. pTreg induced during pregnancy have been shown to persist in the organism for a long time as memory Treg and can be reactivated during subsequent pregnancies [11]. Others have shown that these fetal antigen-specific Treg can also be suppressive towards unrelated antigen via bystander suppression [115]. As a consequence Treg expansion also leads to increased susceptibility towards infections e.g. *Listeria monocytogenes,* while a depletion of Treg restored host defense [15].

In general the trans differentiation of Tcon (e.g. of Th17 cells) into Treg in the periphery is not a frequent event [116]. However it becomes possible under circumstances like pregnancy.

In contrast to pTreg, Treg are usually induced in the thymus during regular CD4+ T cell development. Therefore they are called tTreg. tTreg and pTreg are described to have functional similarities but to show a very limited bidirectional conversion [117,118].

T cells stem from a common lymphoid progenitor (of T and B cells) in the bone marrow. They commit to the T cell lineage and migrate to the thymus where they mature. This also means recombination of the T cell receptor (TCR) gene segments in the germline to generate a surface-bound TCR. More details on TCR rearrangements are following in section 1.10. The developing T cells are selected in the cortex of the thymus at several steps during their maturation to preserve useful specificities: Prelymphocytes that fail to express a TCR die by apoptosis. Immature T cells are also selected to recognize self-major histocompatibility complex (MHC) molecules (MHC class II for CD4+ T cells, MHC class I for CD8+ T cells) loaded with peptide in the thymus. This process is called positive selection. It ensures that the cells completing maturation will be capable of recognizing antigens displayed by MHC molecules on antigen

presenting cells (APCs). Strongly self-reactive T cells are eliminated to prevent the development of autoimmune responses. This process is called negative selection. Thymocytes whose receptors bind to MHC loaded with peptide with intermediate affinity are positively selected and mature to single-positive (CD4+ or CD8+) T lymphocytes. These migrate to the medulla of the thymus, where they are exposed to AIRE+ medullary thymic epithelial cells (mTECs), which express self-tissue-specific antigens and can also mediate negative selection. If interaction of TCR and self-peptide is very mild, the cell will become a naïve CD4+ T cell and will be allowed to emigrate into the periphery. If the cell and its receptor show a very strong interaction with the self-peptide the cell will be negatively selected. However, if the TCR and self-peptide interaction is intermediate, the cell will become a Treg. It will be able to recognize self, but it will act in tolerogenic way and therefore a Treg will help in immune surveillance [60,119].

Treg are necessary to maintain the immunological tolerance to self-antigen and to suppress immune responses that would otherwise be deleterious to its host [75]. Treg regulate the activation of conventional effector T cells, which react to (self)-antigen-specific stimulation. Treg fulfill this function mainly via the transcription factor forkhead box P3 (Foxp3), their critical regulator of development and function. The main function conferred with Foxp3 is the suppressive activity towards non-Treg cells. Foxp3 is essential for Treg development and further inside Treg interacts with transcription factors like nuclear factor of activated T cells (NFAT), acute myeloid leukemia-1 (AML1)/runt-related transcription factor 1 (Runx1), the histone acetyl transferase (HAT)/histone deacetyl transferase (HDAC) complex, and possibly NF-κB. Transcription factor activity promotes expression of e.g. IL-2 and cytotoxic T lymphocyte antigen 4 (CTLA-4) or facilitates the assembly of transcriptional activation complexes on the IL-2 promoter or interferes with IL-2 production. A knockdown of these transcription factors abrogates the suppressive capacity [7,75,120]. Further, Treg constitutively express CD25, the α chain of the IL-2 receptor, on their surface. CD25 however also is an activation marker on Tcon. Human Treg are further characterized by being CD127- (low expressing IL-7r α chain) [121,122].

In the context of autoimmunity Treg are essential in suppressing autoreactive responses. Foxp3 deficiency results in generalized autoimmune inflammation, which can be seen in patients suffering from immunodysregulation polyendocrinopathy enteropathy X-linked syndrome (IPEX) [12,123] and in scurfy mice, in which the Foxp3 gene is depleted [88,89,124,125]. In addition to that, quantitative or functional Treg disturbance is known in a number of autoimmune diseases, including MS [1,126,127], rheumatoid arthritis [78,94,128], systemic lupus erythematosus [129–132] and type I diabetes [2,133,134]. In MS Treg are known to have diminished suppressive potential [5,135,136] and to hold decreased expression of Foxp3 and immunosuppressive CTLA-4 [1,126,127,137,138].

Further Treg are reported to play an important role in controlling both feto-reactive T cells during pregnancy and auto-reactive T cells in autoimmune diseases [3,8–10,107,108,139]. However, it remains currently unknown whether the protective phenotype is predominantly mediated by Treg. And if this is the case, whether it is due to the Treg exerting increased functionality during pregnancy or whether it is due to antigen-specific regulation of disease-causing conventional T cells (Tcon) and immuno-suppressive Treg during pregnancy.

However, it has been suggested that tTreg regulate effector Tcon in an antigen-specific mode [140].

It has been recently shown that a local expansion of Treg in the reproductive tract [13] and draining lymph tissue during pregnancy partially leads to immune protection of the semi-allogenic fetus. It was further

shown that this is due to glucocorticoid resistant Treg being enriched in relative numbers due to the decreasing numbers of glucocorticoid sensitive Tcon [3]. However, there is consensus about the fact that the mechanism behind the protection of autoimmune disease is more complicated than a simple increase of Treg in pregnancy [6,141].

Therefore Treg during pregnancy and EAE are an eligible cell population for identifying pregnancy-induced effects onto autoimmunity.

1.8 Suppressive capacity of Treg

Treg exert their function of maintaining the immunological unresponsiveness to self-antigens and in suppressing excessive noxious immune responses via influencing and counteracting effector function of T cells, which they encounter or are in close proximity with.

Treg usually become activated via antigen exposure in the regional lymph at a much lower concentration of antigen than necessary for naive T cells [75].

Activated Treg mediate their suppressive effects by either directly inhibiting or lysing effector T cells or they indirectly act onto effector T cells via controlling the priming of effector cells through APCs [113], via killing of APCs [142,143] or via inhibition of the maturation and function of dendritic cells (DCs). DCs are APCs and therefore both can activate naïve T cells to become effector T cells. Further Treg can act onto their target cell via direct cell contact or via mechanisms exerting their function from the distance [113]. The best-studied mechanisms are discussed in the following.

Treg can deprive other cells in their vicinity from cytokines like IL-2, a major cytokine for T cell proliferation and differentiation. CD25 is a subunit of the IL-2 receptor (IL-2R), which is expressed at high levels on Treg. But CD25 is also upregulated on effector T cells. Higher IL-2R expression levels on Treg can collect the available IL-2 and thereby deprive it from effector T cells and inhibit their proliferation [144].

Treg can act via surface expression of the co-inhibitory, cytotoxic T lymphocyte antigen 4 (CTLA-4). CTLA-4 is a structural homologue of the co-stimulatory molecule CD28. To some extend CTLA-4 function is obtained by interaction with CD80 and CD86 expressed on APCs. CTLA-4 down-regulates CD80 and CD86 expression, thereby inhibits the antigen-presenting ability of APCs and thus dampens T cell activation [113,145,146]. However, many facets of CTLA-4 synthesis and function remain elusive at the moment [147,148].

Moreover, Treg can modulate T cell function via cell-surface molecules such as CD39 and CD73, two ectoenzymes highly expressed on Treg and important in conversion from adenosine diphosphate (ADP)/ adenosine triphosphate (ATP) to adenosine monophosphate (AMP) and adenosine. They have been shown to assist the development of adenosine and the displacement of cyclice adensoine monophosphate (cAMP), necessary for intracellular signal transduction. As a result, adenosine signaling initiated by Treg cells inhibits proliferation of effector T cells and negatively impacts the function of DCs [113,149].

Furthermore, production of the anti-inflammatory, inhibitory cytokines like IL-10 and TGF-β by Treg, stimulated via contact to DCs, can also lead to suppression of effector T cells and DC function in the vicinity [150].

The lymphocyte-activation gene 3 (Lag3) is another surface protein on Treg binding MHC class II on APCs. It has been shown that Lag3 interactions with MHC class II on DCs can also hamper DC activation and thus inhibit Tcon function [151].

Currently, it remains unknown whether factors mediated through pregnancy, such as changed levels of hormones, alter the suppressive capacities of Treg. The above-mentioned increases of Treg numbers suggest that this is not the only pregnancy adaptation in Treg. They might also increase their main function, the suppressive capacity.

1.9 Metabolism of Treg

The chemical reactions in an organism, relevant for conversion of food to energy, are vital to run all processes of the organism and to generate metabolites and components, like pyruvate, nucleotides and amino acids for e.g. cell synthesis or for getting rid of waste products. These life-sustaining processes are called metabolism.

Pregnancy is associated with many intricate metabolic modifications in order to ensure the energetic demands of the mother and the developing fetus [152]. Women have an about 10% higher calorie demand during pregnancy and need to be supplied with higher amounts of nutrients like folic acid, iodine and vitamin D for healthy development of the fetus [153]. To secure fetal nourishment, glucose, amino acids (aa) and lipids consumed by the feto-placental unit must be supplied by the maternal metabolism [152].
Correct working mechanisms of the immune system are vital for healthy growth and development during pregnancy. Therefore immune cells need to be supplied with reliable energy resources [154].
It is known that in order to gain ATP, the molecular currency of energy in the cell, T cells employ specific metabolic pathways in each phase of their development, differentiation and function. A switch in metabolism can influence cellular phenotype. And also vice versa, cellular fate and developmental stage can also influence the metabolic state. It has been shown that induction of Tcon and Treg required distinct metabolic programs (Fig. 1.3). The metabolic program has to correspond to the T cell subset in order to ensure cellular survival and differentiation [151]. During development T cells employ different metabolic pathways, e.g. developing and quiescent cells in the thymus use OXPHOS, differentiated effector Tcon utilize glycolysis, while Treg and memory T cells employ lipid oxidation (OXPHOS), which is critical for their maintenance, function and self-renewal. Upon an antigen re-challenge the reactivation of memory cells also upregulates glycolysis again [156–160].

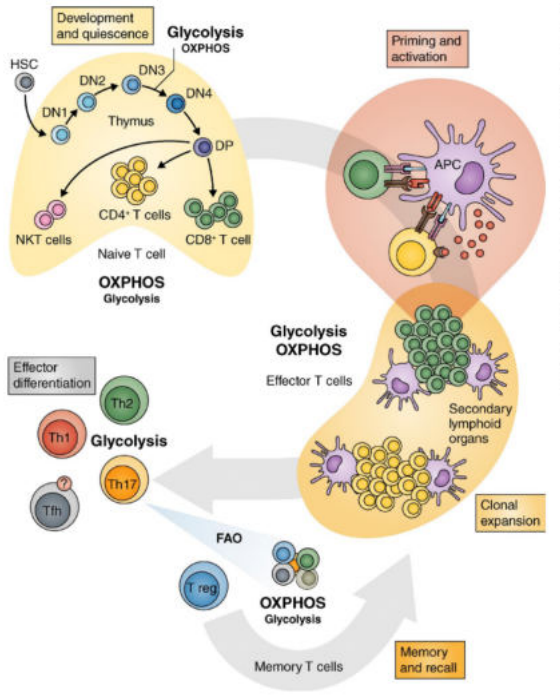

Figure 1. 3 Metabolism is guiding the life cycle of T cells

When naïve T cells develop in the thymus and also when emigrating from the thymus they depend on OXPHOS for their metabolic maintenance. However, they use glycolytic metabolism when rearranging TCR genes. In the secondary lymphoid organs after priming and activation have taken place, clonal expansion leads to a metabolic switch and the transition to an activated effector T cells is accompanied by the usage of glycolysis as well as by elevated OXPHOS activity. Fully differentiated effector CD4+ T cells use glycolysis for their energy consumption. This clearly separates them from Treg and memory T cells, which both mainly relay on fatty acid oxidation (FAO) and OXPHOS. Equally, promoting FAO and catabolic metabolism enhances Treg and memory T cell development. However, upon a second antigen challenge, memory cells quickly increase glycolysis and OXPHOS to fulfill their function [155,159,160]. Figure taken from Buck et al., 2015, 1347 [155].

The two main metabolic pathways used in order to generate ATP and which also drive T cell immunity are glycolysis and oxidative phosphorylation (OXPHOS) [154].

Glycolysis is often used with cellular activation. It takes place at the cytoplasm of a cell and is an oxygen independent pathway. It evolved early in evolution, even before photosynthetic organisms introduced oxygen (O_2) into the atmosphere. Therefore energy had to be produced without O_2. Glycolysis involves a sequence of ten separate reactions, each producing different sugar intermediates. Its net products are two molecules of ATP and two molecules of the reduced form of nicotinamide adenine dinucleotide (NADH), a cofactor which can be used as a reducing agent to donate electrons elsewhere. In aerobic organisms these NADH molecules are donated to the electron transport chain (ETC), which is part of an alternative metabolic pathway at the mitochondria. Furthermore two molecules of pyruvate are generated as a result of glycolysis. Pyruvate is fermented into lactate, in a process called lactic acid fermentation. Thereby NADH is oxidized to NAD^+ via specific enzymes and can be used in further rounds of glycolysis [155,161,162].

The alternative metabolic pathway is oxidative phosphorylation (OXPHOS), which is used by quiescent cells and cells in most normal tissue. OXPHOS takes place at the mitochondria of the cells. It works via breaking down glucose, amino acids and fats in the tricarboxylic acid (TCA) cycle (Fig. 1.4 A) and via the connected processes of the electron transport chain (ETC) (Fig. 1.4 B) to produce ATP. Basically the TCA sets free the energy and the ETC is a redox system, in which electrons from higher energetic levels are given to further lower energetic levels. Hydrogen (H) and oxygen (O_2) are put together to build water (H_2O) in single steps. Free energy is used to build ATP from ADP. Therefore OXPHOS requires O_2 to keep it running and to get rid of protons (H^+) from inside the mitochondrial membrane. In total, oxidation of one molecule of glucose, with the byproducts H_2O and CO_2, produces about 30 molecules of ATP [155,162,163].

At first sight OXPHOS is the much more energy efficient metabolic pathway. Both pathways also produce several side products, which might not sustain the organism with energy in the form of ATP, but may be of instant use in the organism [155].

Furthermore, fatty acid oxidation (FAO) are catabolic reactions generating energy and anabolic processes generating molecules like phospholipids and triglycerides. FAO is a high-energy source yielding much ATP when oxidized to CO_2 and O_2 in the so-called β-oxidation and in the TCA cycle in the mitochondrial matrix. Fatty acids are taken up by the cell and are activated via their transfer into CoA derivatives. Acyl-CoA is generated. Per fatty acid two energetically rich anhydride bonds from ATP are needed. In order to shuttle the acyl rest into the mitochondrion, the mitochondrial enzyme carnitine palmitoyl transferase 1 (Cpt1) is needed. It catalyzes the transfer of the acyl group of the long chain fatty acyl-CoA from coenzyme A to l-carnitine. Thereby acyl carnitine is formed. As acyl carnitine the fatty acid can be transmitted to the inner side of the mitochondrial membrane. The breakdown of fatty acids happens inside the mitochondrial matrix via TCA cycle. Here C_2 units are cleaved off one after the other. FAO is locally and functionally connected with the TCA cycle and the ETC [162].

It has further been shown that T cell fate is controlled through metabolic reprogramming of a fusion protein in the mitochondria. Remodeling of mitochondrial cristae has been shown to happen according to the needs of the cell. Mitochondrial cristae are able to undergo fission or fusion. Fusion in mitochondria of memory T cells establishes the ETC complex, thus encouraging OXPHOS and FAO. On the other side mitochondrial fission in effector T cells leads to an expansion of the mitochondrial cristae, reducing ETC efficiency and thus facilitates aerobic glycolysis [164].

It was identified that "spare respiratory capacity (SRC) is the extra capacity available in a cell to produce energy in response to increased stress or work" (van der Windt et al., 2012, 68 [165]) and therefore is directly connected to increased cell survival [165,166]. Further, SRC has been found to be mediated by cytokine changes and to be the critical regulator of CD8+ T cell memory development [165].

It has been shown, that CD8+ memory T cells, but not effector T cells, possess higher SRC and that this mediates establishment of long-lived memory T cells [165]. Interleukin-15 (IL-15), a cytokine critical for CD8+ memory T cells, regulates SRC and oxidative metabolism by promoting mitochondrial biogenesis and the expression of CPT1a, the metabolic enzyme that controls the rate-limiting step to mitochondrial FAO. These results are an appropriate example of how cytokine changes control the bioenergetic stability of memory T cells after infection by regulating mitochondrial metabolism [165].

Moreover, it has been shown in human and mice that acetyl-CoA carboxylase 1 (ACC1)-mediated fresh synthesis of fatty acid promotes Th17 development. This is in contrast to Treg development. Treg rely on exogenous fatty acids for their development and do not depend on *de novo* fatty acid synthesis. Thus inhibition of ACC1 constrains the formation of Th17 cells and promotes the development of anti-inflammatory Treg. These results show essential differences between Th17 cells and Treg cells in respect of their dependency on ACC1-mediated *de novo* fatty acid synthesis. It has also been speculated that these fundamental differences might be exploited as a new strategy for metabolic immune modulation of Th17 cell–mediated inflammatory diseases [167].

Categorically for Treg it has been shown that the Treg transcription factor Foxp3 masters metabolic adaptations including down regulation of glycolysis, induction of OXPHOS and an increase of the NAD:NADH ratio. These metabolic changes allow Treg to exist in low-glucose and high-lactate environments and to thus maintain their immunosuppressive function under metabolically challenging conditions [157].

In human RRMS patients an immunometabolic profiling of global T cells has demonstrated an impairment in both, glycolysis and mitochondrial respiration compared to healthy controls. This impaired T cell metabolism was shown to be reversible upon *in vivo* treatment with the immunomodulating IFNbeta-1a, which induced glucose uptake via translocation of glucose transporters on the cell surface. This suggests an involvement of an altered metabolism in the pathogenesis of MS and further emphazises the impact of metabolism [168]. In support of this it was identified that a diet with very low calorie and pioglitazone administration reduced the incidence and severity of EAE in C57BL/6 mice [169,170].

As mentioned above the MS treating drug Dimethyl fumarate, usually applied in mild or moderately proceeding RRMS, operates via inactivating aerobic glycolysis in activated myeloid and lymphoid cells - via inactivating the glycolytic enzyme GAPDH. Inactivating glycolysis results in the down-modulation of immune responses, as inflammatory immune cell subsets require aerobic glycolysis. Thus, manipulation of metabolism in Tcon serves as an approved and viable therapeutic target in autoimmune disease [50].

Manipulation studies using drugs to inhibit glycolysis identified an increase in the development of pTreg and could block both, disease mediating Th1 differentiation in an autoimmune mouse model of allergic asthma and also Th17 differentiation in EAE. Other drugs selectively blocking glycolysis showed to reduce effector T cell development and to promote Treg development also in EAE. This further stabilizes the concept of a bidirectional interaction between the immune system and whole-body metabolism. And it shows that cell-intrinsic metabolic capacities of lymphocytes can by themselves dictate the fate and function of the cells and ultimately shape an immune response [171].

These examples provide evidence that metabolism is markedly influencing both lymphocyte/Treg fate and lymphocyte function, also in the EAE model. Therefore investigations of changes in Treg functionality during pregnancy should include measurements of Treg metabolism.

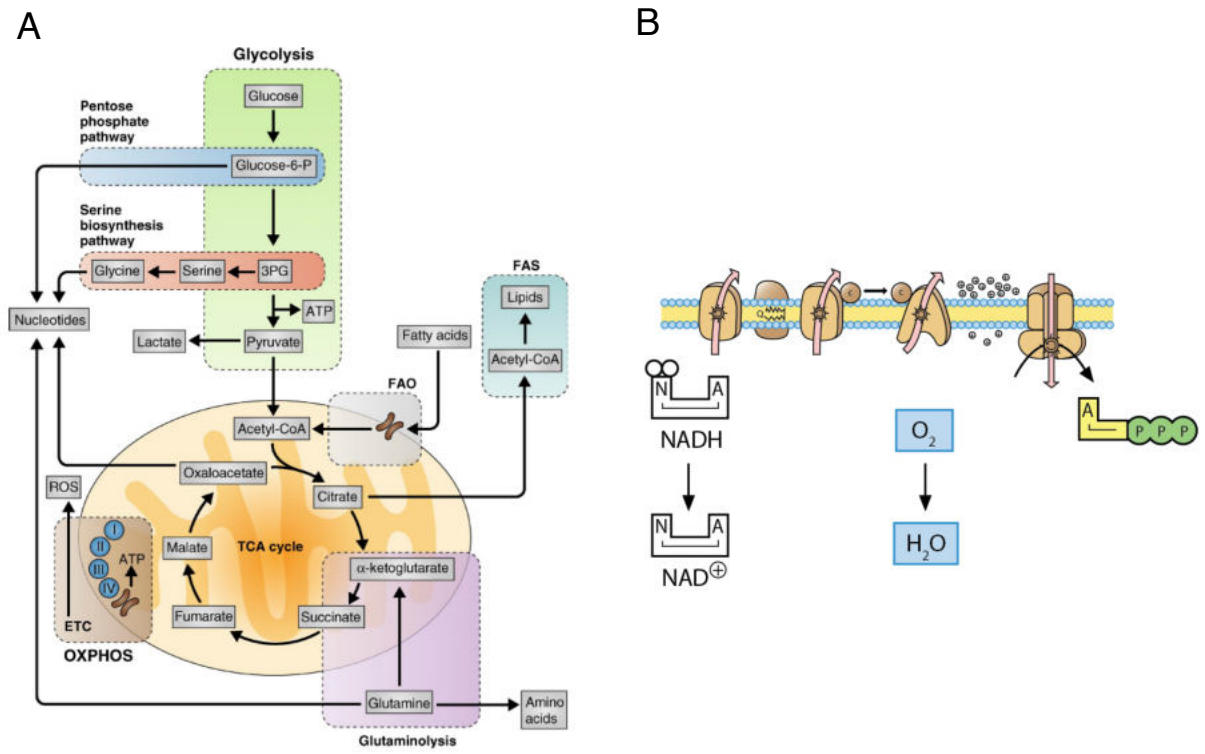

Figure 1. 4 Immunometabolism pathways

Lymphocytes relay either on glycolysis or oxidative phosphorylation (OXPHOS) for energy supply. (**A**) Intermediate steps of metabolic pathways of glycolysis (green), TCA cycle (orange) and OXPHOS (brown) with several intermediates. Figure taken from Buck et al., 2015, 1348 [155]. (**B**) Details of electron transport chain (ETC). Modified from Koolman et al., 2003, 141 [162].

1.10 Treg T cell receptor specificity

An individual has to detect and fight foreign antigen (of pathogens like viruses and bacteria) with an effector response, however self-antigens (from own tissue) have to be tolerated. The discrimination between self and foreign however becomes more difficult when fetal semi-allogen antigen is also present.

In order to detect antigen specifically the antigen-specific TCR evolved. In mice and human it depends on the genetic variability of the TCR locus that the individual is equipped with from its parents and additional recombinatory processes. The TCR is anchored in the plasma membrane on the surface of all T cells and is made up of a heterodimer of two disulfide-linked transmembrane polypeptide chains. The most common form of a TCR is composed of an α and a β chain, less common are γ and δ chains. In the case of α and β chain, both chains are made up of a constant (Cα and Cβ) and a variable (Vα and Vβ) region (Fig. 1.5 C). The genetic information for both chains is encoded in the germ line. For the β chain there is DNA information about the constant region and then many variants of the so-called variable (V), diversifying (D) and junctional (J) regions. In each human individual there are 42 V, 2 D and 12 J regions available. However, only one of each VDJ elements is picked by chance, in order to build a TCR during

somatic recombination (Fig. 1.5 A). The non-used segments are deleted for the individual cell (Fig. 1.5 B). Similarly it happens for the α chain. However, here only different V and J regions exist that are spliced together with the constant region (Fig. 1.5 A). In the human there are in total 43 V regions and 58 J regions from which one is taken each by chance to build a TCR α chain. Additionally, a lymphocyte-specific enzyme called terminaldeoxyribonucleotidyl transferase (TdT) catalyzes random addition of nucleotides that are not part of the germline genes to the junctions between V and D segments and D and J segments, forming so-called N regions. Then the α and a β chain are put together to build the TCR (Fig. 1.5 C). The neighboring regions of the V, D and J segments make up the so-called complementary determining region (CDR3 region) or hyper variable region, which due to recombination has a huge variability (Fig. 1.5 B). In the completed receptor this most variable CDR3 region is located in an area with direct contact to the antigen (Fig. 1.6), therefore it influences the antigen-specificity of the TCR. Overall a human can theoretically build approximately 10^{11} - 10^{15} different TCR sequences. After thymic selection of the completed T cell with its receptor still around 2×10^{7} different TCRs on T cells are possible. The set up in the mouse is very similar to the human. In this way one individual can produce an enormously big amount of different receptors and can effectively fight a vast number of pathogens. After circulation through blood vessels and peripheral tissues T cells are attracted to the site of infection via epithelial cells. When the T cells encounter 'their' specific antigen with 'their' TCR and if they also receive co-stimulation (via the CD3 and CD4 co-receptor molecule) they become activated and exert effector function. Further, activated T cells expand clonally in lymphoid tissue. They proliferate to generate enough antigen-specific effector T cells to eradiate the infection. In clonal expansion the TCR is conserved with cell proliferation. T cells with the same TCR are therefore called clones [60,172,173].

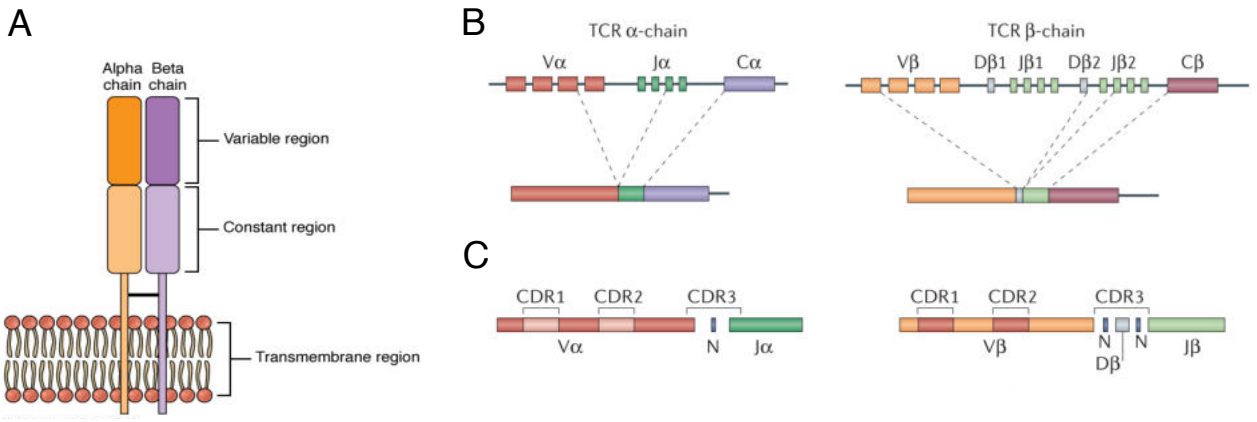

Figure 1. 5 TCR structure and TCR recombination

(**A**) Complete alpha beta TCR on the surface of a T cell. Figure taken from commons.wikimedia.org/wiki/File:2215_Alpha-Beta_T_Cell_Receptor.jpg, (2019-02-7) (2019) [174] (**B**) Germline encoded possibilities for splice variants for building an α and a β chain of a human TCR. (**C**) Already spliced together DNA regions for the α and a β chain for a TCR. Figure in **B** and **C** modified from Turner et al., 2006, 884 [173].

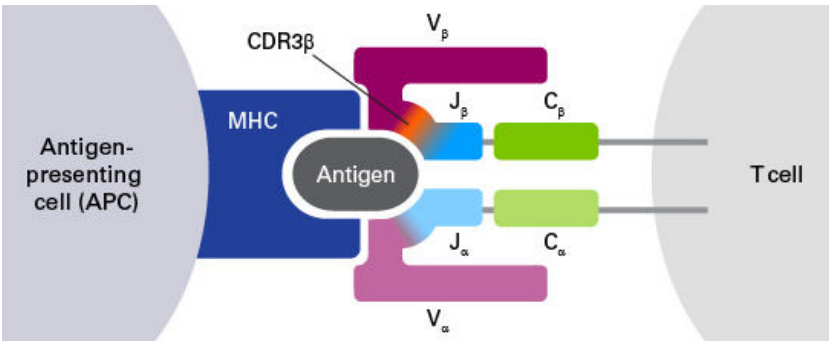

Figure 1. 6 T cell recognizing antigen

Representative drawing of an antigen-specific T cell stimulation. Depicted is a T cell with a TCR on its surface. The TCR recognizes specific antigen, which is presented by the MHC molecule of an APC. Figure taken from www.takarabio.com/areas-of-interest/immunotherapy-research/t-cell-receptor-profiling, (2019-02-7) (2019)[175].

Regarding Treg there are contradictory opinions on the contribution of antigen-specific versus antigen-unspecific regulation of disease-causing Tcon. In Tcon however, antigen-specificity is clearly required for a targeted immune responses. The necessity for Treg to recognize the same antigen in order to properly control the corresponding Tcon response is less evident [10,107,108,139].

In the context of a successful pregnancy there is evidence for the fact that Treg are generated in a fetal antigen-specific manner and thereby limit maternal immune response to the fetus [11,14]. Although Treg expansion is mainly fetal antigen-specific, it has been shown that outside pregnancy these cells are also able to suppress T cell responses to unrelated antigens in form of a bystander suppression [115]. According to this concept T cells in close proximity are activated via other processes e.g. cytokines from nearby activated T cells. Thus non-specific Treg can be activated. This inspires the discussion about whether suppressive Treg effects in pregnancy are mainly mediated through antigen-specific activity [176,177] or via bystander suppression [115].

Similarly in the context of EAE, there are publications arguing for the fact that specificity is required for a Treg and that it needs to react to exactly the same antigen as the Tcon that it regulates [176,177]. However, others state that Treg activity can be evoked via bystander activity [115]. Furthermore, autoreactive immune responses tend to broaden their antigenic scope of application towards unrelated co-presented antigens. This phenomenon is called 'epitope spreading'. In the context of an EAE immunization epitope spreading means that different clones or clonotypes that might be found expanded in EAE are not inevitably MOG-specific. This is the case even though only the MOG_{35-55} peptide has been used for immunization. The activated epitopes often have structural parallels to the original epitope [14,178,179].

Detailed TCR analysis has shown that there is a partial overlap between the repertoires of Treg and non-Treg [113,180–183].

In the context of EAE, the MHC class II restriction of the largely used inbred C57BL/6 mice has been shown to typically lead to a shift in the variety of VDJ segments used for building the TCR. Especially the chain TRBV13.2 is associated with EAE on Tcon and Treg on a population-wide level. Less elevated than TRBV13.2, but associated with EAE are the chains TRBV5, TRBV19, TRBV31 and TRBV20 [118,184–187]. Even though C57BL/6 mice are genetically identical it has been clarified that each individual mouse

begins with a unique TCR repertoire and generates an individual composition of expanded MOG-specific clones [118,184].

Antigen-specificity in the context of both pregnancy and EAE remains currently unknown, but bears promising information that might help to better understand participation of specific mechanism in the pregnancy mediated protection from EAE.

1.11 Aims

The aim of this work is gaining a better understanding of the role of Treg in immune modulation during pregnancy and how this contributes to establishing tolerance in multiple sclerosis.
Very particular questions and hypotheses arise around different aspects of Treg functionality during pregnancy and EAE:
One hypothesis is that the potency of the increased Treg numbers found in the reproductive tract and uterus draining lymph nodes during pregnancy is increased in order that they can perform their purpose in a more appropriate way – adapted to the pregnancy circumstances. Hypothetically an increased functionality of Treg is another specific mechanism of the immune system to protect mother and child. Treg from pregnant mice should show a higher suppressive capacity than Treg stemming from virgin mice, because they have to hinder encephalitogenic Tcon not only from self-reactive activity but also of attacking the fetus. As a 'side effect', more potent suppressor cells protect the CNS in EAE-immunized animals along with the fetus.

Another hypothesis is that the metabolism of Treg is changed during pregnancy. It had been hypothesized already that targeting cell metabolism may represent a new method in stimulating immunity and in influencing inflammatory diseases [154]. Maybe evolution has implemented such mechanisms already and suppresses autoimmunity and inflammation via promoting Treg in pregnancy in the form of increasing their lipid oxidation characteristic. Hypothetically elevated energy supply for increasing amounts of Treg during pregnancy and EAE is met via an increased energy metabolism in Treg. Thus, Treg phenotype and functionality are stabilized to promote effector Tcon suppression that can potentially harm the fetus. Treg are thought to rely on OXPHOS for their energy supply. Thus, the hypothesis is that Treg stemming from pregnant mice show increased OXPHOS levels enabling the Treg to fulfill their function comprehensively.

A third hypothesis is that there are changes in Treg antigen specificity mediated by pregnancy and EAE, measurable on the clonal cell level and that these changes convey protection from EAE disease. Currently, it remains unknown whether Treg in the context of pregnancy and autoimmunity control the disease-causing Tcon with antigen-specific or antigen-unspecific Treg function. Further it remains unknown if changes that pregnancy has onto EAE are at all mirrored in the TCR repertoire of the involved cells. The aim is to analyze the TCR repertoire of Tcon and Treg over the course of pregnancy and EAE in C57BL/6 animals and to explore changes in the TCR repertoire over the course of pregnancy and EAE.

In order to study these hypotheses, the following components are addressed:

- Assessment of Treg functionality via measurements of suppressive capacity of Treg isolated from virgin and pregnant mice

- Comparison of Treg functionality via measurements of energy metabolism of Tcon and Treg originating from virgin and pregnant mice

- Systematic analysis of the TCR β repertoire in Tcon and Treg in virgin and pregnant mice that are either in a naïve or EAE diseased stage

2. Material and Methods

2.1 Mice, material, buffer, media, devices and software

Table 2. 1 Used mouse strains

Mouse strain	Official Symbol	Jax Stock Number	Company
C57BL/6	C57BL/6	000664	The Jackson Laboratory
B6-DEREG	C57BL/6-Tg(Foxp3-DTR/EGFP)23.2Spar/Mmjax	32050	The Jackson Laboratory
BALB/C	BALB/cJ	000651	The Jackson Laboratory

Table 2. 2 Reagents for PCR (for genotyping of B6-DEREG mice)

Reagent	Sequence	Company	Used µl per reaction
H_2O	-	Thermo Fisher Scientific	14,05
Maxima Hot Start Buffer (20µM)	-	Thermo Fisher Scientific	2,5
$MgCl_2$ (25µM)	-	Thermo Fisher Scientific	1,5
dNTPs 10 (mM)	-	Thermo Fisher Scientific	0,5
Primer eGFP 3'(µM)	CGGCGAGCTGCACGCTGCCGTCCTC	biomers	1
Primer eGFP 5'(µM)	CCTACGGCGTGCAGTGCTTCAGC	biomers	1
Primer b-Actin fwd (µM)	AGAGGGAAATCGTGCGTGAC	biomers	1,1
Primer b-Actin rev (µM)	CAATAGTGATGACCTGGCCGT	biomers	1,1
Maxima Hot Start Polymerase	-	Thermo Fisher Scientific	0,25
Template	-	-	2
∑			25

Table 2. 3 Reagents for animal experiments

Reagent	Company
CO_2/O_2 gas mixture (80% CO_2, 20% O_2)	SOL Deutschland
Forceps	Fine Science Tools
MOG_{35-55} Peptide	peptides & elephants
Mycobacterium tuberculosis	Becton Dickinson
O_2 (100%)	SOL Deutschland
PBS	Pan-Biotech
Pertussis toxin	Merck
Scissors	Fine Science Tools
Syringes (different sizes)	B. Braun

Table 2. 4 Reagents for cell culture

Reagent	Company
Anti-CD28 (Clone 37.51)	BioLegend
Anti-CD3 (Clone 145-2C11)	BioLegend
CD90.2 antibody	BioLegend
Collagenase A	Roche
DNase I	Merck
eFluor 670	Thermo Fisher Scientific
Falcon	Cellstar
Filter for Falcon	Greiner
HBSS	Thermo Fisher Scientific
Rabbit complement	Cedarlane
PBS	Pan-Biotech
Percoll	GE Healthcare
Pipette tips	Sarstedt
RPMI 1640 media	Pan-Biotech
Serological pipettes	Sarstedt
Tubes for fluorescence-activated cell scanning and sorting	Becton Dickinson
10 × PBS	Pan-Biotech
96-well plates	Greiner

Table 2. 5 Reagents for complete RPMI Buffer

Consumable	Company	Concentration
B-mercaptoethanol	Sigma-Aldrich	0.1 %
Fetal calf serum (FCS)	Carl Roth	10 %
Penicillin and streptomycin	Thermo Fisher Scientific	1 %
RPMI 1640 media	Pan-Biotech	500 ml

Table 2. 6 Reagents for Erylysis Buffer

Consumable	Company	Concentration
Amoniumchloride (NH_4CL)	Sigma-Aldrich	0.15 M
Millipore Water	generated in-house	500 ml
NA_2EDTA	Thermo Fisher Scientific	0.1 mM
Potassium bicarbonate ($KHCO_3$)	Sigma-Aldrich	10 mM
pH 7.3 – 7.4		

Table 2. 7 Reagents for Magnetic-associated cell sorting (MACS)

	MACS Buffer	
Consumable	**Company**	**Concentration**
2.5 g BSA	Carl Roth	0.5 %
EDTA	Thermo Fisher Scientific	2 mM
500 ml PBS	Pan-Biotech	
Sterile filter (0.4 µM)	Merck	
	Other consumables for MACS	
CD4+CD25+ Regulatory T cell isolation kit, mouse	Miltenyi Biotec	
CD8a (Ly-2) MicroBeads, mouse	Miltenyi Biotec	
MS columns	Miltenyi Biotec	
LD columns	Miltenyi Biotec	

Table 2. 8 Reagents for RNA/DNA or only RNA isolation

Reagent	Company
AllPrep DNA/RNA Micro kit	QIAGEN
B-mercaptoethanol	Sigma-Aldrich
QIAshredder spin columns	QIAGEN
RNAeasy Mini Kit	QIAGEN

Table 2. 9 Reagents for RT-PCR Assays

Consumable	Company
Maxima Hot Start Buffer	Thermo Fisher Scientific
Maxima Hot Start Polymerase	Thermo Fisher Scientific
$MgCl_2$	Thermo Fisher Scientific
dNTPs	Thermo Fisher Scientific
Primer eGFP 3’	biomers
Primer eGFP 5’	biomers
Primer b-Actin fw	biomers
Primer b-Actin rev	biomers

Table 2. 10 TaqMan assays for Quantitative real time PCR (RT-PCR)

Reagent	Company	Code	Dye
Cables1	Thermo Fisher Scientific	Mm00491531_m1	FAM-MGB
Cpt1a	Thermo Fisher Scientific	Mm01231183_m1	FAM-MGB
IL-7r	Thermo Fisher Scientific	Mm00434295_m1	FAM-MGB
TBP	Thermo Fisher Scientific	Mm01277042_m1	FAM-MGB

Table 2. 11 Reagents for copy number assays

Reagent	Company	Code	Dye
AllPrep DNA/RNA Mini kit	QIAGEN	-	-
DNA of respective samples	-	-	-
TaqMan Assay: Beta Actin	Thermo Fisher Scientific	Mm00607939_s1	FAM-MGB
TaqMan Assay: COXII	Thermo Fisher Scientific	Mm03294838_g1	FAM-MGB

Table 2. 12 Reagents for Cell Mito Stress Test

Consumable	Company	Concentration
Cell-Tak Tissue Adhesive	Corning	
Glucose	Sigma-Aldrich	25 mM
L-glutamine	Thermo Fisher Scientific	2.0 mM
Seahorse Calibrant	Agilent	
Seahorse XF base medium	Agilent	per 100 ml
Sodium Bicarbonate Buffer	Sigma-Aldrich	0.1 M-solution contains 8.40 g/L
Sodium hydroxide (NaOH)	Sigma-Aldrich	1 M
Sodium pyruvate	Sigma-Aldrich	1.0 mM
XF Cell Mito Stress Test Assay Medium	Agilent	
XF Cell Mito Stress Test Kit	Agilent	
XFe96 Flux Assay Kit	Agilent	
XF96 Cell culture Microplate	Agilent	

Table 2. 13 Reagents for fatty acid oxidation media (used for Cell Mito Stress Test)

Consumable	**Company**	**Concentration g per 1L 5×**
Calcium chloride (CaCl2)	Sigma-Aldrich	110.00
Magnesium sulfate (MgSO4)	Sigma-Aldrich	120.36
Potassium chloride (KCl)	Sigma-Aldrich	74.55
Sodium chloride (NaCl)	Sigma-Aldrich	58.44
Sodium phosphate (NAH2PO4)	Sigma-Aldrich	119.98
	40 ml from 5x stock diluted in 160 ml millipore water, to reach 1x in 200ml. This was further added by:	
Consumable	**Company**	**Concentration mg per 200ml 1×**
Glucose	Sigma-Aldrich	90.08
HEPES	Sigma-Aldrich	238.3
L-Carnitine	Sigma-Aldrich	19.766

Table 2. 14 Reagents for flow cytometry

Reagent	**Company**
Antibodies for staining	see Table 2.16
Buffer for fluorescence-activated cell scanning	see Table 2.15
Cleaning solution	Becton Dickinson
dd H_2O	generated in house
Flow for fluorescence-activated cell scanning and sorting	Becton Dickinson
Rinse solution	Becton Dickinson

Table 2. 15 Reagents for fluorescence-activated cell sorting buffer

Consumable	**Company**	**Concentration**
Bovine serum albumin (BSA)	Carl Roth	25 g
H_2O	generated in house	5000 ml
Sodium azide	Carl Roth	1 g
10 x PBS	Pan-Biotech	500 ml

Table 2. 16 Antibodies against mouse antigens for flow cytometry

Antibody	Company	Color	Clone	Final dilution used for cell staining (in fluorescence-activated cell scanning buffer)
CD4	BioLegend	Pacific Blue	Clone RM4-5	1:100
CD8	BioLegend	Brilliant Violet 510	Clone 53-6.7	1:100
F_c Block (True Stain anti-mouse CD16/CD32)	BioLegend	-	Clone 93	1:1000
Fixable Dead Cell Stain	Thermo Fisher Scientific	Pacific Orange (V500)	-	Stock dissolved in water-free DMSO, for use 1:1000 diluted in PBS

Table 2. 17 Devices

Device	Company	Comment
Computer	HP	
Centrifuge	Heraeus	
Flow cytometer	Becton Dickinson	
Fluorescence-activated cell sorter	Becton Dickinson	
Freezer (-80 °C)	Sanyo	
Freezer (-20 °C)	Liebherr	
Fume hood	Belec Vario Lab	
Gel documentary device	INTAS Science Imaging	
HT 7900 real-time PCR instrument	Thermo Fisher Scientific	
Incubator	Memmert	
Irradiation unit (Biobeam)	Eckert & Ziegler	
MACS magnet	Miltenyi Biotec	
PCR cycler	Analytik Jena	
pH-meter	Mettler-Toledo	
Qubit 3 Fluorometer	Thermo Fisher Scientific	
Refrigerator	Liebherr	
Spectrophotometer (Nanodrop)	PeqLab	
Sterile hood	Thermo Fisher Scientific	
Table top centrifuge	Thermo Fisher Scientific	
XFe96 Analyzer	Agilent	Available at Huber working group (UKE)

Table 2. 18 Software

Software	Company
Adobe Illustrator CC 2018	Adobe
Adobe Photoshop CC 2018	Adobe
Excel	Microsoft
FACSAria	Becton Dickinson
FACSDiva	Becton Dickinson
FlowJo v10	FlowJo
Graph Pad Prism7	Graph Pad
ImageJ Fiji	Open source
Mixcr 2.1.10	Open source
R scripts	Open source
RQ Manager 1.2.1	Thermo Fischer Scientific
SDS 2.4	Thermo Fischer Scientific
VDJtools 1.1.8	Open source
Wave 2.2.0	Agilent
Windows	Microsoft
Word	Microsoft

2.2 Methods

2.2.1 Mice

C57BL/6 mice or B6-DEREG female mice and BALB/C males were kept under specific pathogen-free conditions in the Central Animal Facility at the University Medical Center Hamburg-Eppendorf. Age-matched adult mice were used in all experiments.

2.2.2 Genotyping

Tail biopsies were taken from newborn genetically modified mice (B6-DEREG) [188]. DNA was extracted from the biopsy using QuickExtract reagent for 6 min at 65 °C at 500 rpm, then for 2 min at 98 °C at 350 rpm. Then the DNA was used as a template in a genotyping PCR (Table 2.2). The amplification program was used as follows: 40 cycles for 10 min at 94 °C, 30 sec at 94 °C, 30 sec at 63 °C, 30 sec at 72 °C. Then samples were incubated for 5 min at 72 °C and afterwards cooled down to 15 °C. The fragment size of the PCR product was analyzed on a 3% agarose gel containing RotiSafe Gel Stain. The amplicons from wild type samples were 150 base pairs long while transgenic animals showed the 150 base pair long amplicon as well as a 350 base pair long amplicon. Pictures of the respective gels were taken with a gel documentary device and were analyzed with Photoshop or ImageJ.

2.2.3 Allogenic mating of mice

Age-matched female mice were mated with BALB/c males for three consecutive nights. Successfully mated females where identified by the presence of a vaginal plug, separated, and weighted on consecutive days to confirm pregnancy. The day of plug was considered gestational day 0.5 (E 0.5). In experiments including postpartum time points, pups were separated and sacrificed at the day of delivery. Consequently virgin mice were used as control animals for the pregnant ones.

2.2.4 Induction of experimental autoimmune encephalomyelitis (EAE)

Mice were anesthetized with O_2/CO_2 mixed gas and subsequently immunized subcutaneously (s.c.) with 200 µg of myelin oligodendrocyte glycoprotein peptide 35-55 ($MOG_{35–55}$) in complete Freund's adjuvant containing 4 mg/mL heat inactivated *Mycobacterium tuberculosis*. In addition, 200 ng pertussis toxin were injected intravenously (i.v.) on the day of immunization and 48 h later. Animals were scored daily for clinical signs by the following system: 0: no clinical deficits; 1: tail weakness; 2: hind limb paresis; 3: partial hind limb paralysis; 3.5: full hind limb paralysis; 4: full hind limb paralysis and forelimb paresis; and 5: premorbid or dead. Animals reaching a clinical score ≥ 4 had to be killed according to the regulations of the Animal Welfare Act. For induction of a pregnancy with a simultaneous EAE animals

were mated first. On gestational day 7.5 (E 7.5) an EAE was induced in addition according to the usual procedure as described above. Animals were typically taken into experiments in late pregnancy, on day E 18.5, as this corresponds to the third trimester phase of a human pregnancy.

2.2.5 Cell isolation

2.2.5.1 Immune cell isolation from lymph nodes and spleen

Mice were anesthetized with O_2/CO_2 gas mixture and killed with CO_2. Inguinal, brachial, auxiliary, superficial cervical and para-aortal lymph nodes as well as the spleen were harvested with sterile instruments and put into ice-cold PBS. Single cell suspensions were prepared by homogenizing spleen and lymph nodes through a 40-µm cell strainer. Cells were pelleted by centrifugation (300 g, 10 min, 4 °C), then resuspended in 1 ml MACS Buffer and treated with 5 ml ice-cold Erylysis Buffer for 2.5 min for lysis of splenic red blood cells. Lysis was stopped by addition of 50 ml MACS Buffer. Cells were pelleted by centrifugation (300 g, 10 min, 4 °C), washed with MACS Buffer and finally resuspended in 5 ml MACS Buffer or PBS, depending on follow up applications like a staining for fluorescence-activated cell sorting or MACS immune cell isolations.

2.2.5.2 Isolation of CNS-infiltrating lymphocytes

For isolation of CNS-infiltrating lymph nodes mice were sacrificed as described above for isolation of peripheral lymphocytes. Immediately after killing mice were intracardially perfused with 10 ml ice-cold PBS to remove leukocytes from blood vessels. Brain and spinal cord were harvested with sterile instruments and put into ice-cold PBS. They were incubated for 1 h at 37 °C in a digestion solution, containing serum free RPMI, 1 mg/ml Collagenase A and 0,1 mg/ml DNaseI with agitation. Brain and spinal cord were homogenized by triturating through a 40-µm cell strainer, washed with 50 ml PBS and pelleted by centrifugation (300 g, 10 min, 4 °C) and washed again with 50 ml PBS. Cells were resuspended with 30% Percoll and 78% Percoll was layered underneath. The gradient was centrifuged (2500 rpm, 30 min, 4 °C) and CNS infiltrating immune cells were removed from the gradient interphase. The cells were washed with PBS and centrifuged again (1800 rpm, 10 min, 4 °C). Cells were resuspended in PBS and again centrifuged (1200 rpm, 7 min, 4 °C). Finally, isolated cells were depleted for CD8 T cells using CD8a Microbeads and MS columns. Cell suspensions were washed with PBS, counted and used in follow-up applications like DNA isolation and TCR sequencing.

2.2.6 Magnetic-activated cell sorting (MACS)

Immune cells were isolated from lymph nodes and spleen according to section 2.2.5. Isolated cells were counted and then cells were used in follow up magnetic isolation protocols:

2.2.6.1 CD4+CD25+ T cell isolation (gain of CD4+CD25+ regulatory T cells)

Magnetic isolation of CD4+ cells:

CD4+ cells were isolated according to the manufacturer's protocol of the CD4+CD25+ Regulatory T Cell Isolation Kit for mouse. Briefly, a control aliquot for pre-fluorescence-activated cell scanning analysis was taken. Cells were centrifuged at 300 g for 10 min at 4 °C and the supernatant was taken off. Cells were resuspended in a mixture of MACS Buffer with a biotinylated antibody cocktail that labels many immune cells but spares the desired CD4+ cell populations. Then antibody-bound non-CD4+ anti-biotin-microbeads were added to the solution to specifically label the CD4+ cells. The suspension was run over an LD coal column placed in a strong magnet to hold back the microbead-labeled cells inside the column and to wash through the unlabeled cells, which in this case are CD4+ cells. The columns were washed again to gain as much unlabeled cells as possible (Fig. 2.1). Another control aliquot was taken at this stage.

Magnetic isolation of CD4+ CD25+ cells:

MACS isolated CD4+ cells were centrifuged again at 300 g for 10 min at 4 °C and the supernatant was taken off. Cells were resuspended in a mixture of MACS Buffer with a biotinylated antibody cocktail that labels only the desired CD25+ cell populations. The suspension was run over a MS coal column placed inside a strong magnet to hold back the micro bead-labeled cells inside the column and to wash through the unlabeled cells. In this case these cells were CD4+ CD25− cells. The column was washed again to wash out all unlabeled cells. A control aliquot was taken at this stage. Then the column was taken out of the magnet and all labeled and therefore kept back cells are washed out to gain the CD4+ CD25+ cells (Fig. 2.1). Another control aliquot was taken at this stage again. Then cells were pelleted by centrifugation at 300 g for 10 min at 4 °C, and stored at –80 °C until RNA isolation or used directly in follow up applications like suppression assays or Cell Mito Stress Test.

Control stainings for fluorescence-activated cell scanning were performed of the MACS separated cell populations taken at different stages of the isolation to check their purity. Therefore cell suspensions were stained with CD4-Pacific Blue and Fc-Block for 15 min at 4 °C in the dark. Cell suspensions were washed with fluorescence-activated cell scanning buffer and taken up in the same buffer for measurements on fluorescence-activated cell scanning device and Diva software. Subsequent analyses of the data e.g. checking of the population purity were performed with FlowJo v10 software.

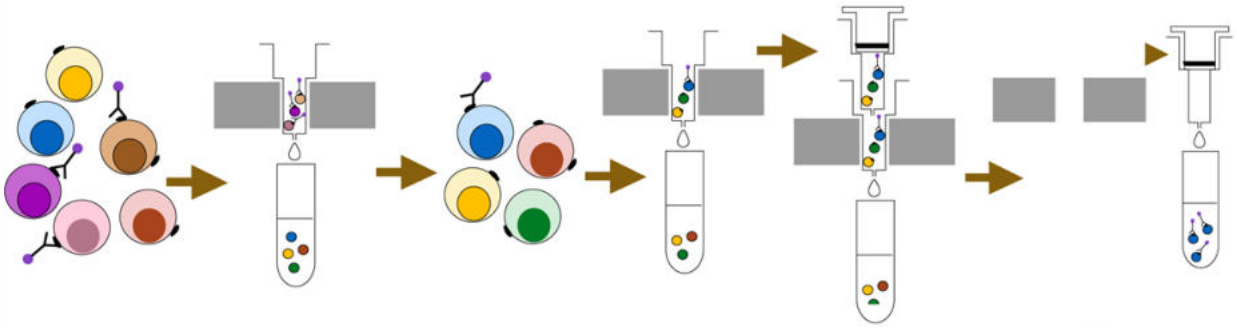

Figure 2. 1 MACS separation method to isolate CD4+CD25+ Treg from mixed lymphocytes

Modified from www.miltenyibiotec.com/DE-en/products/macs-cell-separation/basic-principle-of-magnetic-cell-separation.html (2019-02-11) (2019) [189].

2.2.6.2 CD8 T cell depletion

CD8− cells were isolated according to the manufacturer's protocol of the CD8a Microbeads kit for mouse. Briefly, a control aliquot for pre-fluorescence-activated cell scanning analysis was taken. Cells were centrifuged at 300 g for 10 min at 4 °C and the supernatant was taken off. Cells were resuspended in a mixture of MACS Buffer and microbeads labeling CD8+ immune cells, but sparing all other immune cell populations. The suspension was run over a coal column (size MS) placed in a strong magnet to hold back the microbead-labeled CD8+ cells inside the column and to wash through the unlabeled cells, which in this case are desired CD8− cells. Another control aliquot was taken. As a control the column was taken out of the magnet and all labeled and kept back cells were washed out to also isolate the CD8+ cells. Another control aliquot was taken at this stage again. Cells were then pelleted by centrifugation at 300 g for 10 min at 4 °C, dry frozen in liquid nitrogen and stored at –80 °C until DNA isolation and following TCR sequencing.

Control stainings for fluorescence-activated cell scanning were performed of the MACS separated cell populations taken at different stages of the isolation to check the purity of the cell separations. Therefore the cell suspensions were stained with CD4-FITC, CD8-Briliant Violet 510 and Fc-Block for 15 min at 4 °C in the dark. Cell suspensions were washed with fluorescence-activated cell scanning buffer and then taken up in the same buffer for measurements on the fluorescence-activated cell scanning device and Diva software. Subsequent analyses of the generated data e.g. of the population purity were performed with FlowJo v10 software.

2.2.7 RNA isolation, cDNA synthesis and real-time-polymerase chain reaction (RT-PCR)

2.2.7.1 RNA isolation

Dry frozen pellets of around 0.5×10^6 to 9×10^6 cells were thawed on ice and RNA was isolated using the RNAeasy Mini kit according to the manufacturer's protocol. Briefly, cells were resuspended in 350 µl Lysis Buffer consisting of RLT-Buffer mixed with β-mercaptoethanol (1:100) and were disrupted by passaging through a 30 G needle. Cell debris was removed by centrifugation (full speed, RT, 3 min), then the supernatant was transferred into a new tube. Then an equal volume of 70% ethanol was added and mixed by pipetting up and down and was transferred into an RNAeasy Mini spin column and centrifuged (> 8000 g, RT, 15 sec). Subsequently samples were consecutively washed with 700 µl Buffer RW1 (> 8000 g, RT, 15 sec), 500 µl Buffer RPE (> 8000 g, RT, 15 sec), 500 µl Buffer RPE (> 8000 g, RT, 2 min) and finally only centrifuged (full speed, RT, 1 min). RNA was eluted into a 1.5 ml tube by addition of 30 µl RNase-free water (full speed, RT, 1 min). Purified RNA was quantified on the NanoDrop and stored on ice for direct use or in the –80 °C freezer until library preparation.

2.2.7.2 cDNA synthesis

For cDNA synthesis, RNA was thawed on ice. 500 ng RNA were added to 1 µl random hexamer primer and adjusted to a volume of 12 µl with HPLC-water. Samples were denatured for 5 min at 65 °C. Then 4 µl 5× reaction Buffer were added as well as 1 µl Ribolock RNase Inhibitor, 2 µl of 10 mM dNTP Mix and 1 µl RrevertAid H Minus M-MuLV reverse transcriptase. The reaction was mixed and incubated at 25 °C for 5 min., then reverse transcription was carried out at 42 °C for 60 min and inactivation was performed at 70 °C for 5 min. The transcribed cDNA was stored in the –20 °C freezer or used directly in subsequent purpose.

2.2.7.3 Real-Time-Polymerase Chain Reaction (RT-PCR)

Gene expression was analyzed by real-time PCR in a HT 7900 RT-PCR instrument with TaqMan assays, containing a set of primers and a reporter (see Table 2.9, 2.10 and 2.11). All cDNA samples were diluted 1:10 in RNase-free water and run in triplicates according to the manufacturer's protocol. Briefly, for a single reaction 0.5 µl 20 × TaqMan Gene Assay, 5 µl 2 × TaqMan Gene Expression Master Mix, 2.5 µl RNase-free water were mixed together with 2 µl cDNA template and run in a 96-well plate format. The reaction was initiated by heating up to 50 °C for 2 min, 95 °C for 10 min, followed by 40 cycles of 95 °C for 15 sec and 60 °C for 1 min. In all assays the housekeeping gene tatabox binding protein (TBP) was used as the endogenous control. The gene expression of the genes of interest was calculated by $2^{-\Delta CT}$ and relative to TBP expression. Data analyses were performed with SDS 2.4 and RQ Manager 1.2.1.

2.2.8 Suppression assay

Suppression assays were prepared and carried out according to published protocols [190,191]. CD4+CD25– responder cells were harvested from non-pregnant mice and stimulated for proliferation. Then the ability to limit this proliferation was compared between CD4+CD25+ Treg from pregnant and virgin mice.
In order to enable distinction of the different cells types and in order to measure their proliferation the CD4+CD25− Tcon were stained with 4 µM eFluor670 dye. Therefore cells were centrifuged, counted and aliquoted in 2×10^7 cells per milliliter. eFluor670 was mixed 1:1 with the cell suspension. The mixture was incubated for 10 min at 37 °C. The staining was stopped by addition of complete RPMI, which was incubated for 5 min on ice. Afterwards cells were centrifuged at 300 rpm for 10 min and washed twice with complete RPMI. Then cells were counted and set to a concentration of 1×10^6 per ml.

Additionally, feeder cells were generated to ensure nourishment and antigen presentation in the cultures. Therefore one virgin mouse was anesthetized with the O_2/CO_2 mixture and killed by inhalation of pure CO_2. Its spleen was harvested with sterile instruments into ice-cold PBS. Cells were counted and set to a concentration of 30×10^6 spleenocytes in 900 µl HBSS media. 100 µl rabbit complement was added. Additionally 5 µl anti-CD90.2 antibody were added and incubated together for 30 min at 37 °C with mild agitation. The procedure was stopped by addition of 5 ml HBSS. Cells were centrifuged at 300 g for 10 min at 4 °C and afterwards taken up in 2 ml PBS for irradiation with 40 Gy. Afterwards cells were washed with 2 ml PBS and taken up again in 1 ml complete RPMI. Cells were counted and set to a concentration of 1×10^6 cells per ml. Subsequently the CD4+CD25+ Treg and the CD4+CD25– Tcon were both adjusted to 1×10^6 cells per ml and serial dilutions were carried out for the Treg populations. Cells were plated in 96-well plates with round bottom in descending ratios of Treg and Tcon: 1:1, 1:2, 1:4, 1:8, 1:16. Additionally feeder cells were added in an amount equal to the Tcon cell number. For stimulation anti-CD3 was added to each well at a final concentration of 1 µg/ml. The volume of each well was adjusted to a volume of 200 µl. Suppression assays were incubated at 37 °C for 72 hours. Then wells were harvested and stained with a dead cell staining dye to enable detection of living cells and with CD4-PE for CD4+ cell detection. Then cells were washed, taken up in 300 µl fluorescence-activated cell scanning buffer and measured via the flow cytometer running with Diva software for living cells, cell numbers and cell proliferation. Subsequent analyses were performed using FlowJo v10 software.

2.2.9 Flow cytometry staining

2.2.9.1 Identification of dead cells

Dead cells were identified by using a Fixable Dead Cell Staining Dye. It was used according to the manufacturer's protocol. Briefly, cells were washed twice before the staining with PBS (350 g, RT, 5 min) to remove soluble protein. Then cells were resuspended in PBS mixed with the staining diluent which is labeled with the Fixable Dead Cell Staining dye and incubated for 15 min at 4 °C in the dark. Subsequently cells were washed with PBS (350 g, RT, 5 min) and subjected to surface staining.

2.2.9.2 Surface staining

1×10^6 cells per staining reaction were transferred into a tube for fluorescence-activated cell scanning and were washed with 2 ml fluorescence-activated cell scanning buffer (350 g, RT, 5 min). Cells were resuspended in a master mix solution consisting of F_c receptor block and a cocktail of labeled antibodies of desired surface molecules (Table 2.16). Cells were stained at 4 °C for 30 min in the dark. Then cells were washed with PBS (350 g, RT, 5 min) and either resuspended in 200 µl fluorescence-activated cell scanning buffer for subsequent measurement on the fluorescence-activated cell scanning device and Diva software.

2.2.9.3 Staining for MACS check

MACS isolated immune cell suspensions were stained for flow cytometry measurements with CD4-Pacific Blue and Fc-Block for 30 min at 4 °C in the dark, washed with PBS, filtered and re-suspended in fluorescence-activated cell scanning buffer. Antibodies were usually diluted as indicated in Table 2.16. The cells were then measured on fluorescence-activated cell scanning device with Diva software.

2.2.10 Flow cytometer configurations

The flow cytometer was used with the detector setting shown in Figure 2.2 and Diva software.

Laser	Primary Fluorochrome	Detector	Dichroic Mirror	Bandpass Filter	Other Fluorochromes
488 nm (blue) Laser 1	Side Scatter	F		488/10	
	FITC *Alternative:* GFP	E	505 LP	530/30 513/17	Alexa Fluor 488, CFSE, YFP
	PE	D	550 LP	575/26	Cy3 (Icave: 13% excitation only)
	PE-TxRed	C	600 LP	610/20	PE-Dazzle594 PE-CF594
	PerCP-Cy5.5 *Alternative 1:* PerCP	B	685 LP 635 LP	695/40 670/14	PerCP-eFluor710
	PE-Cy7	A	735 LP	780/60	PE-Vio770
405 nm (violet) Laser 2	Pacific Blue	F		450/50	Alexa Fluor 405 Brilliant Violet 421 BD Horizon V450
	AmCyan	E	505 LP	525/50	BD Horizon V500 Brilliant Violet 510
	BV605	D	600 LP	610/20	
	BV650	C	630 LP	660/20	
	BV711	B	685LP	710/50	
	BV786	A	735LP	780/60	
633 nm (red) Laser 3	APC	C		660/20	Alexa Fluor 647 eFuor 660
	Alexa700	B	710 LP	730/45	
	APC-Cy7	A	755 LP	780/60	APC-eFluor780

Figure 2. 2 Flow cytometer configurations

Depicted detector configurations were used on the flow cytometer.

2.2.11 Flow cytometry gating strategies and cell identification

For purity analysis after MACS or as read out of suppression assays flow cytometry measurements were used. Lymph nodes and spleen or CNS were harvested, single cell suspensions prepared and desired cell populations were isolated via MACS and stained as described above or used in suppression assays. Immune cells sub-populations were identified by the following gating strategy (Fig. 2.3 and Fig. 2.4) on the fluorescence-activated cell scanning device and Diva software. Subsequent data analyses were performed with FlowJo v10 software and Graph Pad Prism 7.

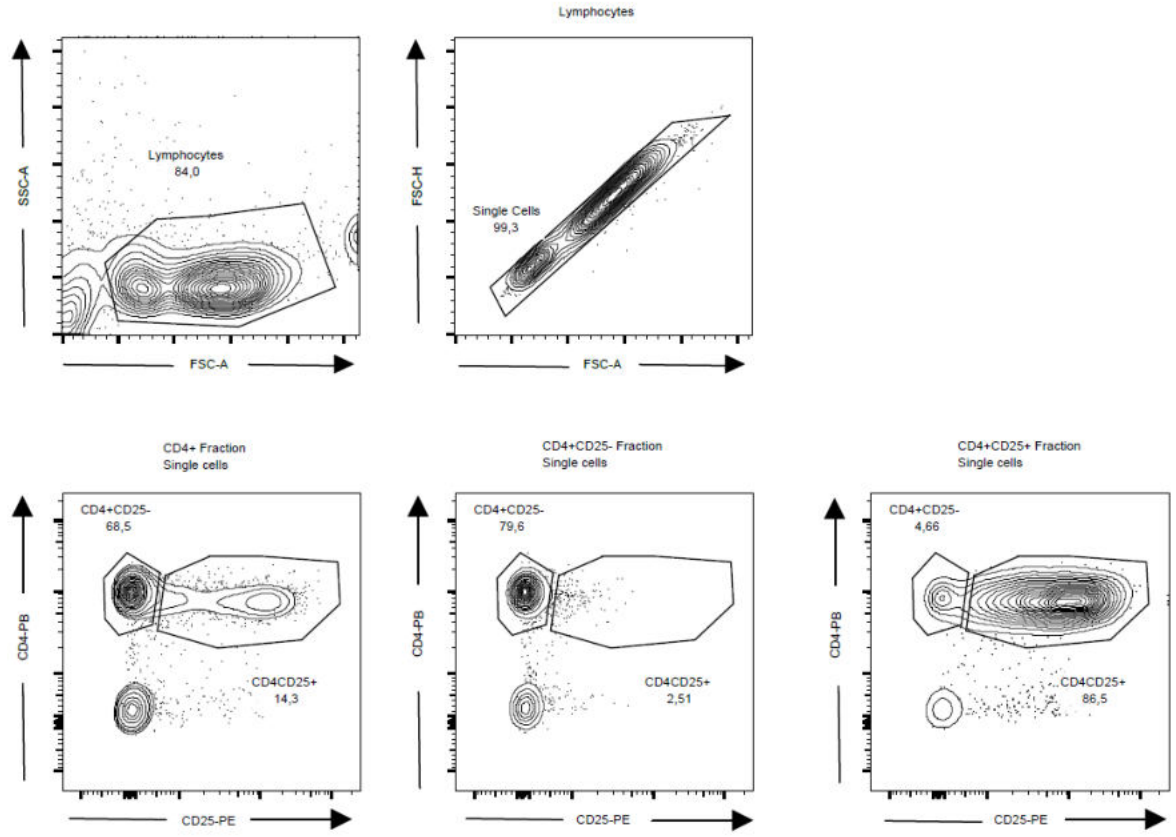

Figure 2. 3 Purity analysis after MACS isolation of CD4+CD25+ Treg and CD4+CD25− Tcon

Lymphocyte populations were identified according to their size and granularity (SSC and FSC). Doublets were excluded by plotting height against area of the forward scatter (FSC-H against FSC-A). Then cells were gated for CD4-PB+ and CD25-PE− populations or for and CD4-PB+ and CD25-PE+ populations to identify Tcon and Treg populations, respectively. Three different aliquots were taken during the cell isolation process (CD4+, CD4+CD25−, CD4+CD25+ fractions) (see section 2.2.6.1). Purity of MACS isolated CD4+CD25+ populations was routinely above 84%.

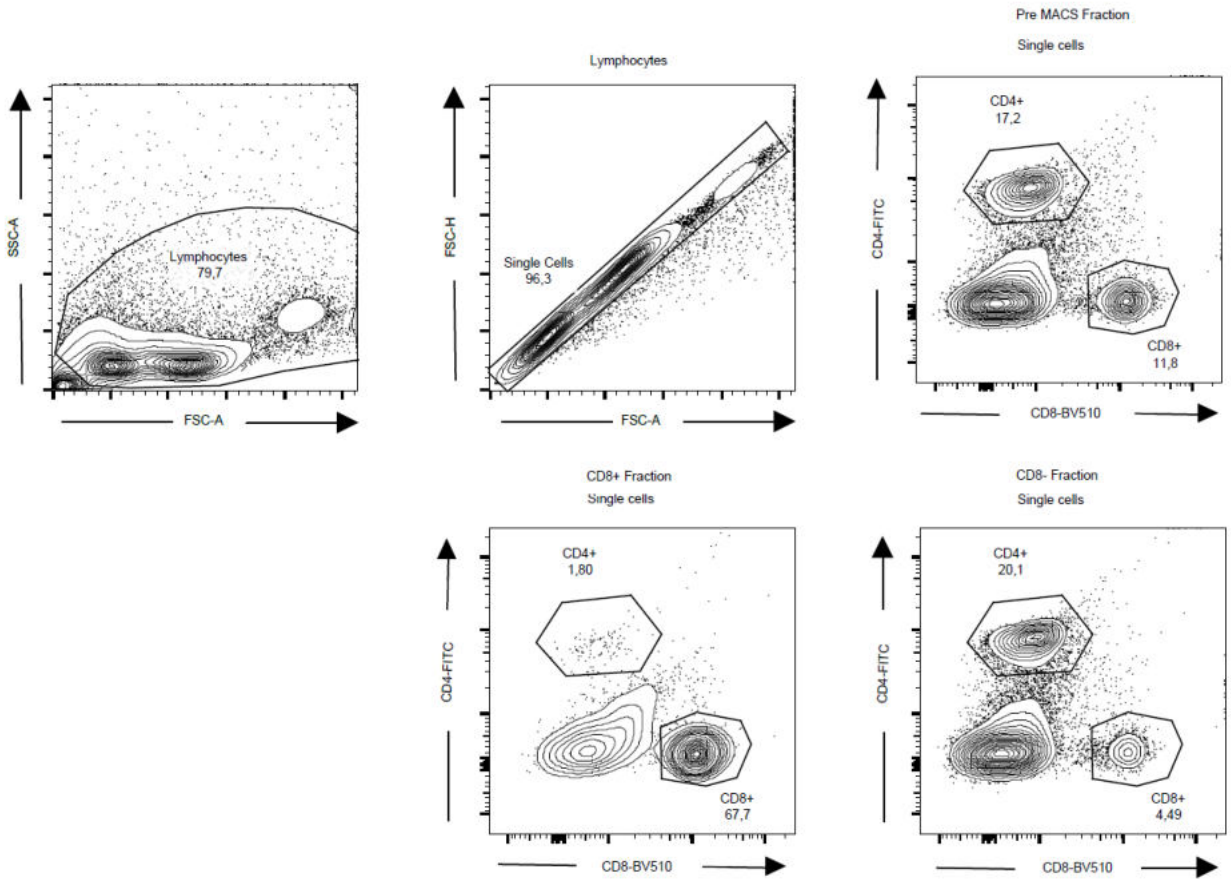

Figure 2. 4 Purity analysis after MACS depletion of CD8+ T cells

Lymphocyte populations were identified according to their size and granularity (SSC and FSC). Doublets were excluded by plotting height against area of the forward scatter (FSC-H against FSC-A). Then cells were gated for CD4-FITC+ and CD8a-BV510− populations or for CD4-FITC− and CD8a-BV510+ populations to identify CD4+ and CD8+ populations, respectively. One aliquot was taken before isolation (pre MACS) and two different aliquots were taken during the cell isolation process (CD8+, CD8− fractions) (see section 2.2.6.2). Purity of MACS isolated CD8− populations routinely contained less than 6% of CD8+ cells.

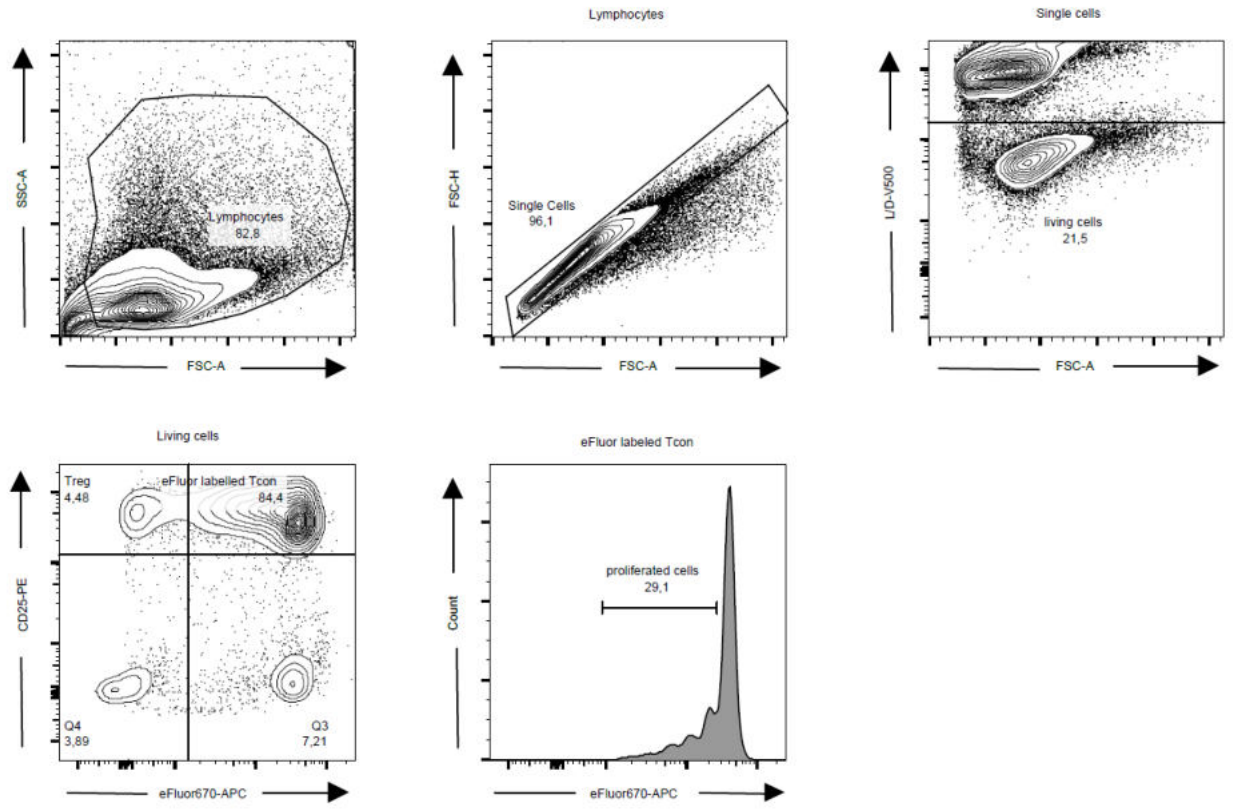

Figure 2. 5 Flow cytometry analysis of Treg suppression assays

Lymphocyte populations were identified according to their size and granularity (SSC and FSC). Doublets were excluded by plotting height against area of the forward scatter (FSC-H against FSC-A). Then cells were gated for dead cell dye-V500− against area of the forward scatter to identify living cells. Dead cells were stained with Fixable Dead Cell Staining Dye in V500, which leaves the living cells unstained. Then living cells were subdivided into either CD25-PE+ and eFluor670− populations (eFluor670 was detected with the APC filter in the APC channel) or into CD25-PE+ and eFluor670+ populations to identify Treg or Tcon, respectively. The percentage of proliferated eFlour670-labeled Tcon was analyzed.

2.2.12 Staining for fluorescence-activated cell sorting

Isolated immune cell suspensions from DEREG mice were stained for fluorescence-activated cell sorting with CD4-Pacific Blue and Fc-Block for 30 min at 4 °C in the dark, washed with PBS, filtered and re-suspended in PBS with EDTA (1:10000). The cells were used in fluorescence-activated cell sorting.

2.2.13 Fluorescence-activated cell sorting configurations

The fluorescence-activated cell sorter was used with the detector settings shown in Figure 2. 6 and Aria software.

Laser	Primary Fluorochrome	Detector	Dichroic Mirror	Bandpass Filter	Other Fluorochromes
488 nm (blue)	FITC *Alternative:* GFP	E	502	530/30 513/17	Alexa Fluor 488, CFSE, YFP
	PE	D	556	585/42	Cy3 (Icave: 13% excitation only)
	PE-TxRed	C	610	616/23	PE-Dazzle594
	PerCP-Cy5.5	B	655	695/40	PerCP-eFluor710?
	PE-Cy7	A	735	780/60	PE-Vio770
405 nm (violet)	Pacific Blue	F		450/50	Alexa Fluor 405 Brilliant Violet 421 BD Horizon V450
	AmCyan	E	502	510/50	BD Horizon V500 Brilliant Violet 510
	BrilliantViolet 605	D	600	610/20	
	BrilliantViolet 650	C	640	670/30	
	BrilliantViolet 711	B	685	710/50	
	BrilliantViolet 786	A	735	780/60	
633 nm (red)	APC	C		660/20	Alexa Fluor 647 eFluor 660
	Alexa700	B	690	730/45	
	APC-Cy7	A	755	780/60	APC-eFluor780

Figure 2. 6 Fluorescence-activated cell sorter configurations

Depicted detector configurations were used on the fluorescence-activated cell sorter running with Aria software.

2.2.14 Fluorescence-activated cell sorting

Cell suspensions were sorted into Tcon (CD4+ Foxp3–) and Treg (CD4+ Foxp3+) populations with the fluorescence-activated cell sorter device and Aria software. Collection tubes were coated with FCS and filled with complete RPMI medium (1% Penicillin Streptomycin, 0.1% β-mercaptoethanol) with 20% FCS. The isolated and stained cell suspensions were inserted into the device and sorted for following parameters: lymphocyte size in FSC-A and SSC-A gates, according to singularity in FSC-H and FSC-A gates, into CD4+Foxp3– and CD4+Foxp3+ cells according to CD4+ staining and DEREG-eGFP positivity of cells extracted from DEREG mice, which contain an eGFP sequence behind the promoter for the Foxp3 gene. Subsequently a purity check was performed to record pureness. Purity of sorted populations was routinely above 95%. Then cells were pelleted by centrifugation at 300 g for 10 min at 4 °C, dry frozen in liquid nitrogen and stored at –80 °C until DNA isolation. A sorting strategy was used as shown below.

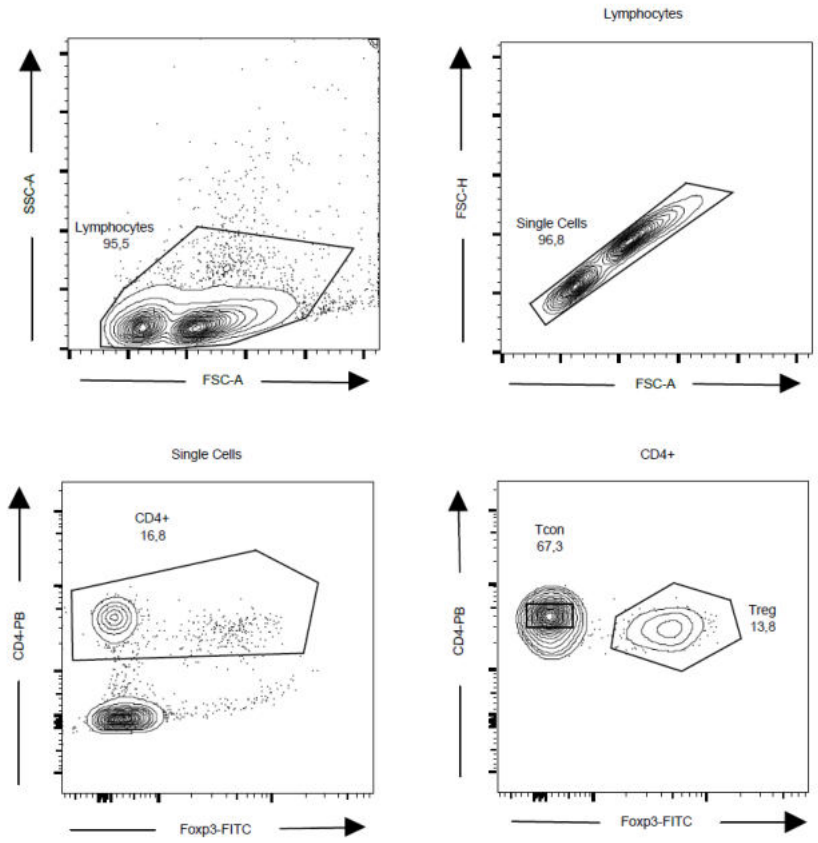

Figure 2. 7 Sorting strategy to isolate Tcon and Treg from DEREG mice

Lymphocyte populations were identified according to their size and granularity (SSC and FSC). Doublets were excluded by plotting height against area of the forward scatter (FSC-H against FSC-A). Cells were gated for CD4-PB+ and Foxp3-eGFP− lymphocyte populations (eGFP was detected with the FITC filter in the FITC channel). Then sorting into CD4-PB+ and Foxp3-eGFP– Tcon and CD4-PB+ Foxp3-eGFP+ Treg was performed. Purity of sorted populations was routinely above 95%.

2.2.15 Cell Mito Stress test

The Cell Mito Stress Test is used in order to analyze cellular mitochondrial respiration and glycolysis. It measures mitochondrial respiration via the O_2 consumption rate (OCR) and at the same time the extracellular acidification rate (ECAR), which provides a measure for the rate of conversion of pyruvate to lactate and is therefore a measurement of glycolysis. Both measurements are performed in parallel in the so-called Seahorse XFe96 analyzer. The assay was carried out according to the manufacturer's protocol. Briefly, cells of interest were plated in a special plate format, which is adjusted to the size of measuring sensors and well ports through which substances can be added. During the runtime of the assay substances can be added into the individual wells (Fig. 2.8 A and B), interfering with the electron transport chain (ETC). The machine mixes the substances in the well and measures OCR and ECAR in real-time via a sensor (Fig. 2.8 A and C). This sensor contains two fluorophores, one for O_2 and one for pH (Fig. 2.8 B and C). The sensor is lowered into the wells up to 200 microns above the cells and thereby creates a

transient micro chamber in which the measurements of oxygen concentration and pH can be accurately performed (Fig. 2.8).

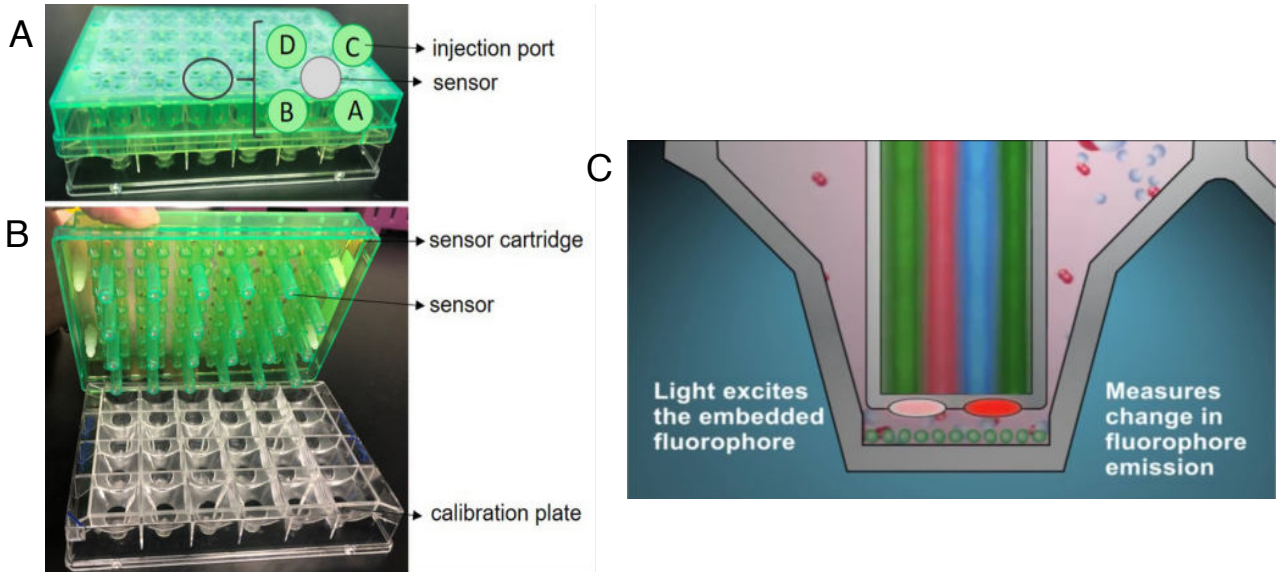

Figure 2. 8 Plates and sensors used for Cell Mito Stress Test

(**A**) Appearance of assay plate for Cell Mito Stress Test. (**B**) Special well format of lower plate and four injection ports (green) above one big well at the bottom (white). In between the injections ports there is the sensor (grey). Figure A and B taken from bio-protocol.org/e2850 (2019-01-29) (2019) [192]. (**C**) When the sensor is lowered into the bottom well it is building a micro chamber in the well plate. Figure taken from www.agilent.com (2019-01-21) (2019) [193].

This allows the measurement of basal respiration, ATP production-coupled respiration, H+ (Proton) leak, maximal and reserve capacities (spare respiratory capacity) and non-mitochondrial respiration. The proton leak, maximal respiration, and non-mitochondrial respiration, can be measured directly. The ATP-linked respiration and spare respiratory capacity are calculated using basal respiration and the other measured parameters [193].

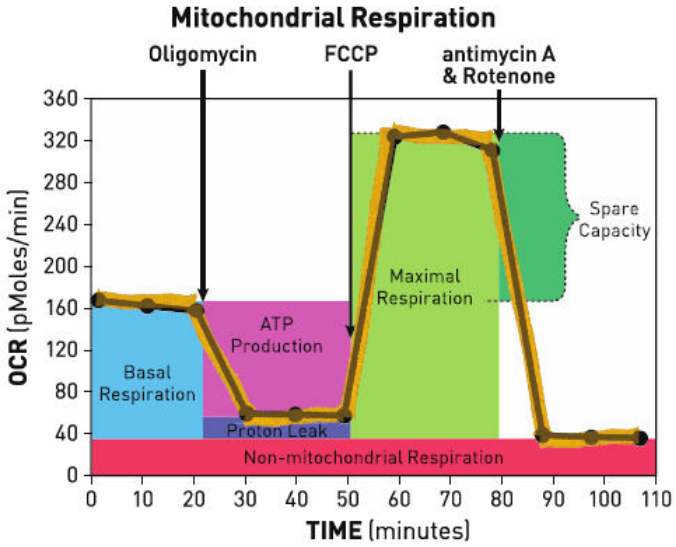

Figure 2. 9 Details on Mitochondrial Respiration measurements in the Cell Mito Stress Test

This test works via the addition of Oligomycin, FCCP, a mix of antimycin A and Rotenone to the desired cells, all interfering with the ETC and continuous measurements of the O_2 consumption rate (OCR). Figure taken from www.agilent.com (2019-01-21) (2019) [193].

Before starting the procedure the Assay Media had to be freshly prepared. Therefore glucose (final concentration: 25 mM per 100 ml), sodium pyruvate (final concentration: 1mM per 100 ml) and L-glutamine (final concentration: 2 mM per 100 ml) were added to the Seahorse XF base medium and were adjusted carefully to a pH of 7.4 using sodium hydroxide. Then the media was sterilized using a 0.2 µM-filter and warmed to 37 °C before use.

Since measurements can only be performed with adherent cells, suspension cells like lymphocytes need to be immobilized on the bottom of the well using the biological adherent Cell-Tak, an extract made from seashells. Therefore the special assay plates were coated one day before the assay. For this purpose 22.4 µg/ml of Cell-Tak, were mixed into a Sodium Bicarbonate Buffer that was set to pH 6.5 – 8.0 and filter sterilized. 1 M sodium hydroxide at half a volume of the used Cell-Tak was added and mixed. The coating solution was dispensed within 10 min after preparation into the wells of the XFe96 cell culture microplate, incubated for 20 in at room temperature, washed two times with Bicarbonate Buffer and set for air drying and storage at 4 °C overnight.

Also one day before the assay Sensor Cartridge and Utility Plate from the XFe96 flux assay kit were calibrated overnight with 200 ul Seahorse XF Calibrant in a non-CO_2 incubator.

On the assay-day, the compounds Oligomycin, FCCP and Rotenone with antimycin A were dissolved in pre-warmed XF Cell Mito Stress Test Assay Medium according to the manufacturer's protocol (Final well concentrations: Oligomycin 1.0 µM, FCCP 0.5 µM, Rotenone/antimycin A 0.5 µM). Next, the 4 ports of the XS Sensor cartridge were loaded with the different compounds, with one compound per port. Ports above wells for baseline measurement were not loaded. Background correction wells were loaded with assay media only.

Next, freshly MACS isolated Tcon and Treg, originally pooled from spleen and lymph node cells, were aliquoted in the desired cell amount (0.5×10^6 and 1×10^6 per well) and were centrifuged at room temperature at 200 g. Cells were taken up in the appropriate volume of pre-warmed media for at least three replicates per group and were seeded in the desired amounts onto the Cell-Tak coated microplates in order to adhere cells to the bottom of the wells. Background correction wells had to be filled with assay media only. Next, the microplate was centrifuged at room temperature at 200 g without brake for 1 min to spread the cells evenly in the wells. Next, the plate had to be transferred into a 37 °C incubator not supplemented with CO_2 for 25-30 min to ensure that the cells could completely sink down and attach to the well bottom. Afterwards, 130 µl of warm assay media had to be gently added and the microplate and all had to be incubated without CO_2 again for 15-25 min.

Next, the previously compound filled Sensor Plate was put on top of the Utility Plate from the overnight incubation with calibrant. On top of each other they are put into the XFe96 Analyzer device for calibration inside the machine. Afterwards only the lower Utility Plate, is exchanged for the microplate seeded with the desired cells. Then the assay was run with the adequate protocol as also recommended by the manufacturer. The settings are mix-wait-measure cycles with 3 min – 0 min – 3 min, with 3 basal measurements taken prior to the first port injection, leading to addition of the first compound, and 3 rate measurements taken after each injection.

At the beginning, the basal respiration is measured when no additional compound has yet been added to the wells, and the mitochondrial ETC was working as usual for the cell population (Fig. 2.9). Then Oligomycin was added through the first port into the wells of the lower plate. Oligomycin is a blocker of complex five of the ETC and therefore the ETC was forced to stop. Therefore the following mix-wait measure cycle measured the slowing down of the ATP production that is still possible without action of the complex five, and also the proton leak, when no ATP production is taking place any more (Fig. 2.9). Comparing the basal respiration with the proton leak, the actual ATP production of the cells can be calculated. Next, FCCP was added through another port into wells. FCCP produces a H^+ gradient shortcut into the mitochondrial membrane. Therefore H^+ Ions can pass through this hole in the membrane making H^+ available inside the mitochondrion to produce ATD from ADP. Therefore here the maximal respiration could be measured (Fig. 2.9). Subtracting the basal respiration from the measured maximal respiration one can get the spare respiratory capacity (SPC), a spare energy reserve available to a cell in a situation of increased stress or work [165]. This can be important for long-term survival and function of the cells. As a third compound rotenone and antimycin A were added to the wells. These substances are blockers of complex one and three of the ETC. By blocking them no H^+ Ions can be transported out of the mitochondrion. Inside the mitochondrial matrix too many H^+ gather, therefore NADH can hardly be oxidized to NAD^+ any more, as H^+ are everywhere. Therefore the whole ETC comes to a stop and eventually the cells die because their energy supply system broke down (Fig. 2.9).

These metabolism measurements were performed in Tcon and Treg extracted via the MACS isolation method (see 2.2.6.1) from pregnant and virgin animals. The assays were conducted either with manufacturer's media and 0.5×10^6 cells or with fatty acid media, which was homemade (as shown in Table 2.13) and 1×10^6 cells per well. Using these high cell numbers often meant pooling several animals in order to reach the high numbers. Per animal about 0.5×10^6 Treg can be extracted.

Subsequent data analyses were performed with the desktop version of the Wave 2.2.0 software for XFe96 Analyzer and additionally with Graph Pad Prism 7. Statistical analysis was performed with Graph Pad

Prism 7 and individually per phase of Cell Mito Stress Test (baseline measurements, ATP production phase, maximal respiration phase, ETC stop phase).

2.2.16 Isolation of genomic DNA

Dry frozen pellets were thawed on ice and DNA was isolated according to the manufacturer's protocol of the AllPrep DNA/RNA Micro kit. Briefly, cells were resuspended in 350 µl Lysis Buffer consisting of RLT-Buffer mixed with β-mercaptoethanol (1:100). The lysate was pipetted into QIAshredder spin columns to disrupt the lysate completely. DNA and RNA fractions were separated by centrifugation (> 8000 g, RT, 30 sec).

The column containing the DNA was stored at RT for later DNA purification while the flow-through was used for direct RNA purification in a new tube. An equal volume of 70% ethanol was added to the flow-through and mixed well by pipetting up and down and was transferred into an RNAeasy MinElute spin column and centrifuged (> 8000 g, RT, 15 sec). Subsequently samples were consecutively washed with 700 µl Buffer RW1 (> 8000 g, RT, 15 sec), 500 µl Buffer RPE (> 8000 g, RT, 15 sec), 500 µl Buffer RPE (> 8000 g, RT, 15 sec). For purification 500 µl of 80% ethanol were added (> 8000 g, RT, 2 min) and finally only centrifugation (full speed, RT, 5 min). RNA was eluted into a 1.5 ml tube by addition of 14 µl RNase-free water, which was incubated in the column for 3 min before centrifugation (full speed, RT, 1 min). Purified RNA was quantified on a Qubit 3 Fluorometer and stored in the –80 °C freezer until further use.

Then genomic DNA was purified. Samples were washed from the set aside AllPrep DNA column with 500 µl Buffer AW1 (> 8000 g, RT, 15 sec), 500 µl Buffer AW2 (full speed, RT, 2 min) and finally only centrifugated (full speed, RT, 1 min). DNA was eluted into a 1.5 ml tube by addition of 30 µl EB Buffer that was preheated to 70 °C. This was incubated at RT for 5 min and then centrifuged (> full speed, RT, 1 min). Again 30 µl EB Buffer were added and incubated at RT for 5 min and then centrifuged (> full speed, RT, 1 min) to reach a total volume of 60 µl purified DNA. Purified DNA was quantified on a Qubit 3 Fluorometer and stored at –80 °C until library preparation.

Isolation of genomic DNA as described in 2.2.16 was performed by Dr. Jan Jäger, research assistant at INIMS.

2.2.17 Library preparation and TCR-sequencing

The amplification of the TCRβ gene rearrangements (also called library preparation) was performed by HS Diagnomics (Berlin) using 100 ng input DNA per sample and a combination of specific primers for amplification of all IGMT-listed mouse V/J segments. In a second PCR step universal Illumina adapter sequences including additional barcodes were added to the generated TCRβ amplicons. To prevent and/or to identify carry-over contaminations the K-box method was utilized, which is a series of three synergistically acting short sequence elements [194]. Amplicon sequencing was performed at the

Transcriptome and Genome Analysis Laboratory (Universitätsmedizin Göttingen) on the MiSeq platform generating 0.5 -1×10^6 paired-end reads (2 × 150 bp) per sample.

2.2.18 TCR-sequencing analysis

Productive TCR β rearrangements were extracted from fastq files using mixcr 2.1.10 [195] with standard parameters. Down-stream analysis was performed with VDJtools 1.1.8 [196] and custom R scripts. As a metric for skewing of the TCR repertoire by clonal expansion the metric 'clonality' was used, defined as (1–normalized Shannon Wiener Index). Clonality values approaching 0 indicate a very even distribution of clonotype abundances, whereas values approaching 1 indicate an increasingly asymmetric distribution in which a few clonotypes are present at high frequencies. Usage of TRBV and TRBJ segments was calculated by using the VDJtools function 'CalcSegmentUsage' and pairing of V and J segments in representative samples was visualized in circus plots via 'PlotFancyVJUsage'. Data set wide similarity of CDR3aa sequence usage was assessed by calculating the pairwise overlap between samples by 'CalcPairwiseDistances' with standard parameters. Pairwise distances were projected into a 2D plane by multidimensional scaling (MASS package) and color-coded by experimental condition. Overlap between peripheral and CNS samples was calculated and visualized using the VDJtools function 'OverlapPair' with standard parameters. The color-coding was extended to the top 100 clonotypes (default is 20). EAE clonotypes were required to be present in at least two of three analyzed CNS samples (see Fig. 3.18 B in results part). Tracking of EAE clonotypes in independent data sets were performed on the level of CDR3aa sequence and quantified as cumulative abundance within each sample. All plots were either generated by VDJtools, GraphPad Prism 7 or the R package ggplot2.

All bioinformatic processing of the TCR-sequencing data as described in 2.2.18 was performed by Dr. Dr. Jan Broder Engler, bioinformatician at INIMS. Analysis and visualization of the data were performed in cooperation with Dr. Dr. Jan Broder Engler.

2.2.19 Statistical analysis

Statistical analysis was performed with Graph Pad Prism 7. Data were shown as mean values ± SEM. *N* values refer to the number of biological replicates. Differences between two groups were determined by unpaired Student's *t* tests. Comparisons between three or more groups were performed by two-way ANOVA with Sidak's post hoc test. Significant results are indicated by asterisks *$P < 0.05$; **$P < 0.01$.

2.2.20 Data availability

Data generated for the TCR-sequencing part of this study are available through the Gene Expression Omnibus (GEO) [197] under accession number GSE122894.

3. Results

3.1 Suppressive capacity of Treg from virgin and pregnant mice

Suppressive capacity – hindering Tcon in their proliferation, by means of direct and indirect contact – is the most important function of a Treg and is of particular importance during pregnancy and autoimmunity. Several aspects imply that an increased suppressive potential is ensured during pregnancy.

To explore Treg functionality, the overall suppressive capacity of Treg to limit Tcon proliferation was analyzed. Treg extracted from virgin and pregnant mice were analyzed in parallel suppression assays and their functionality was compared.

Treg extracted from virgin and pregnant mice were isolated via the MACS method. Responder Tcon cells were isolated equally, but in all cases from non-pregnant mice, to rule out an effect of pregnancy on Tcon as a potential confounder. Tcon were stained with eFluor670 to assess their proliferation. Both immune cell types were mixed in the well plates with descending ratios of Treg (1:1, 1:2, 1:4, 1:8, 1:16, 0:1) and with constant Tcon numbers. The mix was stimulated with anti-CD3 and feeder cells for co-stimulation and kept in the incubator for 72 hours before analysis.

Treg originating from pregnant animals did not show a higher capability of overall suppression of Tcon proliferation than Treg from non-pregnant animals did ($P = 0.9784$ for % proliferated cell, $P = 0.4550$ for relative proliferation). Instead suppressive capacity of Treg was found to be comparable in the virgin and pregnant state (Fig. 3.1).

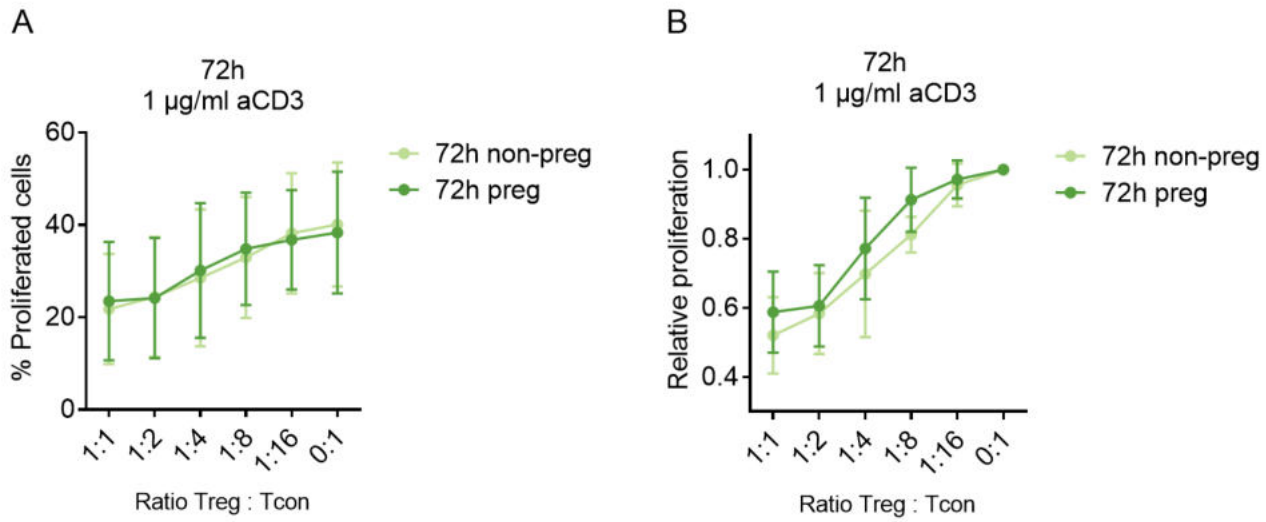

Figure 3. 1 Suppressive capacity of Treg is alike in virgin and pregnant mice

Suppressive capacity shown in (**A**) as % proliferated cells or in (**B**) as relative proliferation normalized to the 0:1 Tcon:Treg ratio. Measurements were performed with Treg extracted from pregnant mice (dark green lines) and Treg extracted from non-pregnant mice (light green lines). Tcon were extracted in all cases from non-pregnant mice ($n = 3$ biological replicates per group). Assays were measured 72 h after cultivation of Tcon and Treg together with feeder cells and anti-CD3. Tcon were plated in constant numbers, Treg were plated in descending ratios (1:1, 1:2, 1:4, 1:8, 1:16, 0:1). Data are presented as mean values ± SEM. Statistical analysis was performed by two-way ANOVA with subsequent Sidak's multiple comparison post hoc test. *$P < 0.05$; **$P < 0.01$.

3.2 Immunometabolism in Tcon and Treg from virgin versus pregnant mice

Immunometabolism has been shown to be crucial in manifesting a cellular fate, to induce a change of cell identity and in some cases to render cells more potent than others. Such an advantage of functionality could supposedly be a mechanism rendering more potency also to Treg during pregnancy. In order to cautiously approach immunometabolism in Treg during pregnancy a validation of already existing microarray data, carried out by Dr. Dr. Jan Broder Engler at INIMS, pointing towards increased immunometabolism was performed first. Measurements of mitochondrial DNA followed and subsequently immunometabolism experiments in Treg extracted from pregnant animals were carried out.

3.2.1 Validation of differential gene expression in Tcon and Treg from virgin versus pregnant mice

Functionality of a cell is essentially influenced by the genes, which encode the necessary information to build up proteins needed for the fulfillment of particular functions. Different environmental circumstances can have influence on which genes are translated and transcribed at particular times. Previously generated microarray data were available, showing differences in gene expression patterns in Treg extracted from pregnant or virgin mice. The microarray showed a number of genes to be down regulated with pregnancy

and only few genes to be upregulated during pregnancy, among them IL-7r, Cables1 and Cpt1a. In order to confirm these upregulated genes, RT-PCR experiments were performed as a validation. The relative gene expression of IL-7r, Cables1 and Cpt1a was checked in Tcon and Treg taken from non-pregnant (E0) and pregnant (E18.5) mice, as well as from mice that had been pregnant, had delivered and were at post partum day 5 (PP5).

Expression of the genes Il-7r, Cables1 and Cpt1a was found to be increased with pregnancy in Treg (Il-7r: $P = 0.0027$; Cables1: $P < 0.0001$; Cpt1a: $P = 0.0458$) and similarly to be decreased again after pregnancy (Il-7r: $P = 0.0005$; Cables1: $P = 0.0007$; Cpt1a: $P = 0.0148$) (Fig. 3.2). This was true for the Treg samples and in a similar but slightly milder pattern also for the Tcon samples (Cables1: $P = 0.0006$) (Fig. 3.2). Therefore the differentially regulated gene expression in pregnancy shown by the available microarray analysis was validated via RT-PCR.

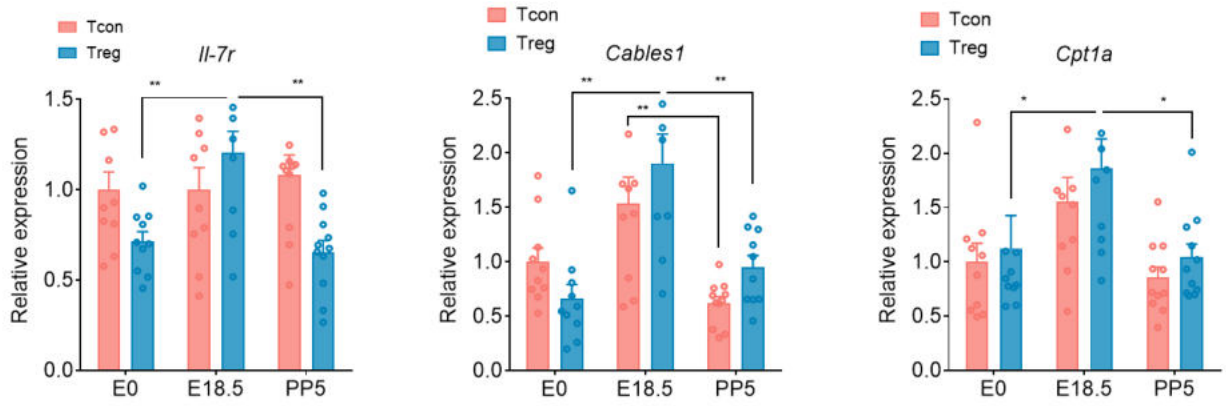

Figure 3. 2 Expression of IL-7r, Cables1 and Cpt1a over the course of pregnancy by RT-PCR

Used Tcon and Treg were extracted from virgin (E0) or pregnant (E18.5) mice, or from mice at post partum day 5 (PP5) ($n = 10$ biological replicates per group). Data are presented as mean values + SEM. Statistical analysis was performed by two-way ANOVA with subsequent Sidak's multiple comparison post hoc test $*P < 0.05$; $**P < 0.01$.

From what is known so far about most of these genes, some of them seem to have a very obvious influence onto Treg functionality e.g. Il-7r. Il-7r (Interleukin-7 receptor, also known as CD127) is an important mediator in T cell proliferation, differentiation and activation [60]. Further it has a crucial role in VDJ recombination during lymphocyte development [198]. Cables1 (Cdk5 and Abl enzyme substrate 1) is involved as a negative regulator in cell cycle progression and as a proliferation determinant. It had also been shown to be involved in Cushing disease. In a healthy state human CABLES1 inhibits proliferation to antagonize proliferation mediated by glucocorticoids (GCs) [199]. Therefore Cables1 has important influence onto immune cell proliferation, but rather negatively influences cell proliferation than promoting it. Therefore Cables1 was assessed to rather not be causal for increased Treg function.

However, Cpt1a is known to play an important role in cellular metabolism. It is the only mitochondrial enzyme responsible for catalyzing the transfer of a specific fatty acid group into the mitochondrion. Once this fatty acid is transported into the mitochondrial matrix via Cpt1a it is available for further use in fatty acid oxidation (FAO) and oxidative phosphorylation (OXPHOS). Therefore it is part of the multistep process of acid break down to produce energy for the cell [200]. Metabolism constitutes a fundamental

function of each cell to survive and to be able to fulfill its function. This rendered Cpt1a as a relevant player possibly causing an increase in Treg metabolic functionality.

Taken together previously available microarray data was validated via RT-PCR measurements and in particular validation of Cpt1a upregulation during pregnancy supported the assumption that metabolism is altered in Treg in the pregnant state.

3.2.2 Relative mitochondrial DNA content in Treg extracted from virgin versus pregnant mice

To further confirm a change in metabolism of Tcon and Treg during pregnancy mitochondrial DNA (mtDNA) expression was assessed. Therefore copy number assays were performed on Tcon and Treg extracted from non-pregnant or pregnant animals. DNA of these cells was isolated and used in RT-PCR set up. Comparisons of the relative DNA content of the mitochondrial encoded gene cytochrome C oxidase subunit 2 (COX II) and the nuclear encoded β actin gene were performed.

Results showed a trend towards a relatively higher mitochondrial DNA content in Treg from pregnant origin compared to non-pregnant Treg (Fig. 3.3). The mitochondrial DNA content of Tcon was found to be unchanged by pregnancy. These findings further support the microarray and RT-PCR results indicating tendency towards a change of metabolism in Treg in the pregnant state.

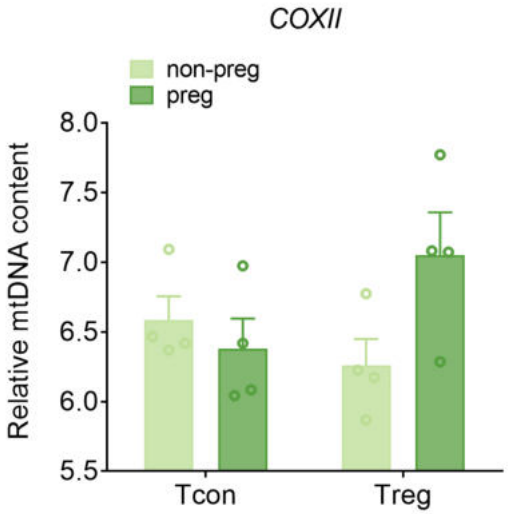

Figure 3. 3 Relative mtDNA content in Tcon and Treg extracted from virgin versus pregnant mice

RT-PCR measurements of relative mitochondrial DNA content, performed on mitochondrial encoded COX II gene and nuclear encoded β actin performed on Tcon and Treg extracted from pregnant and non-pregnant animals ($n = 4$ biological replicates per group). Data are presented as mean values + SEM. Statistical analysis was performed by two-way ANOVA with subsequent Sidak's multiple comparison post hoc test. *$P < 0.05$; **$P < 0.01$.

3.2.3 Immunometabolism measurements in Tcon and Treg extracted from virgin versus pregnant mice

Several aspects indicating a pregnancy-mediated increase of metabolism in Treg have been identified. Immunometabolism has been shown to be essential in determining a cellular phenotype, to mediate a change of cell fate and also in conveying increased functionality to cells. Thus, immunometabolism measurements of Treg were assessed as a function crucial to Treg.

Assays were performed from Tcon and Treg extracted from pregnant and non-pregnant animals. Cells were isolated in parallel via the MACS method and were referred to the immunometabolism measurements.

Cell Mito Stress Test assays were conducted with manufacturer's 'Seahorse' media and 0.5×10^6 cells per assay well (Fig. 3.4, Fig. 3.5 and Fig. 3.6) to measure mitochondrial respiration (OXPHOS) as well as extracellular acidification rate (ECAR, as a measurement of glycolysis) of Tcon and Treg extracted from virgin or pregnant female mice. Measurements were repeated with self made fatty acid adjusted media (Table 2.13) and higher cell numbers of 1×10^6 cells per assay well (Fig. 3.7, Fig. 3.8 and Fig. 3.9) to enable and further stimulate the analyzed cells to use fatty acids as energy source and to work out usage of aerobic OXPHOS pathway.

OCR measurements with both media and with both immune cell amounts from pregnant versus non-pregnant conditions started at slightly different levels of basal respiration (Fig. 3.4 A, Fig. 3.5 A: comparing non-pregnant and pregnant Treg $P = 0.0115$, comparing Tcon and Treg in the pregnant status $P = 0.0094$, Fig. 3.7 A and Fig. 3.8 A). After the addition of Oligomycin, when ATP production is measured, all Tcon and Treg groups showed a similar decrease of ATP production (Fig 3.4 A, Fig. 3.5 B, Fig. 3.7 A and Fig. 3.8 B). After the addition of FCCP maximal respiration is measured. The Tcon groups with cells of both virgin and pregnant origin showed a higher increase in their maximal respiration than the Treg groups of both virgin and pregnant origin did (Fig. 3.4 A, Fig 3.5 C: comparing Tcon and Treg in the non-pregnant status $P = 0.0043$ and in the pregnant status $P = 0.0013$, Fig. 3.7 A and Fig. 3.8 C). Tcon were high in maximal respiration and Treg were comparably low. Pregnancy did neither increase nor decrease an effect of the cell type. After final addition of rotenone and antimycin A Tcon and Treg respiration comes to stop (Fig. 3.4 A, 3.5 D, Fig. 3.7 A and Fig. 3.8 D).

During the glycolysis (ECAR) measurements with both media and with both immune cell amounts Tcon and Treg behaved overall similar to the OCR measurements (Fig. 3.4 B and 3.7 B). All different cell groups started at more widely spread ECAR baseline measurements (Fig. 3.4 B, Fig. 3.6 A, Fig. 3.7 B and Fig. 3.9 A). After the addition of Oligomycin, all Tcon and Treg groups showed a similar increasing ECAR behavior with manufacturer's media (Fig. 3.4 B, Fig. 3.6 B). Among the fatty acid media measurements all groups were stable or increased in both Treg groups (Fig. 3.4 B, Fig. 3.6 B, Fig. 3.7 B and Fig. 3.9 B: comparing Tcon and Treg in the non-pregnant status $P = 0.0221$, comparing non-pregnant and pregnant Treg $P = 0.0240$). After the second assay stimulus (with FCCP) the Tcon showed a trend towards a higher ECAR, regardless of the pregnancy status (Fig. 3.4 B, Fig. 3.6 C: comparing Tcon and Treg in the non-pregnant status $P = 0.0438$, Fig. 3.7 B and Fig. 3.9 C). After final addition of rotenone and antimycin A Tcon and Treg ECAR came to stop (Fig. 3.4 B, Fig. 3.6 D: comparing Tcon an Treg populations in the non-pregnant status $P = 0.0288$, Fig. 3.7 B and Fig. 3.9 D).

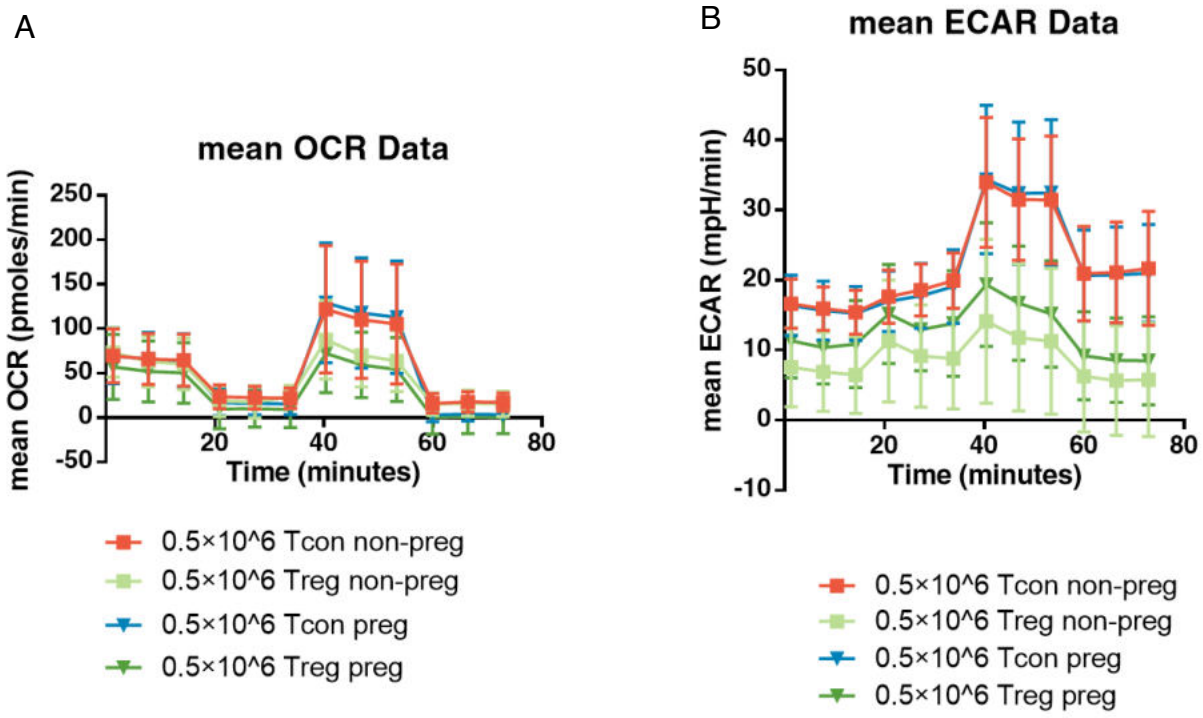

Figure 3. 4 Immunometabolism measurements with manufacturer's media show OXPHOS and glycolysis to be increased in Tcon, independent of the pregnancy status

(**A**) O_2 consumption rate (OCR) and (**B**) extracellular acidification rate (ECAR) measurements performed on Tcon and Treg from non-pregnant versus pregnant mice. Measurements were performed on 0.5×10^6 cells per well, using manufacturer's medium, (n = 4 biological replicates per group). Data are presented as mean values ± SEM. Statistical testing was performed by two-way ANOVA with subsequent Sidak's multiple comparison post hoc test per separated Cell Mito Stress Test phase (Fig. 3.5 and Fig. 3.6) with *$P < 0.05$; **$P < 0.01$.

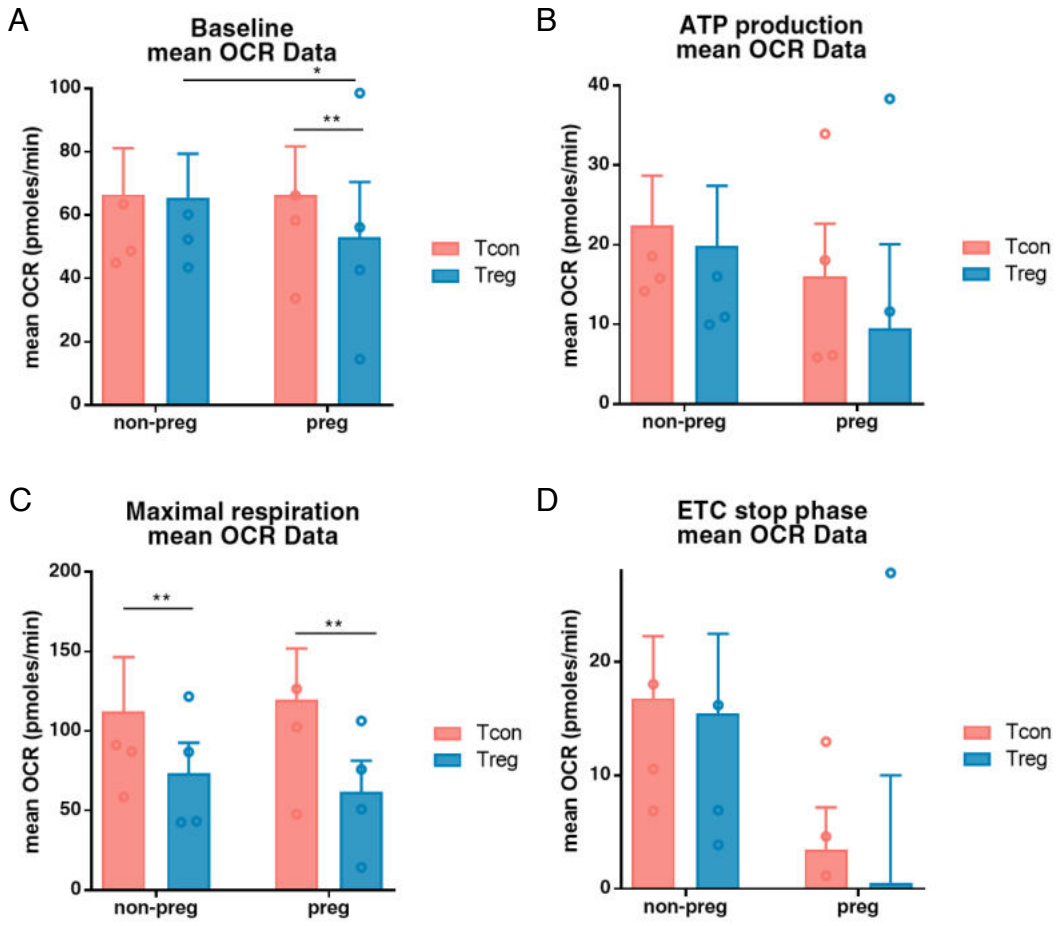

Figure 3. 5 OCR measurements with manufacturer's media, separated by measurement phases

OCR data as shown in Fig. 3.4 but separated by Cell Mito Stress Test measurement phases (Fig. 2.7): (**A**) baseline measurements, (**B**) ATP production phase, (**C**) maximal respiration phase, (**D**) ETC stop phase, in order to perform statistical analysis. Measurements were performed on 0.5×10^6 cells per well, using manufacturer's medium, ($n = 4$ biological replicates per group). Data are presented as mean values + SEM. Statistical analysis was performed by two-way ANOVA with subsequent Sidak's multiple comparison post hoc test. *$P < 0.05$; **$P < 0.01$.

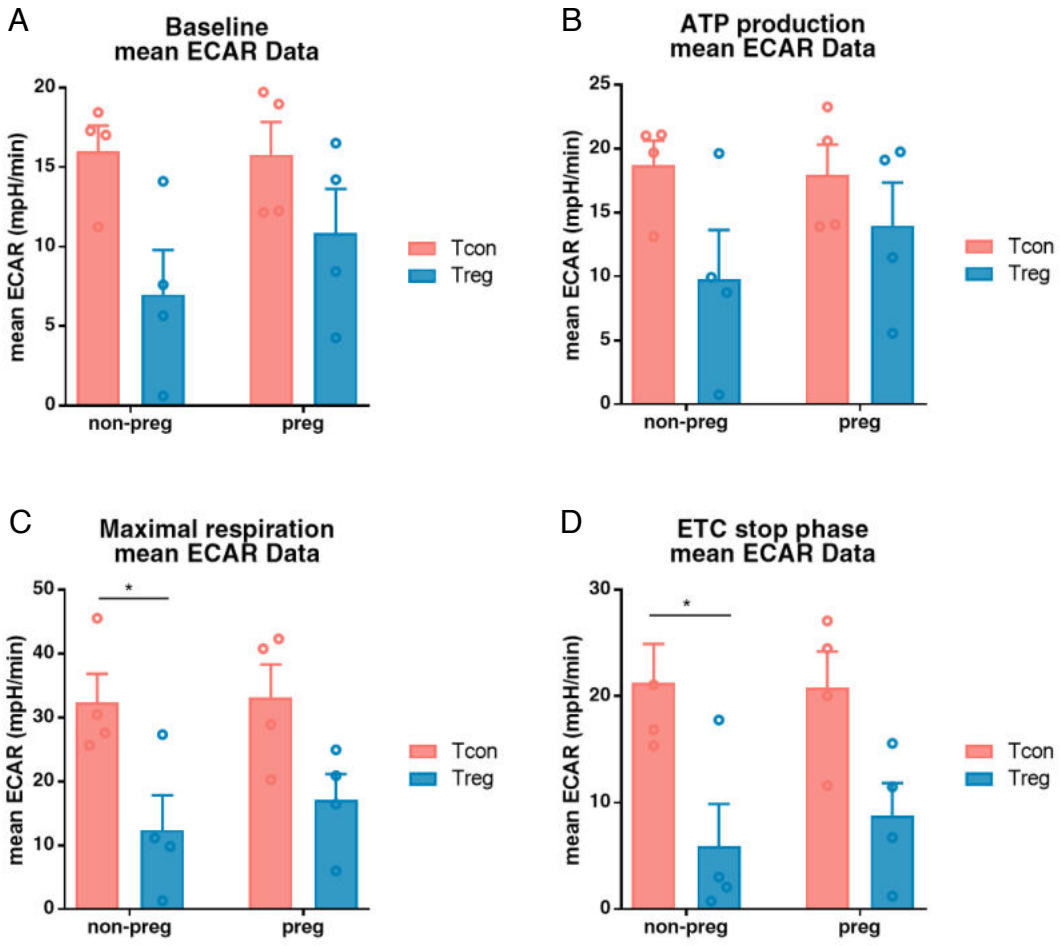

Figure 3. 6 ECAR measurements with manufacturer's media, separated by measurement phases

ECAR data as shown in Fig. 3.4 but separated by Cell Mito Stress Test measurement phases (Fig. 2.7): (**A**) baseline measurements, (**B**) ATP production phase, (**C**) maximal respiration phase, (**D**) ETC stop phase, in order to perform statistical analysis. Measurements were performed on 0.5×10^6 cells per well, using manufacturer's medium, ($n = 4$ biological replicates per group). Data are presented as mean values + SEM. Statistical analysis was performed by two-way ANOVA with subsequent Sidak's multiple comparison post hoc test. *$P < 0.05$; **$P < 0.01$.

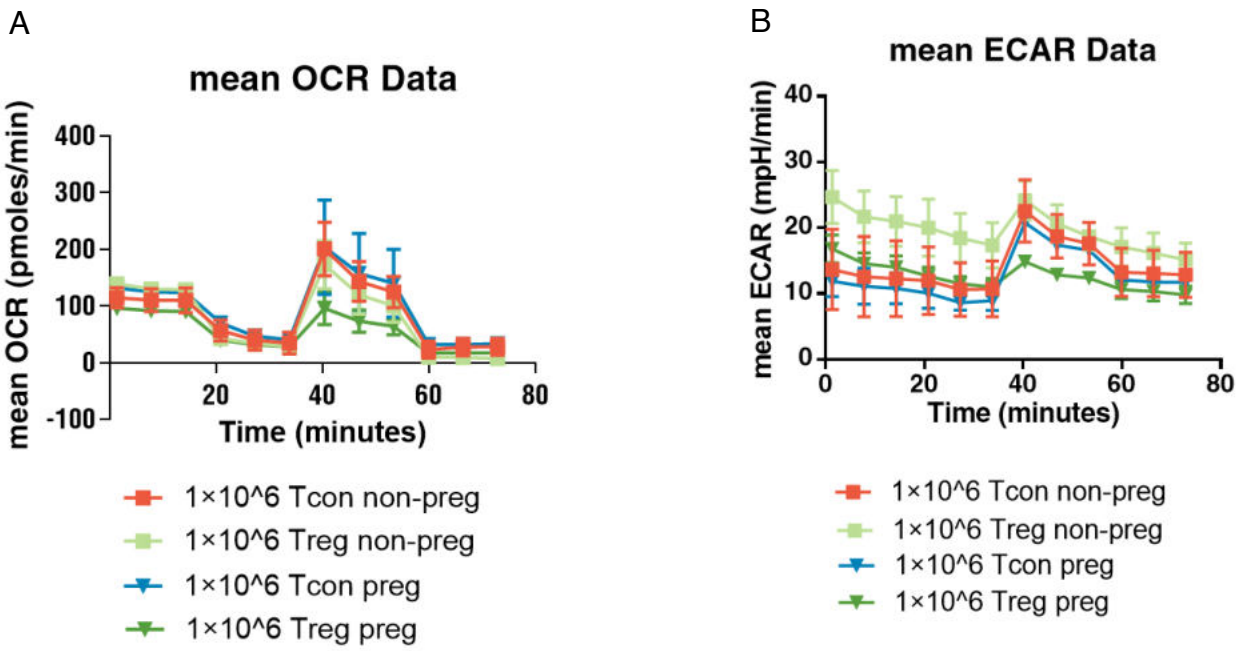

Figure 3. 7 Immunometabolism measurements with fatty acid media show a trend for OXPHOS and glycolysis to be increased in Tcon, independent of the pregnancy status

(**A**) O_2 consumption rate (OCR) and (**B**) extracellular acidification rate (ECAR) measurements performed on Tcon and Treg stemming from non-pregnant versus pregnant mice. Measurements were performed on 1×10^6 cells per data point, using self-made fatty acid medium ($n = 2$ biological replicates per group). Data are presented as mean values ± SEM. Statistical analysis was performed by two-way ANOVA with subsequent Sidak's multiple comparison post hoc test per separated Cell Mito Stress Test phase (Fig. 3.8 and Fig. 3.9) with. $*P < 0.05$; $**P < 0.01$.

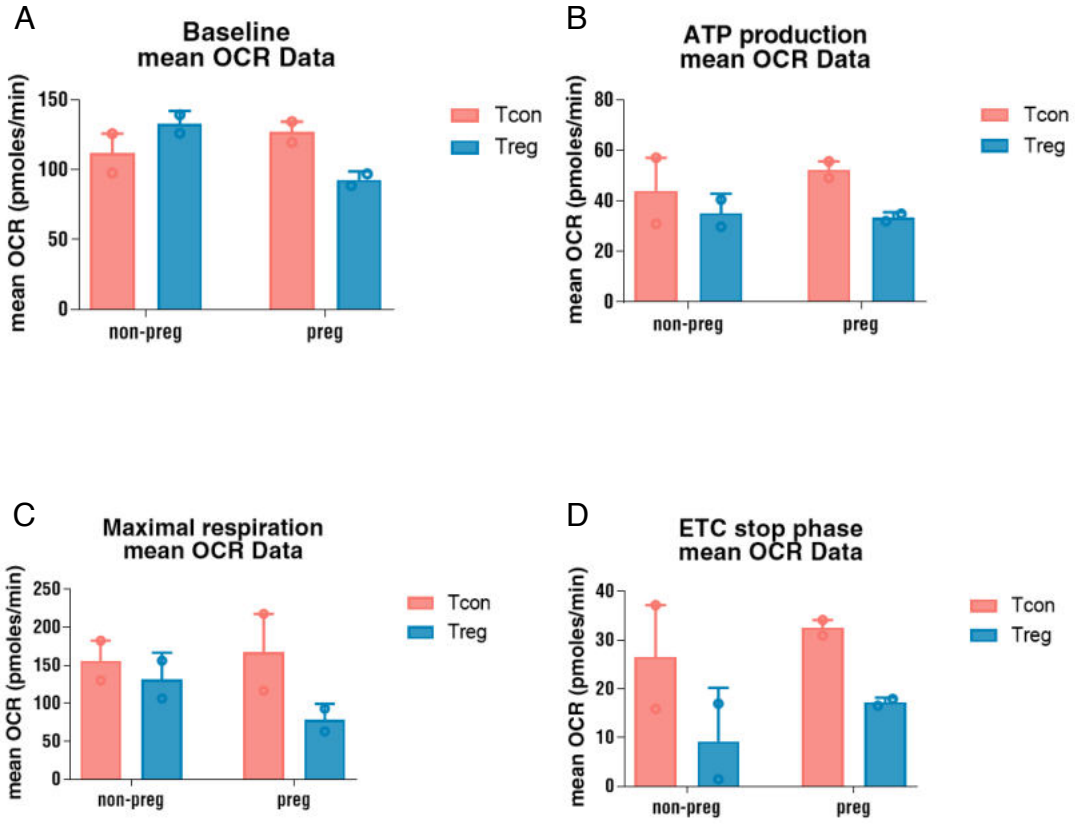

Figure 3. 8 OCR measurements with fatty acid media, separated by measurement phases

OCR data as shown in Fig. 3.7 but separated by Cell Mito Stress Test measurement phases (Fig. 2.7): (**A**) baseline measurements, (**B**) ATP production phase, (**C**) maximal respiration phase, (**D**) ETC stop phase, in order to perform statistical analysis. Measurements were performed on 1×10^6 cells per data point, using self-made fatty acid medium ($n = 2$ biological replicates per group). Data are presented as mean values + SEM. Statistical analysis was performed by two-way ANOVA with subsequent Sidak's multiple comparison post hoc test. *$P < 0.05$; **$P < 0.01$.

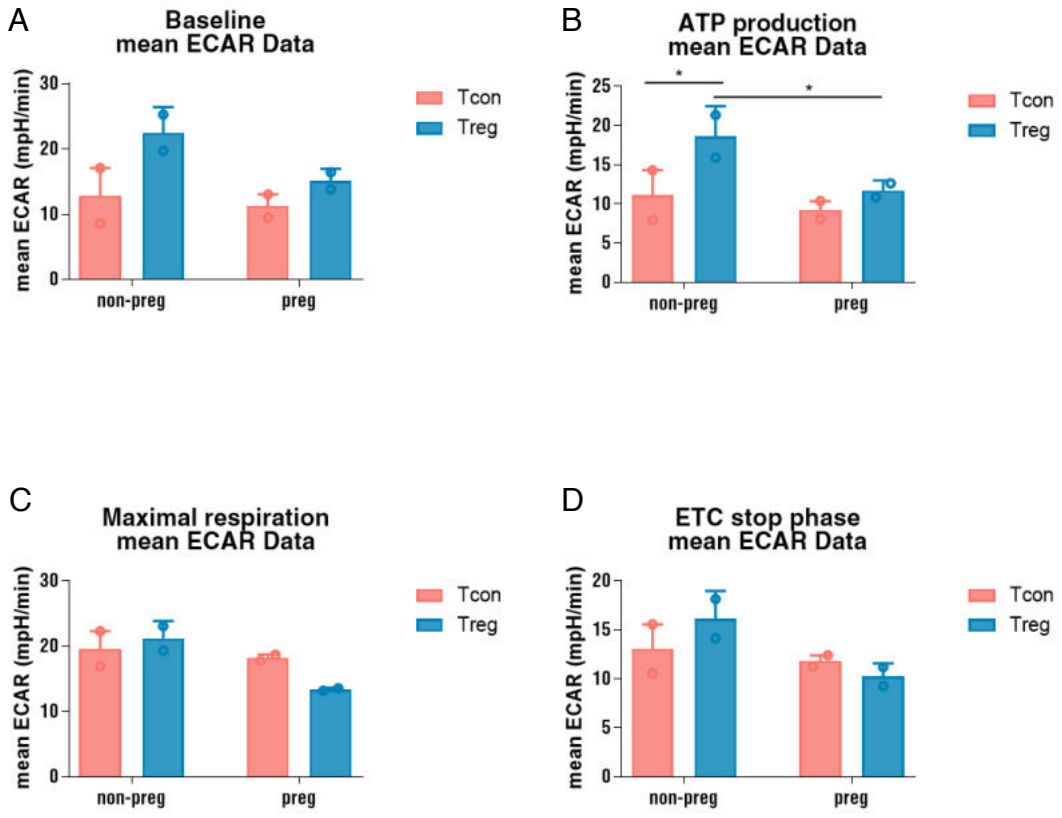

Figure 3. 9 ECAR measurements with fatty acid media, separated by measurement phases

ECAR data as shown in Fig. 3.7 but separated by Cell Mito Stress Test measurement phases (Fig. 2.7): (**A**) baseline measurements, (**B**) ATP production phase, (**C**) maximal respiration phase, (**D**) ETC stop phase, in order to perform statistical analysis. Measurements were performed on 1×10^6 cells per data point, using self-made fatty acid medium ($n = 2$ biological replicates per group). Data are presented as mean values + SEM. Statistical analysis was performed by two-way ANOVA with subsequent Sidak's multiple comparison post hoc test. *$P < 0.05$; **$P < 0.01$.

In summary, OXPHOS and glycolysis were not found to be increased in Treg compared to Tcon regardless of the pregnancy status. Instead, in contrast OXPHOS and glycolysis showed in parts a trend and in parts a significant higher activity in Tcon without and during pregnancy. This was not markedly influenced by an increase of cell numbers or addition of fatty acids in the media. Taken together with the previous assessments of Tcon and Treg in microarray, RT-PCR and relative DNA content measurements the results on energy metabolism are inconclusive. Therefore overall immunometabolism in Tcon and Treg during pregnancy remains to be further examined.

3.3 TCR β repertoire sequencing in Tcon and Treg during EAE and simultaneous pregnancy

Specific TCR engagement drives T cell activation. Thus the specificity of the TCR repertoire is the activity-determining feature of T cells. Analysis of the TCR repertoire in the context of EAE and a simultaneous pregnancy have not been realized so far but bear the potential to recognize changes mediated by these two conditions on the clonal level. Thus, the TCR repertoire was analyzed as the third aspect of function. 'Clonal' in this context means that cells are descendants of the same ancestor, so that they are genetically identical and appear in higher cell numbers after stimulation and clonal expansion. Clonal expansion includes that the exact genetic identity of the TCR is preserved with cell division.

Tcon and Treg extracted from mice at different gestational and EAE disease stages were analyzed systematically via TCR sequencing and subsequent data analysis.

3.3.1 TCR β repertoire clonality analyses in EAE and pregnancy

Spleens and lymph nodes from four experimental groups were collected. One group consisted of non-pregnant naïve, animals. Naïve means that these animals are not immunized and will not develop any EAE disease. Immunized mice will develop first EAE disease signs at seven days after immunization. Another group of animals was pregnant and also naïve. Thus, these two groups were healthy (Fig. 3.10 A). A third group of animals was non-pregnant and EAE diseased. These animals showed acute disease activity (Fig. 3.10 B). A fourth group of animals was pregnant and additionally an EAE had been induced in them (Fig. 3.10 A). Due to the pregnancy this last group was completely protected from EAE disease activity at the time point of sample collection (day 10-12 post immunization) (Fig. 3.10 B). Later, after delivery these mice would have developed an overshooting EAE, if they had not been sampled at this time point already. DEREG mice were used here in order to accomplish isolation of Tcon and Treg from spleen and lymph nodes via sorting Foxp3-eGFP-negative and Foxp3-eGFP-postive CD4+ T cells, respectively (Fig. 3.10 C).

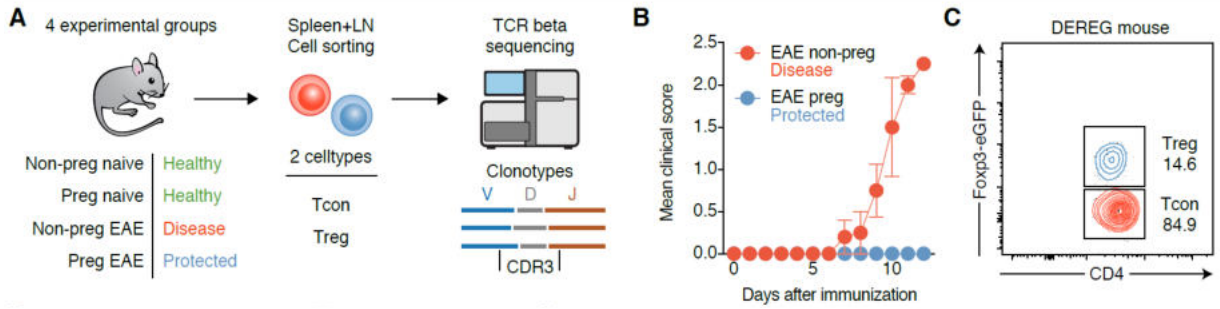

Figure 3. 10 Experimental set up, EAE disease course and used mice

(**A**) Scheme of experimental setup (*n* = 5 biological replicates per group). (**B**) Representative EAE disease courses of non-pregnant (*n* = 5) and pregnant (*n* = 7) B6-DEREG mice. Animals were sampled for TCR-sequencing on day 10-11 after immunization, corresponding to gestational day E18.5. (**C**) Representative gating for fluorescence-activated cell sorting of the CD4+Foxp3-eGFP− Tcon and CD4+Foxp3-eGFP+ Treg from B6- DEREG mice.

Next the genomic DNA of the cells was extracted and library preparation was performed by HS Diagnomics, Berlin. Then the TCR β sequencing was performed at the transcriptomics laboratory at the Universitätsmedizin Göttingen (Fig. 3.10 A). From the generated libraries, around 0.5 million reads were recovered per sample and were mapped onto publically available TCR locus sequences to filter out sequences that are relevant for the desired TCR sequence analyses from sequences of other undesired T cell regions (Fig. 3.11 A). From these TCR mapped sequences around 75% encoded CDR3 nucleotide (CDR3nt) sequences representing productive TCR re-arrangements, which can form working TCRs (Fig. 3.11 B). Raw sequencing fastq files were analyzed at INIMS for the usage of V, D and J segments of the TCRs, for information on nucleotide and amino acid sequences of CDR3 region of the TCRs and also for the frequencies of the sequences.

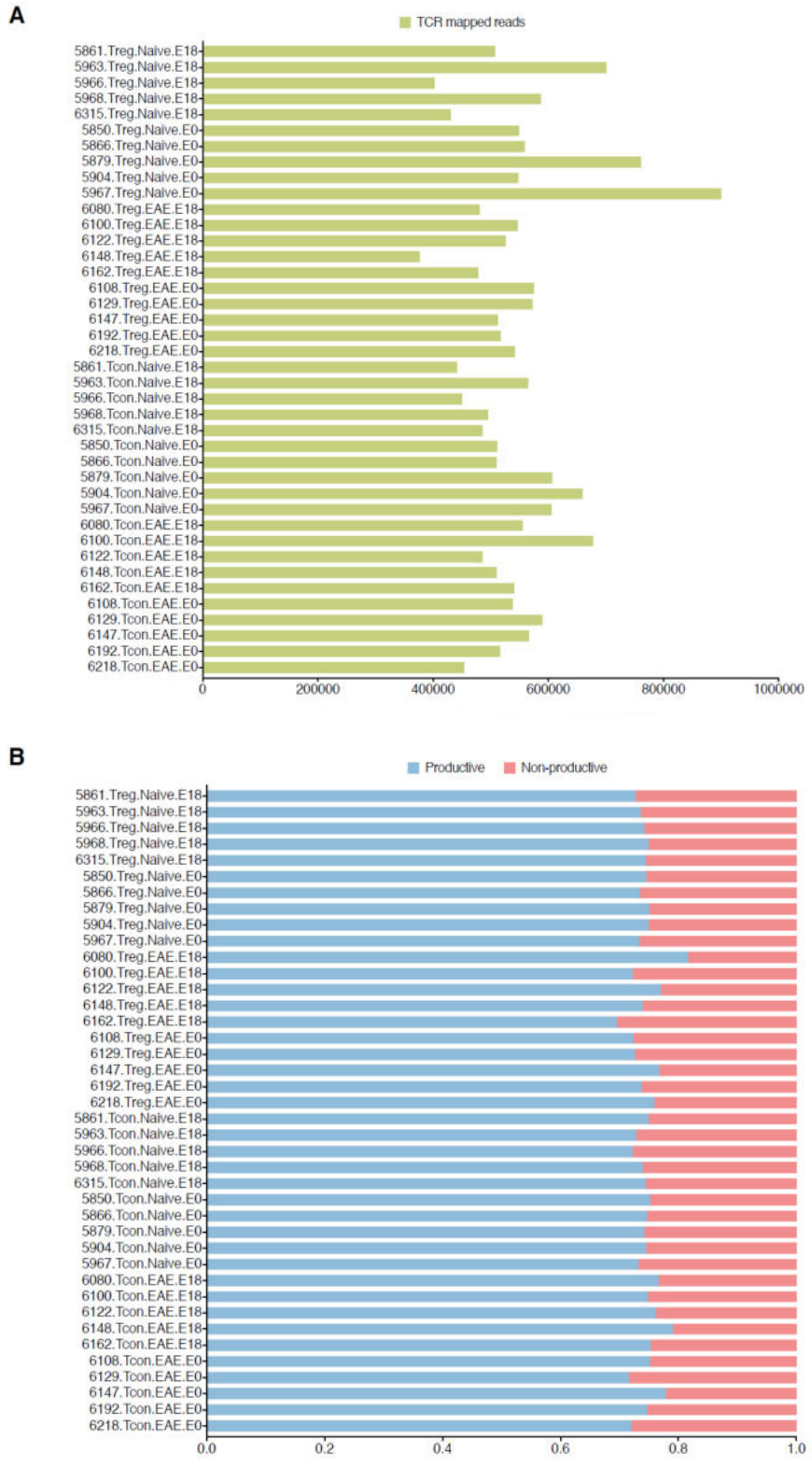

Figure 3. 11 TCR-sequencing quality control

(**A**) Number of reads mapped to the TCR locus is ~0.5 million. (**B**) Relative abundance of productive (~75%) versus non-productive (~25%) TCR re-arrangements.

As an initial analysis, the distribution of clonotype abundances was investigated in two representative animals. Clonotype abundance showed to be clearly smaller in the naïve sample than in the EAE sample. This indicates that during EAE the TCR repertoire becomes more clonal, so more dominated by one or few expanded clones and less evenly distributed, as it is the case for the naïve sample (Fig. 3.12 A). In line with this sample clonality was used to measure global TCR repertoire alterations. Clonality is a combined value, taking into account the number of unique clones combined in one value with the distribution of the clones. Figure 3.12 A can also be seen as an illustration of clonality. Looking at all experimental groups together a strong clonal expansion was detected in EAE samples in contrast to naïve samples ($P < 0.0001$; Fig. 3.12 B). Clonality was also found to be increased in Tcon and Treg subsets of virgin as well as pregnant mice. However, when considering pregnancy separately it did not result in obvious clonality shifts (Tcon, non-pregnant, naive versus EAE: $P = 0.0497$; Tcon, pregnant, naïve versus EAE: $P = 0.0028$; Treg, non-pregnant, naïve versus EAE: $P = 0.0120$; Treg, pregnant, naïve versus EAE: $P = 0.0032$; Fig. 3.12 C).

Therefore, clonality of the TCR repertoire revealed to be predominantly driven by immunization.

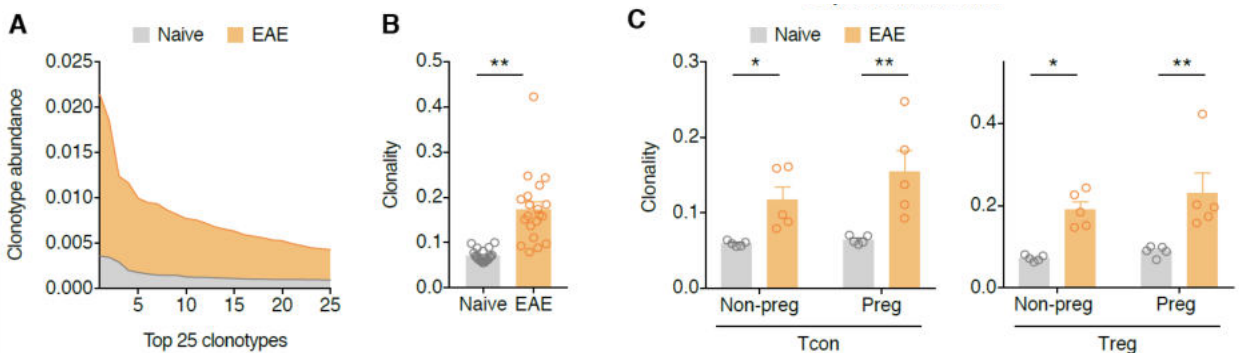

Figure 3. 12 EAE but not pregnancy increases TCR repertoire clonality

(**A**) Clonotype abundance curves (top 25 clonotypes) of representative naïve and EAE samples. (**B**) Clonality analysis of naïve versus EAE samples ($n = 20$ per group). (**C**) Clonality analysis of naïve versus EAE samples, grouped by T cell subtype (Tcon versus Treg) and gestational state (non-pregnant versus pregnant) with $n = 5$ biological replicates per group. Data are presented as mean values + SEM. Statistical analysis was performed by unpaired Student's *t* test in **B** and two-way ANOVA with subsequent Sidak's multiple comparison post hoc test in **C**. $*P < 0.05$; $**P < 0.01$.

3.3.2 Usage analysis of TRBV and TRBJ chains in pregnant EAE mice

In order to perform a more detailed characterization of the TCR specificity the next more detailed level of investigating the TCR was applied. The usage of TRB β V (TRBV) and TRB β J (TRBJ) chain segments for building the TCRs was analyzed, as this can yield initial information of antigen-specificity. Overall the TRBV and TRBJ chain segment usage was barely influenced by the disease state (Fig. 3.13 and Fig. 3.14). A published global induction of the TRBV segments 13.2, 19, 20 and 31 in CNS infiltrates of EAE animals [118,184,186] was not detected in this peripheral EAE sample set. In fact EAE immunization affected the TRBV (Fig. 3.13) and TRBJ (Fig. 3.14) segment usage very faintly. TRBV20 and TRBV31 usage was

significantly increased in Tcon samples in the non-pregnant state (TRBV20: $P = 0.0087$; TRBV31: $P = 0.0403$). TRBV19 was used in significantly higher amounts in Tcon during pregnancy (TRBV19: $P = 0.0171$; Fig. 3.13 A). An exception was the dominant EAE-associated TRBV segment 13.2, which was used in significantly higher amounts in Treg of pregnant EAE animals only ($P = 0.0003$; Fig. 3.13 B). Overall, TRBV usage was mildly changed and TRBJ usage was completely unaltered by EAE and pregnancy. It is documented in the literature that expansion of the TRBV13.2 segment involves MOG-specific clones [118,184–186,201]. However, in the present data set such a TRBV13.2 chain expansion was limited to the group of Treg from pregnant EAE mice. Therefore pregnancy seemed to selectively expand Treg clonotypes that incorporate putatively EAE-associated TCRs. In this way pregnancy might contribute to control encephalitogenic Tcon responses of the same antigen specificity.

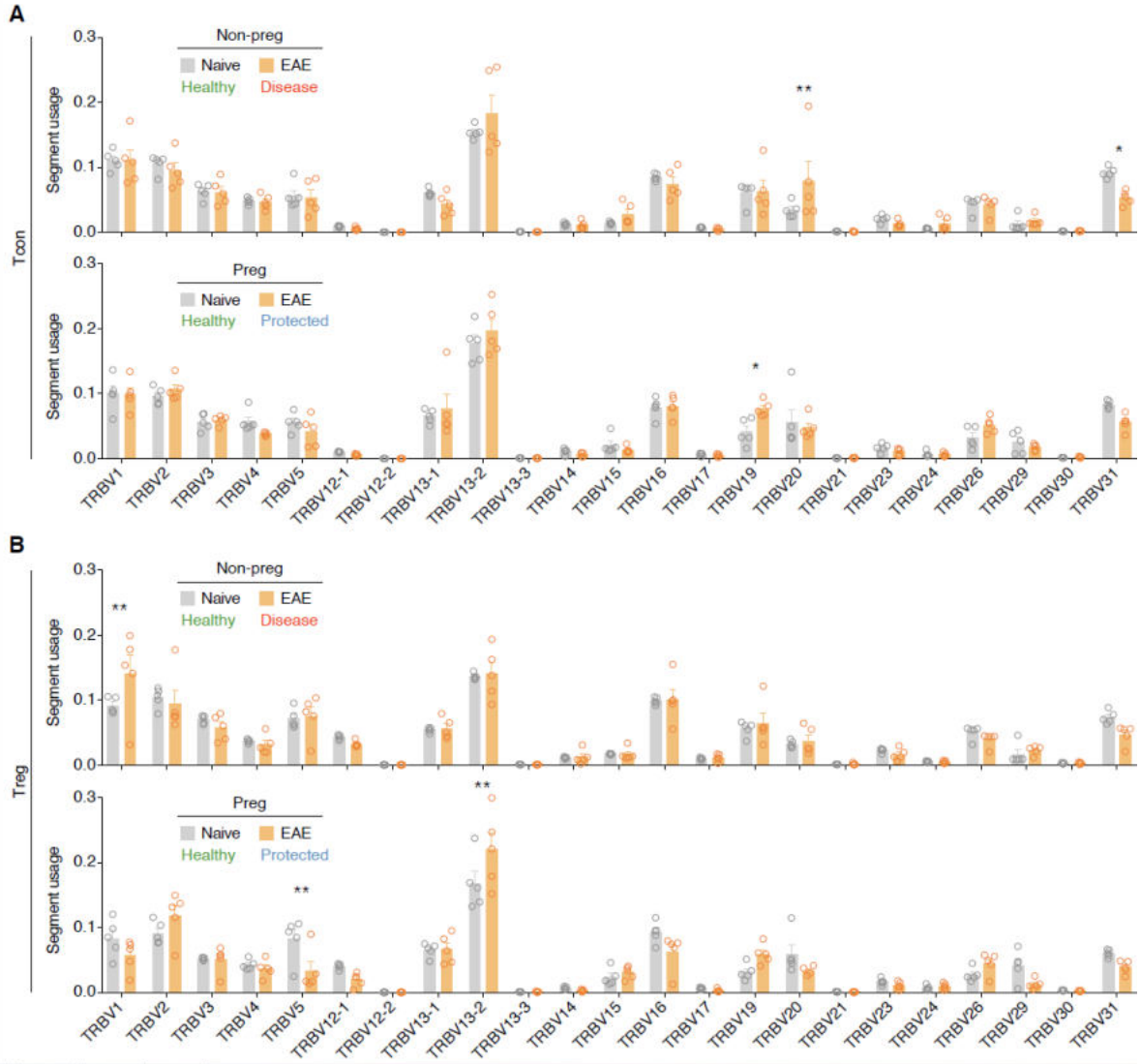

Figure 3. 13 Treg show increased usage of EAE-associated TRBV13.2 in pregnancy-protected EAE mice

TRBV segment usage of Tcon (**A**) and Treg (**B**) isolated from naïve versus EAE mice, grouped by gestational state (non-pregnant versus pregnant) with $n = 5$ biological replicates per group. Data are presented as mean values + SEM. Statistical analysis was performed by two-way ANOVA with subsequent Sidak's multiple comparison post hoc test. $*P < 0.05$; $**P < 0.01$.

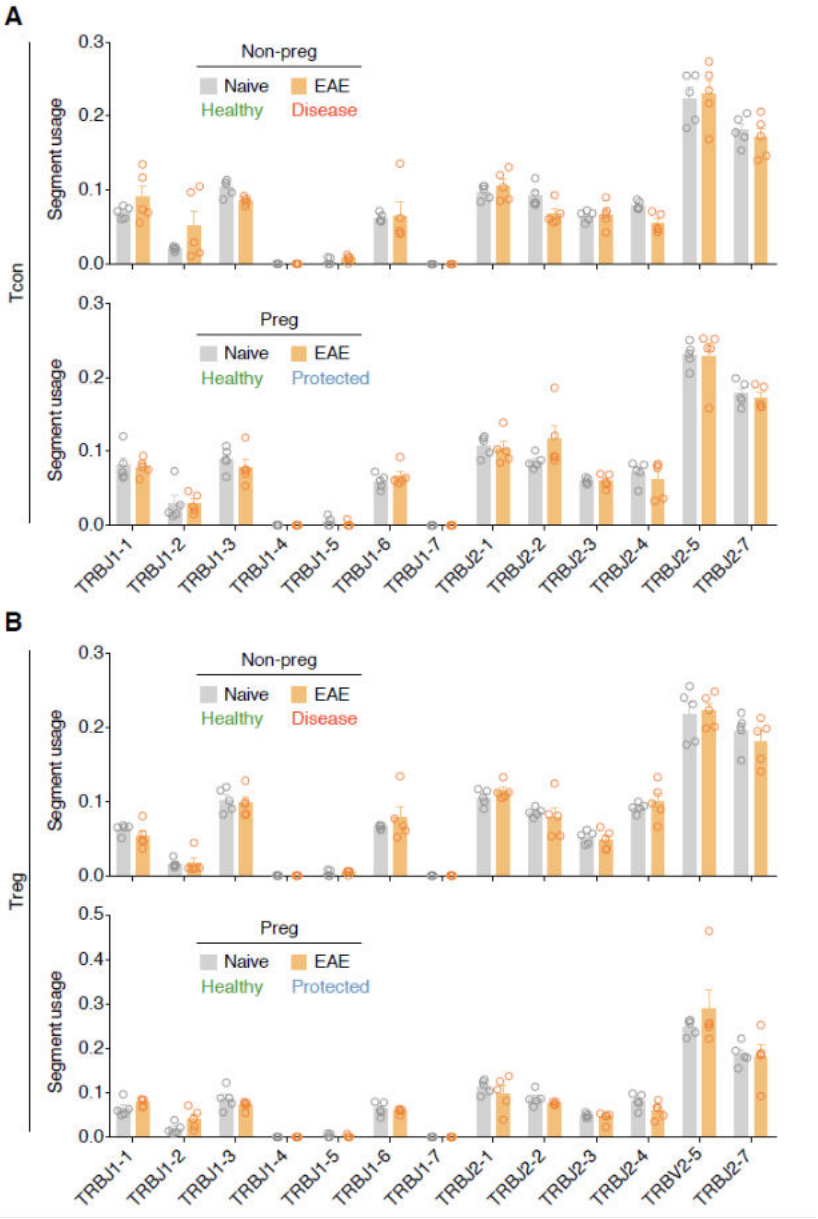

Figure 3. 14 TRBJ usage is unchanged by EAE and pregnancy

TRBJ segment usage of Tcon (**A**) and Treg (**B**) isolated from naïve versus EAE mice, grouped by gestational state (non-pregnant versus pregnant) with $n = 5$ biological replicates per group. Data are presented as mean values + SEM. Statistical analysis was performed by two-way ANOVA with subsequent Sidak's multiple comparison post hoc test. $*P < 0.05$; $**P < 0.01$.

3.3.3 Usage of CDR3aa during EAE and pregnancy

Analysis of TRBV and TRBJ chain segments revealed few pregnancy specific changes. However, TRB chain analysis is only an approximate measurement of receptor specificity. In order to perform an even

more detailed characterization of the TRB the CDR3 region amino acid sequences - the most variable region - were analyzed next. For this purpose pairwise distances between samples were calculated and the results were projected into a 2D plane by multidimensional scaling (Fig. 3.15). This was done in order to analyze the overall similarity of CDR3aa sequence usage in the data set. Data that are depicted close together are very similar to each other. Data points that are far away from one another are more different from each other. Additional color-coding of the immunization status and the T cell subtype displayed a clear separation of naïve versus EAE and Tcon versus Treg samples (Fig. 3.15 A-B). This suggested that the overall variance in CDR3aa usage was markedly driven by these two parameters. In comparison, color-coding of gestational state (non-pregnant versus pregnant) resulted in an intermingled picture (Fig. 3.15 C). Therefore pregnancy acts as a much weaker factor of shared CDR3aa usage than the parameters of disease state or T cell subset. Remarkably, only one experimental group was found to display a permanent clustering across all three parameters. This group consisted of Treg samples from pregnant EAE mice (Fig. 3.15 A-C, dashed circle). This suggests that these samples were tied together by a strong CDR3aa similarity.

In summary, these results show disease status and T cell subtype to be strong determinants of CDR3aa usage. Strikingly, the CDR3aa similarity of Tcon versus Treg was not masked by EAE immunization, but rather intensified. The tight clustering of Treg from pregnant EAE mice suggests a selective pressure affecting Treg under this specific condition, which mirrors the protective effect of pregnancy onto EAE.

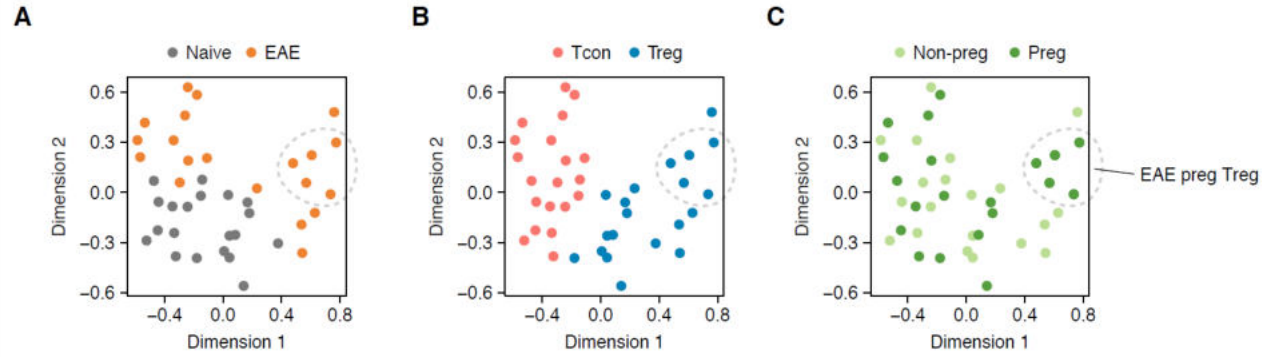

Figure 3. 15 Usage of CDR3aa sequences is driven by immunization and T cell subtypes

Multi-dimensional scaling plots of CDR3aa similarity across samples. Color-coding of naïve versus EAE (**A**), Tcon versus Treg (**B**) and non-pregnant versus pregnant (**C**) samples (*n = 5* biological replicates per group). Dashed line highlights Treg samples of pregnant EAE animals.

3.3.4 Sampling of peripheral and CNS-infiltrating T cells and analysis of TCR β repertoire clonality, TRBV and TRBJ chain segments

Even though C57BL/6 mice are genetically identical, each mouse owns an individual TCR repertoire. In order to determine 'public' EAE clonotypes a new cohort was sampled. 'Public' in this context means that clonotypes are associated with encephalitogenic activity in EAE and are shared by individual mice. CD4+ T cells from peripheral spleen and lymph nodes were collected as well as CNS-infiltrating CD4+ T cells.

This was an independent cohort of three virgin EAE mice (Fig. 3.16 A). The samples were further depleted for CD8+ T cells in order to achieve a closer similarity primary cohort, which was sorted for CD4+ cells (Fig. 3.10). The intention of collecting a second cohort was to detect such EAE-driving public clonotypes that appeared suitable to examine their occurrence during EAE and pregnancy in the first data set. It was determined that CNS samples showed a distinct increase of clonality in relation to peripheral samples from the same mouse (P = 0.0026; Fig. 3.16 B), which was expected. This revealed a local accumulation or expansion of encephalitogenic TCRs in the CNS tissue. These could be Tcon as well as Treg clonotypes as it is known from the EAE model that both cell types infiltrate the CNS [202,203]. Next, the usage of TRBV and TRBJ segments was considered, initially in one representative animal. It was identified that peripherally TRBV2, TRBV13.2, TRBV20, TRBJ2-1, TRBJ2-5 and TRBJ2-7 were the most dominantly used chain segments. In the same animal centrally TRBV13.2, TRBV19, TRBV20, TRBJ2.1, TRBJ2.5, TRBJ2.7 were the most highly abundant chain segments (Fig. 3.16 C). Considering all three animals and the whole analyzed spectrum of TRBV and TRBJ chain segment expression in EAE the segment usage was found to be barely influenced by the central or peripheral origin of the samples (Fig. 3.16 D). A significant increase of TRBV13.2 (P < 0.0001) and TRBV20 usage was found (P = 0.0054; Fig. 3.16 C-D, Fig. 3.17). This is in accordance with already described EAE infiltrates [118,184,186] and found similarly in the primary data set (Fig. 3.13). There is no significant change in TRBJ segment usage, comparing the central or peripheral origin of the samples.

Taken together, the obtained CNS samples are similar to the primary data set and are an adequate source for the identification of EAE-associated clonotypes.

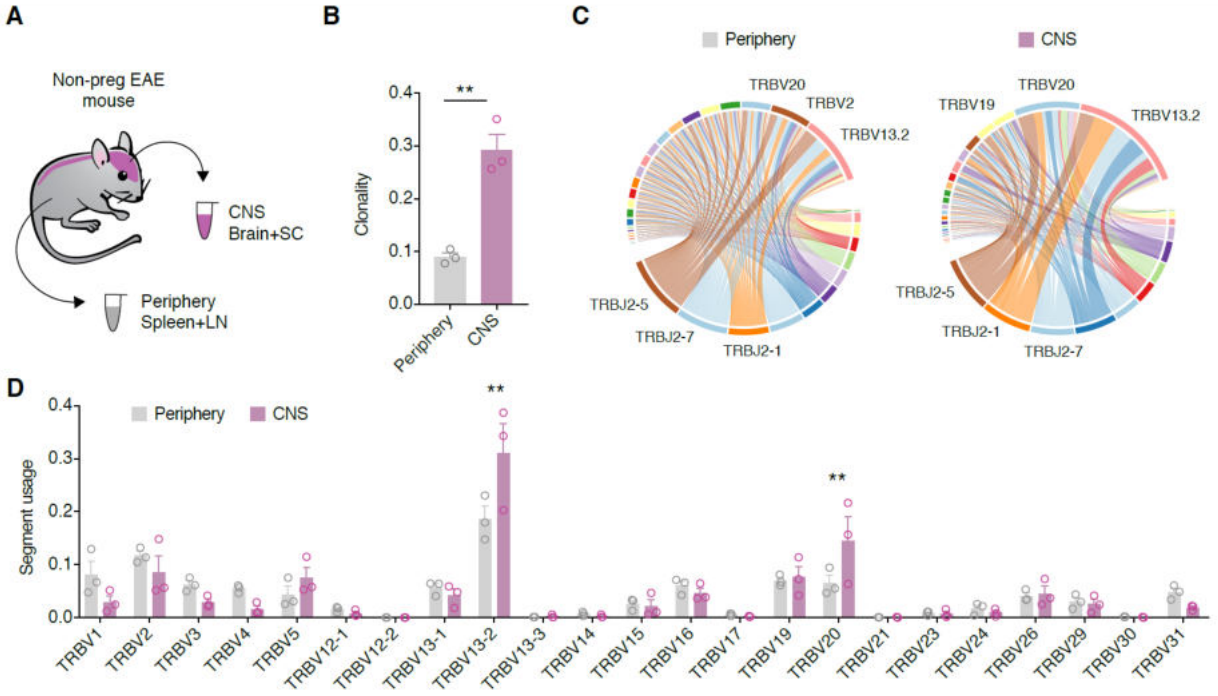

Figure 3. 16 CNS-infiltrating T cells show preferred usage of TRBV13.2 and TRBV20

(**A**) Scheme for sampling of CNS-infiltrating (brain and spinal cord) versus peripheral (spleen and lymph nodes) CD4+ T cells (n = 3 non-pregnant EAE mice at day 14 after immunization). (**B**) Clonality analysis of peripheral versus CNS samples (n = 3 biological replicates per group). (**C**) Circus plots showing relative abundance and pairing of TRBV and TRBJ segments in peripheral versus CNS samples of one representative animal. (**D**) TRBV segment usage in peripheral versus CNS samples (n = 3 biological replicates per group). Data are presented as mean values + SEM. Statistical analysis was performed by unpaired Student's t test in **B** and two-way ANOVA with subsequent Sidak's multiple comparison post hoc test in **D**. *$P < 0.05$; **$P < 0.01$.

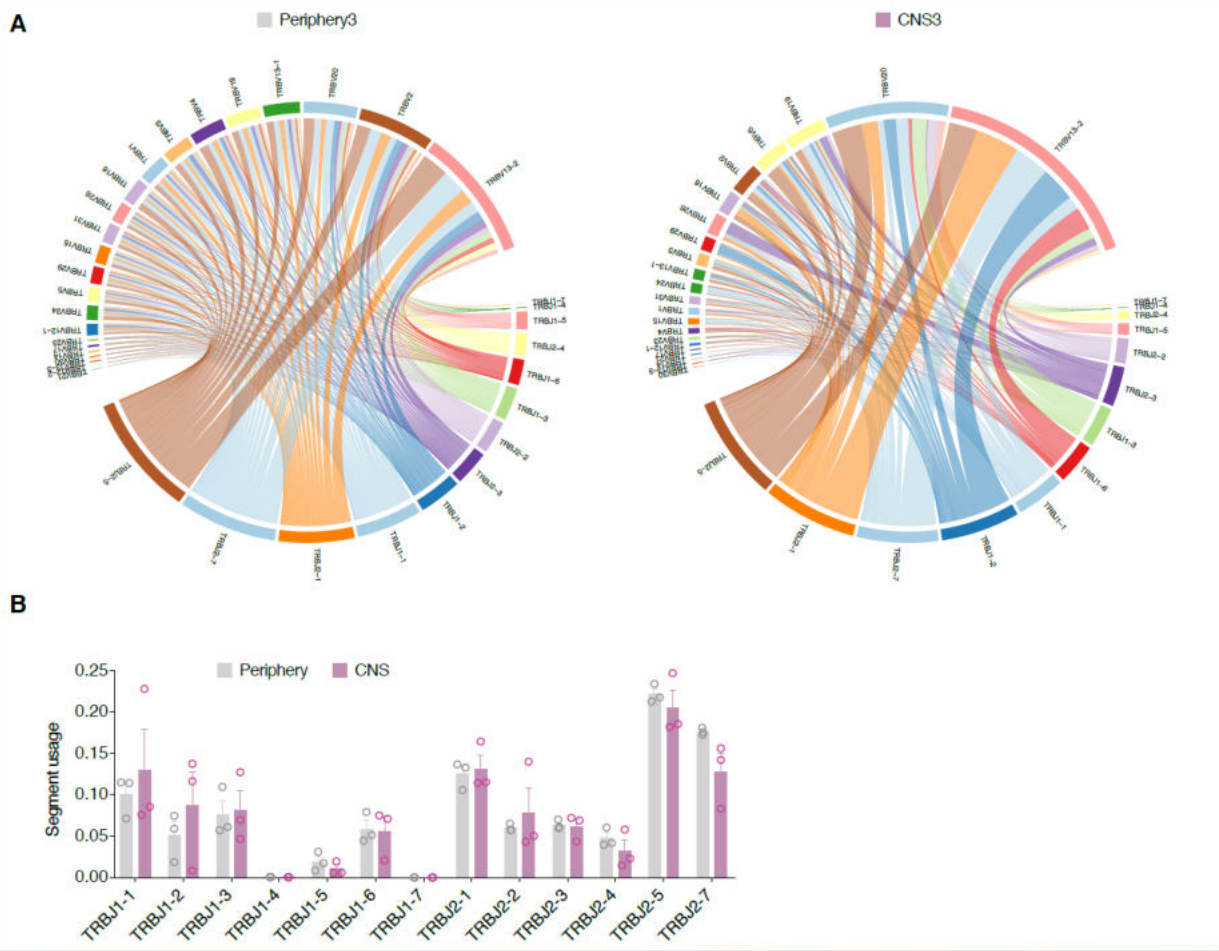

Figure 3. 17 TRBV/J pairing and TRBJ usage in periphery versus CNS

(**A**) Magnification of circus plots from Fig. 3.16 C with labels for all TRBV and TRBJ segments. (**B**) TRBJ segment usage in peripheral versus CNS samples (n = 3 biological replicates per group). Data are presented as mean values + SEM. Statistical analysis was performed by two-way ANOVA with subsequent Sidak's multiple comparison post hoc test in **B**. *$P < 0.05$; **$P < 0.01$.

3.3.5 Usage of CNS sample comparisons for identification of EAE clonotypes

In order to identify public EAE-associated C57BL/6 TCRs the overlap of CDR3 nucleotide sequences (CDR3nt) within and across individual mice and sample locations was investigated via comparisons as shown in Fig. 3.18 A. First, clonotypes that were shared between different EAE mice in the peripheral lymphatic tissue were identified and tracked. Therefore the periphery of animal one was compared with the periphery of animal two. The periphery of animal two was compared with the periphery of animal three, as well as comparisons of the periphery of animal three were made with animal one (Fig. 3.18 A, top row). This comparison showed a limited clonotype overlap of ~4%, which underscored the huge inter-individual heterogeneity of peripheral TCR repertoires that seems to be present even within individuals from an inbreed line and even after they have been immunized with the same MOG_{35-55} peptide antigen.

Then periphery and CNS were compared within the same mouse. This meant comparisons of the periphery of animal one with the CNS of animal one, and respectively with animal two and three. This type of comparison detected a consistent expansion of shared clonotypes from the periphery (~5%) towards the CNS (~40%) (Fig. 3.18 A, middle row). These findings are in concordance with a published antigen-specific infiltration and/or local proliferation of EAE clonotypes within the CNS [204]. Eventually, CNS samples were compared across all three individual mice. This showed a striking overlap, which was observed despite the fact that these are inter-individual comparisons (Fig. 3.18 A, bottom row). Clonotypes shared between CNS1 and CNS2 were identified with a cumulative abundance of ~45% in CNS1 and ~75% in CNS2. Clonotypes shared between CNS1 and CNS3 amounted up to ~90% of productive TCR reads in CNS3 (Fig. 3.18 A, bottom row). Thus, even though there was a high peripheral diversity found in-between different mice, CNS-infiltrating clonotypes showed a remarkable overlap among these animals.

Further analysis of the overlap between the CNS samples of different animals was done by plotting the identified shared clonotypes in a Venn diagram (Fig. 3.18 B). Thereby 918 CDR3nt clonotypes were found to be shared by at least two CNS samples. This included 91 clonotypes, which were present in all three CNS samples. It seemed to be reasonable that these 918 identified EAE clonotypes were suitable to track EAE-specific responses in the primary sample set. Effectively, the cumulative abundance of EAE clonotypes was significantly increased in EAE-immunized animals in comparison to naïve animals ($P < 0.0001$; Fig. 3.18 C). 1,000 randomly selected peripheral clonotypes were tracked as a negative control and were found to be unchanged by EAE immunization (Fig. 3.18 D).

It is vital to note that the cohort used for the discovery of EAE clonotypes was entirely independent of the cohort of Tcon and Treg, which were sampled for the analysis during EAE and pregnancy. Therefore, this strategy allows creating an encompassing clonotype list, which can be used to track EAE responses in any other cohort of MOG_{35-55}-immunized C57BL/6 mice.

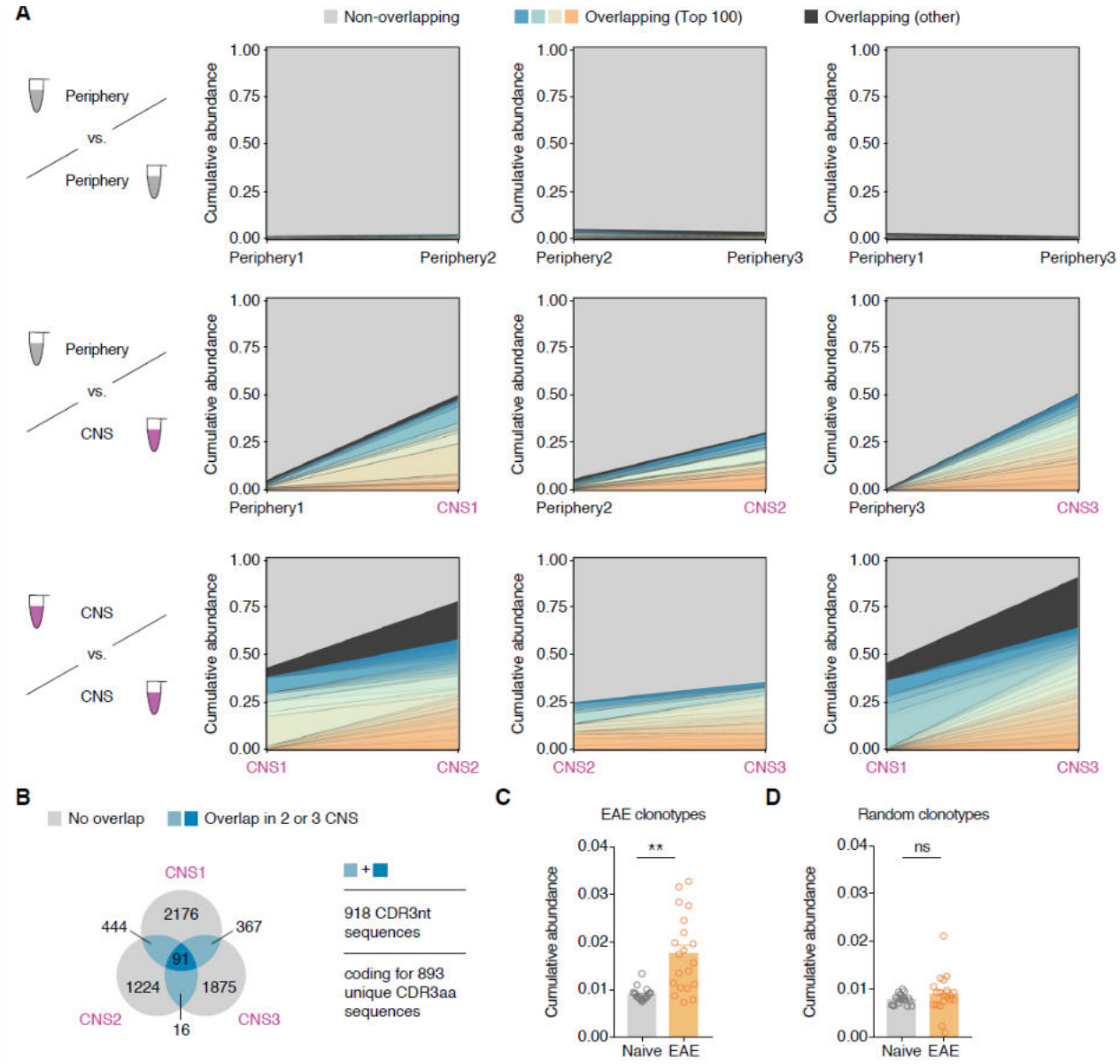

Figure 3. 18 CNS samples enable identification of EAE clonotypes

(**A**) Cumulative abundance of clonotypes shared between peripheral samples across mice (top row), between peripheral and CNS samples of the same mouse (middle row) and between CNS samples across mice (bottom row). Non-overlapping clones are depicted in light grey, top 100 overlapping clones are depicted by colors (light blue to orange), remaining overlapping clones that were not part of the top 100 are depicted in dark grey. (**B**) Venn diagram of overlap between CNS samples. Clonotypes present in at least 2 of 3 CNS samples were considered EAE clonotypes (**C** and **D**) Cumulative abundance of EAE clonotypes (**C**) and 1000 random clonotypes (**D**) in naïve versus EAE samples (n = 20 per group) of the main data set (see Fig. 3.10 A). Statistical analysis was performed by unpaired Student's t test in **C** and **D**. *$P < 0.05$; **$P < 0.01$.

3.3.6 EAE clonotype-tracking in peripheral data set

Subsequent to the identification of EAE clonotypes and their backtracking in the peripheral sample set the EAE clonotypes were plotted in an abundance heat map. Therein each EAE clonotype was shown as a separate row (Fig. 3.19 A and Fig. 3.20). Altogether, 918 CDR3nt clonotypes coding for 893 unique CDR3aa sequences were identified (Fig. 3.18 B). These included 489 clonotypes (~55%), which were found in at least one sample of the main data set and were ordered by the number of samples they were detected in (Fig. 3.20). When pointing the focus onto the top 50 clonotypes (Fig. 3.19 A), it can be detected that clonotypes contributing to Tcon responses in EAE (marked in red) were not identical to those that contributed to Treg responses (marked in blue). Furthermore, Tcon EAE clonotypes made a rather consistent pattern across gestational stages and across animals of the same experimental group. However, EAE clonotype usage by Treg was more sporadic in individual mice and gestational stages (Fig. 3.19 A).

In order to quantitatively analyze changes mediated by EAE induction and EAE protection during pregnancy the cumulative abundance of EAE clonotypes were analyzed across all four experimental groups. Tcon revealed a strong increase of public EAE clonotype abundance in immunized versus naïve animals, regardless of whether they were pregnant or not (non-pregnant, naïve versus EAE: $P = 0.0327$; pregnant, naïve versus EAE: $P = 0.0002$; Fig. 3.19 B). However, in Treg the EAE immunization alone did not lead to an expansion of public EAE clonotypes ($P = 0.9840$). Whereas only in the additional presence of pregnancy Treg increased their usage of public EAE clonotypes ($P = 0.0007$; Fig. 3.19 B). Remarkably, 1,000 peripherally identified random clonotypes did not show any significant changes, which supported the finding that an induction of EAE clonotype abundance was in fact antigen specific (Fig. 3.19 C). Supposing that the specificity for EAE-related antigen enhances the power of these Treg to control encephalitogenic Tcon, this finding mirrors the suppression of disease activity in pregnant EAE mice (Fig. 3.10 B).

Taken together, these results demonstrate that pregnancy was required to generate detectable EAE clonotype expansion in Treg of EAE mice. Additionally, Tcon and Treg showed a different usage of EAE-associated CDR3aa sequences, which is consistent with a distinct clonal origin of both cell types.

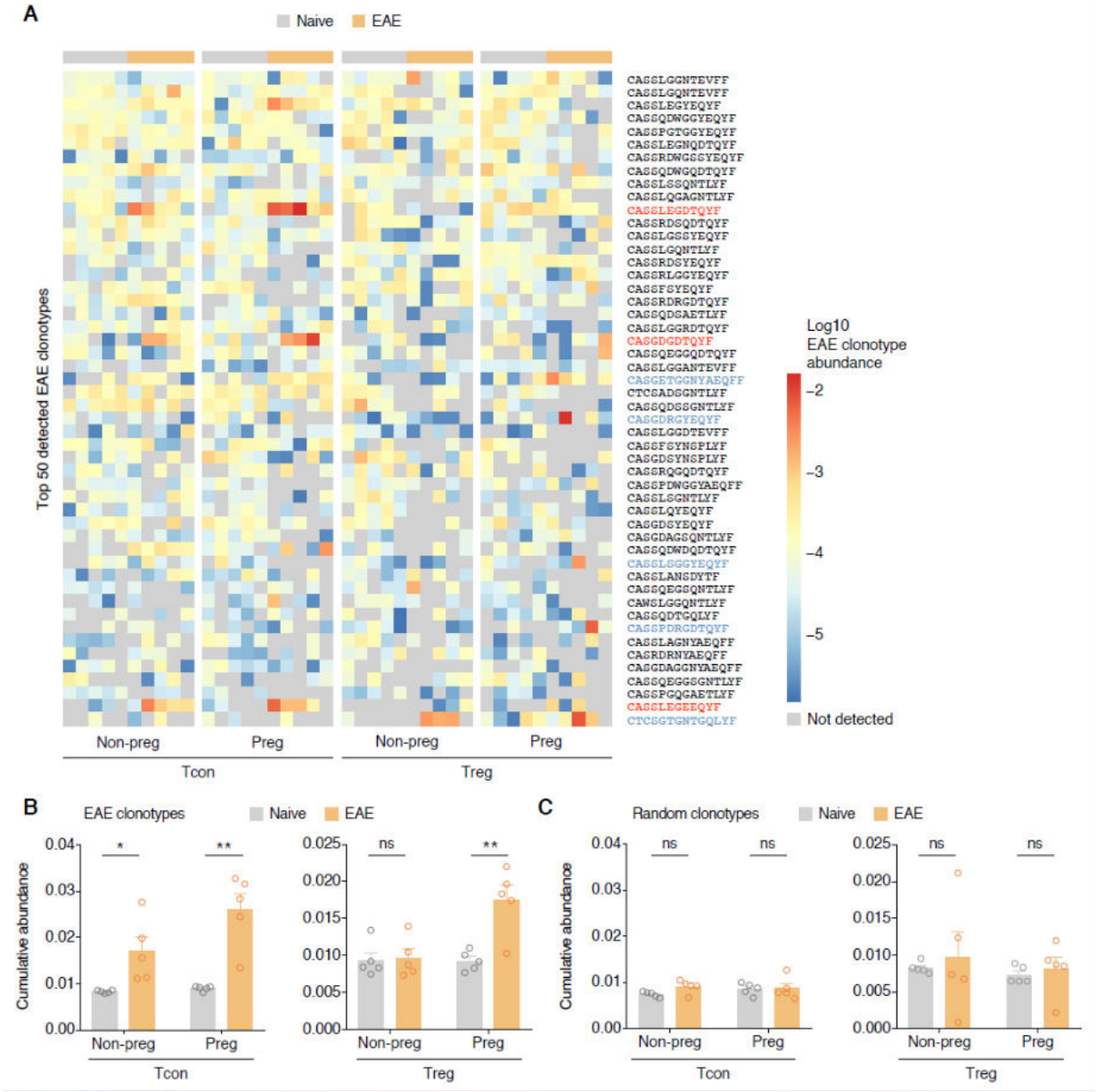

Figure 3. 19 Pregnancy is required to expand EAE clonotypes within Treg

(**A**) Abundance heatmap of top 50 EAE clonotypes across samples. Light grey color in heatmap indicates that clonotype was not detected in the respective sample. (**B** and **C**) Cumulative abundance of EAE clonotypes (**B**) and 1000 random clonotypes (**C**) in naïve versus EAE samples, grouped by T cell subtype (Tcon versus Treg) and gestational state (non-pregnant versus pregnant). Data (n = 5 biological replicates per group) are presented as mean values + SEM. Statistical analysis was performed by two-way ANOVA with subsequent Sidak's multiple comparison post hoc test in **B** and **C**. *$P < 0.05$; **$P < 0.01$.

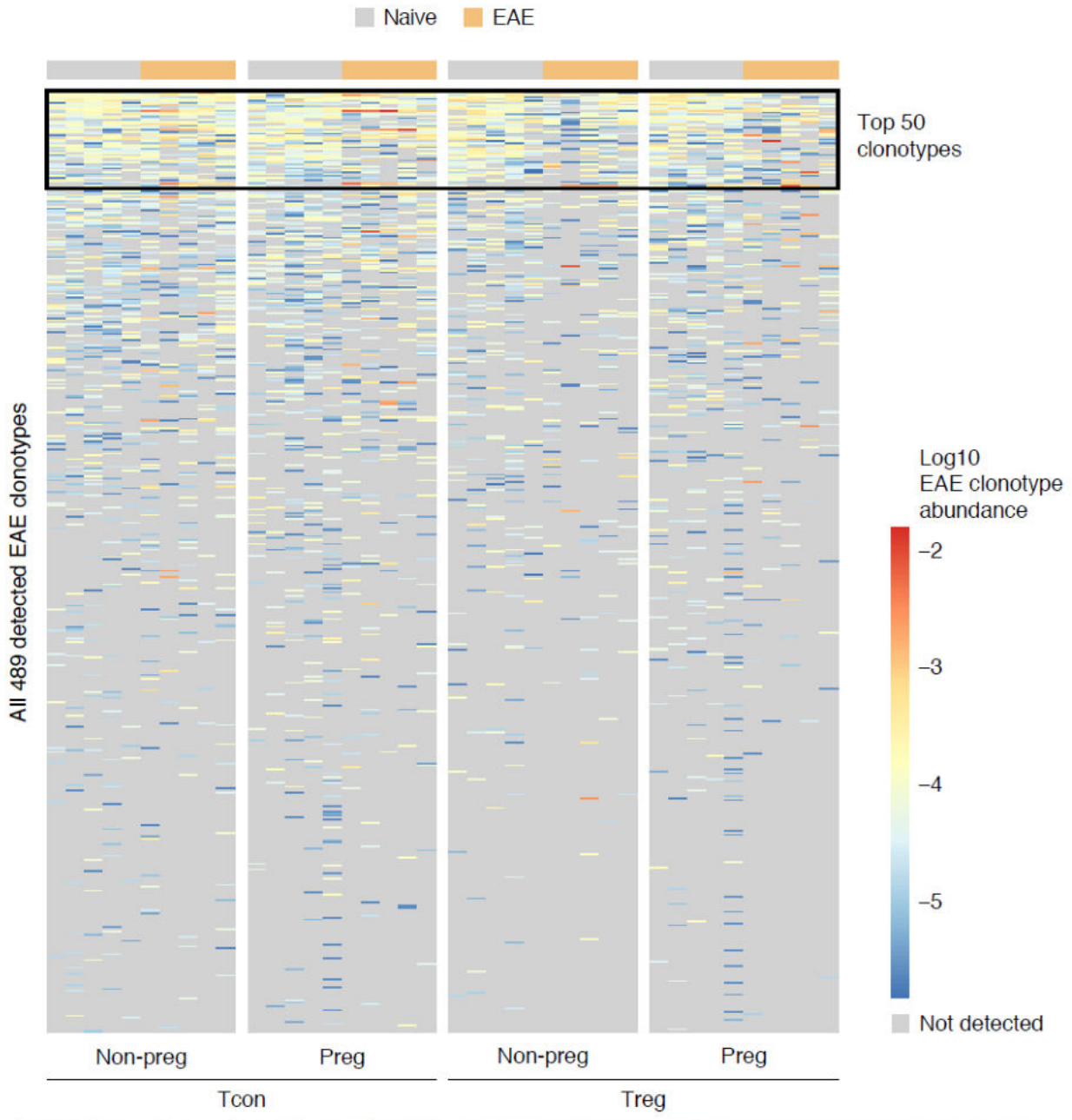

Figure 3. 20 Abundance heatmap of EAE clonotypes

Complete abundance heatmap of all 489 detected EAE clonotypes across samples (n = 5 biological replicates per group). Detailed heatmap of top 50 clonotypes is depicted in Fig. 3.19 A. Grey color indicates that clonotype was not detected in the respective sample.

4. Discussion

This work brings together the fields of EAE, pregnancy and Treg. With regard to the EAE and pregnancy conditions this work analyzes different functional aspects of Treg, namely suppressive capacity, immunometabolism and TCRs. Each of these fields is a complicated territory of its own. This thesis tries to unravel if and how these aspects execute the protective effect of pregnancy in autoimmunity.

Currently, MS is an incurable autoimmune disease affecting increasing numbers of patients in their most productive time of life. Since it had been clarified that against previous counseling generally MS patients can become pregnant and that a pregnancy actually leads to an amelioration phase of the disease, a change of thinking occurred [2,5]. Researchers soon realized the potential in this phenomenon and tried to mimic it artificially with pregnancy hormones [101,205], with rather sparse success so far. This exemplifies the complexity of the phenomenon. Advances have been made in understanding the immunological processes of pregnancy [74,77,87,91]. Knowledge on sex effects and hormonal aspects of the ameliorating phenomenon is advancing [3,6,38] and an animal model was generated to mimic the human phenomenon of disease amelioration during pregnancy, and enabling examination of more details [3]. Aspects of Treg limiting autoimmunity came more into focus [78]. Recently, Treg numbers were found to be increased in the reproductive tract and uterus draining lymph nodes during pregnancy and EAE. It was further identified that this was mediated via a change in glucocorticoid sensitivity of different T cell subsets [3]. Along with the known working mechanisms of the branch of Treg and recent data, taken in the EAE and simultaneous pregnancy set up at INIMS (Microarray, CTLA-4 measurements), many facts indicated that Treg not only increase in numbers but might also enhance their functions and become more potent in fulfilling them. It was hypothesized that such an increased Treg functionality mediates the suppression of MS and EAE symptoms during pregnancy.

Thus the superior goal of this work is a better understanding of the role of Treg in pregnancy-mediated protection from multiple sclerosis.

To achieve this goal this work analyzes the most important functionalities of Treg taken from donor mice in the virgin and pregnant state as well as in the naïve or EAE diseased state.

The work consists of three main pillars of Treg functionality: Treg suppressive capacity, Treg metabolism and the TCR repertoire of Treg.

In summary Treg suppressive capacity and Treg metabolism show inconclusive results during pregnancy.

Treg extracted from pregnant animals do not show a higher suppressive capacity than Treg from non-pregnant animals.

Pre-investigations on immunometabolism performed via RT-PCR and measurement of mtDNA indicated an increase of metabolism in Treg extracted from pregnant mice. However, measurements of OXPHOS were not found to be increased in Treg isolated from pregnant compared to non-pregnant animals. Instead OXPHOS as well as glycolysis showed higher activity in Tcon before and during pregnancy.

Analyses of the TCR repertoire of Treg with and without pregnancy and EAE suggest that pregnancy is a prerequisite for the expansion of Treg that target EAE-related antigens.

4.1 Suppressive capacity

Treg have evolved during evolution in order to regulate function of the immune system that would otherwise get out of control due to misdirected or unavoidable mechanisms in the life of a complex organism [106,120,136]. One vital aspect of Treg function is their suppressive potential. One main aim of this work is to examine whether the suppressive capacity of Treg is different when originating from virgin or pregnant donors. It was found that Treg extracted from pregnant animals do not show a higher capability of overall suppression of Tcon proliferation than Treg from non-pregnant animals. Instead suppressive capacity of Treg was found to be unchanged in the virgin and pregnant state.

This surprising outcome poses further questions, such as if suppressive capacity does not change during pregnancy or whether it was impossible to pick up a difference due to methodological limitations. Many details, such as increased expression of the cytotoxic protein CTLA-4 on Treg extracted from pregnant animals, further supported the hypothesis of an increased suppressive potential in Treg during pregnancy [3,148]. Treg hinder effector Tcon directed to attack the fetus and similarly might also hinder encephalitogenic Tcon of attacking the CNS in EAE-immunized animals.

The measured suppression in all suppression assays was not as high as shown by others [190,191,206], even though the assays were performed in a similar set up, were tightly titrated, tested and then performed repeatedly in the described way with steady results.

Essentially, suppression assays look at the overall suppressive capacity of Treg. They do not look at changes in particular cell contact dependent or independent kinds of suppression that Treg generally use for suppression [113,150]. Such more detailed investigations could be achieved by performing e.g. capturing assays of e.g. IL-2, IL-10, TGF-β to pick up changes of e.g. IL-2 levels in the vicinity of Treg extracted from virgin or pregnant mice in a similar set up with Tcon and Treg mixed together.

Another aspect is that Treg also mediate indirect suppressive function via interfering with and reducing activity of DCs and APCs, which as a consequence do not activate Tcon any more. However, untreated APCs are not part of the set up of a classical suppression assay, were Tcon and Treg are mixed, adjusted with feeder cells and anti-CD3 stimuli for co-stimulation. Feeder cells are intended to work as APCs in this set up, however they might not have available complete APC functionality, as they have been irradiated and treated with anti-CD90.2, to block their co-stimulation and proliferation. Blocking of feeder cell proliferation is intended in the assay to purely measure proliferation rates of responder cells. But this also reduces the assay sensitivity in regard to suppressive function mediated via APCs. Therefore, even though the performed classical suppression assays are a standard procedure in measuring suppressive capacity, they leave gaps of knowledge. Refining suppression assays could mean e.g. to exchange feeder cells for DCs and as final read out still use Tcon proliferation.

At the beginning it was envisaged to also perform fine-tuned MOG-driven suppression assays in a similar way as the performed CD3 driven assays. However, as the results of the CD3 driven suppression assays were sparse, MOG-driven suppression assays were thought to be rather unpromising and were not carried out.

Moreover, different suppression assay read out methods via Bromodeoxyuridine (BrdU) stainings instead of cell proliferations dyes like eFluor670 or via continuous live cell imaging methods, including a camera

inside the incubator and thus monitoring of cells continuously and without subsequent staining methods, imposed new problems that remained unsolved. BrdU staining turned out to be unreliable in the suppression assay set up. In the continuous live cell imaging keeping apart different cell types over long time periods of the analyses turned out to be difficult with available dyes and flat-bottom well format is needed for the scanning camera, which is not optimal for Tcon and Treg proliferation.

Another possible limitation of suppression assays is the pooling of groups of Treg from different sites of the body and several mice. This limitation can neither be solved by continuous live cell imaging nor by fine tuned suppression assays. On average around $0{,}5\times10^6$ cells can be isolated per mouse. For one assay with all experimental conditions a minimum of $\sim2\times10^6$ cells is needed. Of course it would be best if those cells could all be isolated from the same mouse at the same site of the body and very close to the uterus. However, this is not possible due to limited Treg numbers, which are further spread over different sites of their body. With current technology suppressive capacity of Treg cannot be measured on an individual Treg level. It is still conceivable that individual Treg are more potent in their suppressive capacity, but that their signal is lost in the pool of cells analyzed together in the same assay well.

Furthermore, there is the potential for a loss of 'pregnancy phenotype' in the cells *in vitro* due to the long lasting cell isolation methods to gain separate Tcon and Treg populations or due to changes in surrounding hormone levels, as the cell isolation and the assay procedure itself take place outside a pregnancy environment.

Taken together, the results leave room for speculation that suppressive capacity might be different and even increased in Treg extracted from pregnant mice.

Others have shown that a diminished suppressive potency of maternal Treg contributes to recurrent pregnancy loss, e.g. the production of IL-10 and TGFβ was shown to be reduced to 2% and 1% respectively in pregnancy loss, compared with 9% and 14% among gestational aged-matched controls [207]. Such a decrease of suppressive capacity was not seen in the here newly generated data. Thus similarities are rather implausible as the mice were distinctly pregnant.

It has been published and stated above already that Treg are necessary to regulate maternal immune responses against the semi-allogenic fetus during pregnancy [8–12,208]. Treg numbers during pregnancy are increased in the reproductive tract [13] and the uterus draining lymph nodes, especially during the late phase of pregnancy [3] in order to preserve the fetus during gestation. An increase in Treg suppressive functionality in parallel was very likely, as increased local numbers increase the action spectrum of Treg but an increase in suppressive function would multiply their efficacy by far more. Such a strong affectivity is presumably needed in order to lead to an effect as strong as a temporal disease protection as seen during pregnancy and EAE. Such simultaneous numerical and functional changes have been shown for Treg analyzed from pregnant human rheumatoid arthritis patients [130], which suggests further that a similar mechanism is also true in other autoimmune diseases like MS.

Especially the suppressive function of Treg has been shown to be hampered in MS patients [135,209] and therefore during an amelioration phase of disease symptoms, as during pregnancy, a reversing effect like pregnancy mediated increase of suppressive function would be realistic.

It has been shown that increased numbers of activated CD4+CD25+ cells exist in the decidua in normal human pregnancies [210]. And it was further demonstrated that enhanced expression of FoxP3, which occurs

in pregnant mice and in mice treated exogenously with estrogen pellets, results in a simultaneous increase in functional suppression within the CD4+CD25^{bright} Treg fraction of spleenocytes [211].

This is in contrast to the here-generated data but is in congruence with the hypothesis stated at the beginning that Treg during pregnancy have a higher suppressive capacity.

In an attempt to re-determine the frequency, phenotype and function of circulating Treg in human pregnancy it was shown by another group that in contrast to previous reports [211] Treg from pregnant women showed the same suppressive capacity as non-pregnant women. This was determined based on suppressing IL-2, TNF-α, and IFN-γ secretion from responder cells while they efficiently produced IL-4 and IL-10. These findings support the view of hormones (especially progesterone) as critical regulators of Treg in pregnancy [212]. Again pregnancy mediated hormonal changes have also lead to the hypothesis investigated here. Recently published data showed that pregnancy mediated changes of glucocorticoid levels lead to a change in lymphocyte numbers - an increase of Treg and decrease of Tcon - in the reproductive tract and uterus draining lymph nodes [3], suggesting the assumption that this will not be the only pregnancy mediated change. Instead the function of Treg could be modified as well with a high probability.

Also contradictory to other publications in the field the authors of the same study found Treg numbers to be reduced in the circulation in the second trimester of pregnancy [212]. This discrepancy to more recently published data could be explained by the fact that in new publications [3] as well as in the here present study Treg were extracted from secondary lymphatic organs rather than peripheral blood. Thus, different organs could be an explanation for different results.

Also these authors comment on the fact that the CD4+ CD25+ population (CD4^{dim} CD25^{high} were used to identify Treg in their study, CD4+ CD25+ were used in the here presented data) is no functionally or phenotypically homogenous cell population but consists of suppressor and also effector cells [212]. This demonstrates again the difficulty to accurately define the suppressive capacity of big groups of Treg.

Overall their results are in line with the here newly generated data that suppressive capacity of Treg extracted during pregnancy is found to be unchanged compared to cells extracted from non-pregnant donors. Thus, they encourage the perspective that pregnancy does not lead to functional changes in respect to Treg suppressive capacity.

It seems that higher numbers of Treg with a suppressive potential are sufficient to meat the changed requirements during pregnancy like e.g. necessity to limit effector Tcon and DC function in the decidua in order to protect the developing fetus [74,88].

However, the authors also point out that opposing data on Treg in pregnancy exist [86,210–212]. Thus they suggest a reevaluation of these opposing data [212]. They differ in important details like pregnancy time point, site of cell extraction, composition of cell sub-types and used analysis methods.

Other aspects of Treg function beside suppressive capacity were also analyzed for changes due to pregnancy.

4.2 Immunometabolism

Like suppressive capacity, metabolism is another functional aspect of Treg. Like any other cell Treg need to be supplied with energy via a cell type matching metabolic pathway to sustain function. Immunometabolism can sustain, amplify or even change the phenotype and thus the function of a cell [155]. Altered metabolism has been shown for diverse immune cell subsets and changes in T cell metabolism have been identified in MS patients [165,168,213].

Thus, as the second aim immunometabolism of Tcon and Treg extracted from mice in virgin and pregnant state was investigated.

Relative expression data analysis of Treg confirmed the previously identified upregulation of three genes specific to the pregnancy state. Among those were genes with already established function in Treg (e.g. IL-7). New potential was detected in the gene Cpt1a, encoding for a unique enzyme necessary in FAO pathway and OXPHOS.

Additionally, measurements of relative mitochondrial DNA amounts in Treg from pregnant versus non-pregnant donors further suggested the hypothesis of increased mitochondrial function during pregnancy and supported the hypothesis that increased metabolism is taking place during pregnancy.

Measurements of immunometabolism in Tcon and Treg originating from virgin or pregnant mice were carried out but did not support an increased usage of OXPHOS by Treg during pregnancy. OXPHOS was not found to be increased in Treg isolated from pregnant animals but in contrast showed higher activity in Tcon before and during pregnancy. Similarly, Tcon were also found to show higher activity of glycolysis.

This finding was surprising. Reasons could be that Tcon and Treg from pregnant animals could have lost their 'pregnant phenotype' already after the long cell extraction period outside the pregnancy environment, lasting around 5 hours. When the cells were finally put into the assay there might be no difference left to detect.
Also, Tcon performance might have been better because they were more stable and more active in the *in vitro* assays.
However, this remains speculative.

Another drawback of the Cell Mito Stress Test is, similar as discussed above for the suppression assays, that only a global measurement of a pool of cells can be generated by the assay. Energy metabolism is performed with 0.5×10^6 to 1×10^6 cells per well at once. The assay is at least run in triplicates. On average around 0.5×10^6 cells can be isolated per mouse, which is not enough for all parallel set ups. As explained above cells need to be pooled from spleen and different lymph nodes of several mice. Actually it is already challenging to have enough mice from different pregnancy states simultaneously, e.g. ~20-25 mice to isolate enough cells for all different parameters tested in parallel. Still, currently the Cell Mito Stress Test is the most accurate technique available and state of the art in measuring energy metabolism with as little external influence as possible. However, for the aims of this work, measurements on an individual cell level would be most desirable, but are currently impossible.

This means that potentially changes in relevant subgroups of Treg might exist, but were lost in the pool of cells analyzed together in one assay well.

Different metabolism measurements of e.g. fatty acid levels present in the blood of virgin versus pregnant mice via a high performance liquid chromatography had been envisaged but could not be carried out due to the fact that mice, especially the non-pregnant ones, have too little amounts of blood in their circulation for the clinical measurement standard.

Taken together, Tcon and Treg energy metabolism remains inconclusive during virgin and pregnant state.

In lymphocytes like CD8 cells, specific engagement of particular metabolic pathways had effectively been shown to promote particularly required lymphocyte function. In particular SRC was identified to render the establishment of CD8 memory cells. SPC and required OXPHOS were shown to be markedly controlled by the cytokine IL-15 and Cpta1 a metabolic enzyme controlling the rate-limiting step to FAO [165]. Furthermore the transformation of the ultrastructure of mitochondria via fission and fusion had been shown to determine metabolism directly and thus to distinctly influence cell function [164]. These mechanisms show distinctly that lymphocyte function controls metabolism and vice versa that metabolism controls lymphocyte function [155]. It was well conceivable that such mechanisms as shown for CD8+ memory cells and for activated effector and memory T cells might also govern the function of Treg during pregnancy and thus aid to mediate a protective phenotype during autoimmune disease. This hypothesis was especially supported by the finding that a changed expression pattern of Cpt1a was validated for Treg. Cpt1a was identified to also govern functional changes in CD8+ memory T cells. However, the described analyses suggest the assumption that such metabolic changes are not influencing Treg during pregnancy.

The here presented metabolism data are in contrast to reports showing that generally Treg are reported to use OXPHOS and FAO but not glycolysis for energy consumption [154,155,214]. Therefore the results indicate a reduced sustenance of Treg - at least in comparison to Tcon - with energy and thus indicate a reduced ability to fulfill their functions properly. Such reduced Treg functionality is a discrepancy to the noticed protection from autoimmune disease during pregnancy, possibly attributed to the actions of Treg, but is more in line with the above cited study showing that circulating Treg numbers and functionality are reduced during pregnancy [212].

Tcon in contrast are reported to generally relay on glycolysis as an activated effector cell. Not fully developed Tcon also rely on OXPHOS [154,155,214]. This could mean that the analyzed Tcon, which are extracted from secondary lymphoid organs, are no activated effector T cells, but instead are resting Tcon relying on OXPHOS. Developing Tcon that are being primed or perform TCR rearrangements and therefore - as shown by others - rather use glycolysis [154,155,214]. In this case the here presented data show regularly working processes in Tcon, but do not aid to unravel the enigma of how pregnancy mediates a temporal protection of autoimmune disease.

This leads to two deductions: Either Treg do not participate in the pregnancy mediated protection form autoimmunity, which is against admitted data by other researchers [3,8,108]. Or Treg are such a diverse population that one overall metabolic pattern generated for putatively different subtypes of Treg is not meaningful. The here analyzed Treg have been extracted from sites all over the mouse body and are not exclusively coming for the uterus draining lymph nodes, for which pregnancy changes are known [3,8,86]. Thus as stated above already individual Treg analyses are preferable, but are impossible today.

Strikingly, it was found out that glycolysis controls the induction of human peripherally induced Treg by modulating the expression of the exon 2 splicing variant of FOXP3. The authors of this study found out that such highly suppressive human pTreg are generated without the presence of exogenous regulatory-

type cytokines (like e.g. TGF or IL-10) following suboptimal stimulation of Tcon via the TCR. They are the highly glycolytic and metabolically active fraction of proliferating Tcon and depended for their induction on the expression of Foxp3 splicing variants containing exon 2 (FOXP3-E2). Among all splicing variants of human FOXP3, the variant produced from FOXP3-E2 has been shown to serve a major role in conferring suppressive ability to Treg. Therefore, they analyzed the metabolic determinants that led to the induction of FOXP3-E2 in human pTreg and found that glycolysis controlled the generation of pTreg cells through localization of the glycolytic enzyme enolase-1 to the nucleus. This is a finding which they also confirmed in studies with RRMS or Type 1 Diabetes (T1D) patients, in whom they observe impaired glycolysis and Foxp3-E2 expression in pTreg [213].

This study supports the belief that the here-analyzed Treg from pregnant donors are to a greater extend pTreg rather than tTreg. Thus the measurements from Treg also show standard levels of glycolysis in their metabolic profiles and not only OXPHOS. Still a gathered metabolic profile of different subtypes of cells is not very accurate, but as specific as possible with available techniques. Against this hypothesis is the fact the authors found out that the splice variant produced from FOXP3-E2, responsible for pTreg induction, is supposed to confer suppressive ability to Treg [213]. This is in contrast to the here-generated data.

The role of immunometabolism during pregnancy with regard to the molecular and cellular mechanisms remains ill defined. It is well known that maternal nutritional status and nutritional behavior influence pregnancy outcome and can influence the offspring's immunometabolism and also its health later in life, presumably also via epigenetic modifications. However the mechanistic link is still missing [215]. So far, detailed studies have either been performed on the nutritional behavior of mothers before and during pregnancy and its impact on fetal development and offspring's health later in life. Or detailed analyses have been performed on metabolism of different types of lymphocytes outside pregnancy. However, detailed mechanistic studies looking at particular lymphocyte type metabolism during pregnancy are lacking so far.

4.3 Treg specificity

The TCR specificity of a T cell is determining the way it is activated and thus its function [113,180,216,217]. Treg during pregnancy arise in a fetal antigen-specific manner [11,14], but can also act in an antigen-independent manner in the form of bystander suppression [115]. Thus unraveling possible specificity shifts, driven by pregnancy and a simultaneous EAE, bear the potential of understanding the mechanism of pregnancy-mediated EAE amelioration. Specificity changes happen on a clonal scale within the TCR repertoire. Activation happens in the first place on individual cell level but multiplies when individual cells expand clonally after activation. Expanding T cell clones are genetically identical and are present in higher numbers. Therefore TCR repertoire and clonality analyses help to identify how cells are activated and can give further information about how many cells share the same features under particular circumstances. This enables assumptions about the repertoire as a whole. Thus, clarifying the antigen-specificity of the TCR repertoire means investigating another main function of Treg.

The TCR repertoires of Tcon and Treg from virgin and pregnant mice were analyzed in a naïve state, EAE diseased state or in a MOG_{35-55} immunized and pregnant state. In the case of MOG_{35-55} immunization and a simultaneous pregnancy, mice were protected from the development of EAE disease symptoms, although the animals were immunized.

As a first measure clonality analyses were performed. They indicated a consistent clonal expansion in EAE samples in both Tcon and Treg. In contrast, pregnancy alone or in addition to immunization did not increase clonality. Clonal expansion induced by BALB/c-associated antigens, expressed by semi-allogeneic fetuses in the pregnant mice, could not be picked up.

Usage of CDR3aa was clearly driven by MOG_{35-55} peptide immunization, whereas the effect of virgin versus pregnant was only marginally recognizable. These results might be based on the fact that peptide immunization in EAE was specifically designed to give rise to supra-physiologic immune responses. Expansion of fetus-specific clones are traceable but to a much subtler extend [11]. From a clonal perspective this leads to the conclusion that pregnancy, with all the changes that it brings along, probably has a subtler effect on the TCR repertoire as previously anticipated. A change in Tcon clonality in EAE diseased versus pregnancy-protected animals was not detected, which implies that the protection during pregnancy cannot be explained by a complete blockage of clonal expansion of MOG_{35-55}-reactive Tcon clones. However, in the animals analyzed here, pregnancy resulted in a complete suppression of disease activity, which was previously shown to be accompanied by reduced immune cell infiltration into the CNS [3].

Analyses of the TRBV and TRBJ segment usage did not show induction of previously reported EAE-associated segments TRBV5, TRBV19, TRBV31 and TRBV20 along with EAE in the periphery. The highly EAE-associated TRBV segment 13.2 [118,184,186,201] was found to be enriched in CNS infiltrates and was only increased in Treg of pregnancy-protected EAE animals. These results indirectly suggest an expansion of EAE-related clonotypes in the Treg compartment, which is dependent on the presence of pregnancy. In order to further consolidate the indications of an expanded EAE-related Treg pool in pregnancy, more profound strategies to identify and track EAE-related clonotypes were explored.

An independent cohort of non-pregnant EAE mice was sampled and was sequenced as well. Unlike the first cohort this second one also contained CNS infiltrating cell samples. This new data set allowed determining the overlap of EAE-associated clonotypes across the periphery of individual mice, in periphery versus CNS within individuals and also across the CNS of individual mice. Overlap in the periphery was found to be limited, but frequencies of shared clonotypes increased towards the CNS. Strikingly, inter-individual overlap between CNS samples was extensive, which allowed the identification of 918 public EAE clonotypes appearing in at least two of the analyzed CNS. Further, these EAE clonotypes could be tracked in the primary cohort. From this tracking of the 918 CNS identified EAE-associated clonotypes in the main experimental cohort, clonotypes across pregnancy and EAE were assembled. A list of detected EAE-associated clonotypes was compiled. Other researchers can use this list as a resource and track EAE clonotypes in any other $MOG_{35–55}$-immunized C57BL/6 mouse cohort.

Comparable identification strategies might also be possible in human studies of autoimmunity and simultaneous pregnancy. However, access to CNS infiltrating cells in the human is practically impossible. Here cerebrospinal fluid (CSF) could be used or blood extracted lymphocytes could be re-stimulated *in vitro* with myelin peptide pools to identify MS specific clonotypes in a similar approach.

Tracking of the identified 918 EAE clonotypes in the primary dataset suggests that pregnancy is a required condition for the increase of EAE clonotypes in the Treg compartment. The tracking of 1,000 peripherally identified random clonotypes in the primary data set shows no dynamic across immunization, cell type and gestational stage. Thus it works as a negative control and demonstrates the specificity of the identified EAE clonotypes. These findings indicate that pregnancy can shift the EAE-specific immune response towards tolerance.

The rather big number of 918 clonotypes that were identified to be EAE clonotypes indicate that despite the fact that these are inter-individual comparisons, C57BL/6 mice regularly respond with a specific population wide 'public' pattern in their CNS to MOG_{35-55} immunization and thus that the presented results are robust findings.

A conceivable explanation of why identification was possible even in the periphery and also of the whole pregnancy protection phenomenon is that induced MOG_{35-55} antigen might be transported to the uterus draining lymph nodes and is then presented in the tolerogenic microenvironment of the uterus. Then the locally expanding numbers of Treg mediate their immunoregulatory effect, which is seen in MS and EAE. Hypothetically, also due to this sequence of processes the EAE clonotype signal could be picked up via sampling peripheral lymph nodes and performing TCR repertoire analysis. Yet, it remains unknown to which extend antigen-presenting cells deliver the $MOG_{35–55}$ epitope to these specific locations after a subcutaneous administration.

A further remarkable finding is the restricted usage of certain CDR3aa within Treg and Tcon, as seen in the distinct clustering of both cell types in CDR3aa-based multidimensional scaling and also in the heatmap of EAE clonotypes, where separate clonotype usage is identified in Tcon and Treg. These findings go along with other assessments identifying Tcon and Treg to clearly differ in clonal composition [118,218]. Thus the present data supports the notion that Tcon and Treg are recruited from different clonal pools during thymic development [219] and that trans-differentiation between both subtypes is limited [118].

As the results shown by the heatmap suggest the assumption that Treg and Tcon do not share exactly the same sequences this leaves room for the speculation that the concept of bystander activation could at least share a part of disease amelioration mediated potentially via EAE-associated Treg. EAE-associated Treg, activated through antigen with the sequences shown in the heatmap, might be able to suppress specific Tcon, which were not found, but might also be able to suppress T cells with other specificities. This has been shown to be the case in antigen-specific Treg that express a specific TCR after retroviral transduction. Further IL-2 production of neighboring effector cells could activate disease-modifying Treg to suppress local effectors. This depiction of soluble factors as mediators underlying bystander suppression are in favor of the fact that regulatory function is not solely made by Treg own actions [115].

In addition it should be stated accurately that the here-performed clonal analyses are in fact analyses of the TCR β chains only. A more profound TCR clonality analyses comprises information about the α and the corresponding β chain of the TCRs. Thus the here presented data show only one part of the situation. However, this part is very meaningful already. To also gain information about the corresponding α chain a pairSEQ approach should be performed [220]. This could refine TCR information and enables e.g. to conclude the respective peptide recognized by the individual TCR. However, the recognized peptide is not of primary interest to this study, as here the immunization peptide is known to be MOG_{35-55}.

Taken together, the data-driven analysis of the TCR β repertoire suggests that pregnancy is a prerequisite for the expansion of Treg that target EAE-related antigens. Autoantigen-specific Treg are powerful suppressors of autoreactive responses [78,140,176,177] and therefore the here newly generated results are potentially suited to explain parts of the strong protection from EAE during pregnancy. However, the targeted expansion of autoreactive Treg during pregnancy has to be independently validated and further investigated, including the exploration of the therapeutic potential in MS and other autoimmune diseases.

An expansion of EAE-recognizing Treg mediated by pregnancy is a very specific effect leading to the protection from autoimmunity during pregnancy. At the beginning of this work much broader effects had been hypothesized, like a general increase of Treg suppressive capacity or increased overall Treg metabolism. Concluding from the here-generated data the means of pregnancy to protect an individual from CNS autoimmunity is established via a very precise clonal expansion of Treg, which have EAE specific receptors. This offers an example par excellence to understand endogenous and antigen-specific immune tolerance induction and might have the potential to further unravel autoimmune disease modifying mechanisms.

When taking together all three investigated aspects of Treg functionality, suppressive capacity and metabolism remain unresolved during pregnancy. The TCR repertoire data indeed suggest clonotype specific - rather than global - immunoregulation during pregnancy that might contribute to amelioration of EAE. The TCR repertoire analyses begin to shed light on the underlying mechanisms of the interaction of autoimmunity and pregnancy and their effect on the TCR repertoire in Tcon and Treg.

Further, the here proposed cell-specific and even antigen-specific mechanisms contributing to EAE disease amelioration during pregnancy might be an explanation for why it has been difficult to encompassingly mimic the protective effect of pregnancy in MS with global immunomodulators like estrogens [101,205]. However, further work on the targeted expansion of autoreactive Treg during pregnancy is required.

A potential next step in order to re-identify antigen-specific Treg during pregnancy could be the use of a MOG tetramer. A tetramer is a MHC/peptide multimer, gained via biotinylation, that is capable of engaging more than one copy of the TCR on the surface of a T cell. It thereby increases the avidity of the interaction [221]. Thus attempts to re-identify MOG-reactive cells in samples taken from virgin versus pregnant could potentially identify MOG specific clones and show a difference between the groups of mice. Still a MOG tetramer staining in a fresh cohort of mice in peripheral samples and without pre-enrichment of tetramer-positive cells will bear problems. This re-identification would relay on the identification of first Foxp3+ cells and subsequently on the identification of activated lymphocytes (CD44+) and MOG tetramer positive cells within the Foxp3+ population. However, Foxp3+ cells make up a little cell population of about 10% of the CD4+ cells of a mouse. The subsequent identification of CD44+ and MOG tetramer positive cells in the Foxp3+ population will be rather limited.

Furthermore a purchasable MOG tetramer also needs to proof functionality in terms of showing reliable results and actual specificity for the MOG-specific TCRs.

However, the in this thesis identified and expanded EAE-associated clonotypes are not necessarily MOG_{35-55}-specific, which is the reason why they are called ‘EAE clonotypes’ and which is also the reason why they were traceable only via this complex strategy. A purchasable MOG_{38-49} tetramer [222] covers only a part of the used MOG_{35-55} peptide and further covers only parts of the clonally expanded EAE clone

population. Many alongside expanded antigen patterns cannot be detected with such a tetramer. Due to their restricted specificity tetramers are only able to stain individual CDR3 regions. Thus, only a small number of the over 800 identified EAE clonotypes could be detected per tetramer. Possibly, using a pool of myelin specific tetramers could be successful.

Another conceivable possibility to re-identify MOG-reactive clones is an *in vitro* re-stimulation of Tcon and Treg in culture taken from virgin versus pregnant mice with MOG peptide. Here again the restricted specificity of the MOG_{38-55} tetramer constitutes a limitation. MOG_{35-55} peptide usage would similar to the *in vivo* situation in the EAE mouse model re-stimulate and lead to the increase of a whole spectrum of EAE-associated clonotypes in the *in vitro* cultures. But again only a fraction of these re-stimulated EAE associated clones could be detected with a MOG_{38-55} tetramer staining. Expanded cells from the cultures might appear to be rather unspecific and show only limited MOG_{38-55} specificity.

Because a comprehensive recording of multiple EAE clonotypes across pregnancy and EAE can only be achieved by TCR sequencing; to date this appears to be the only method allowing this kind of analyses.

More approaches by other researchers to track disease modifying myelin-specific Tcon and Treg during EAE, but outside pregnancy, with a MOG_{35-55}-tetramer in *Foxp3gfp* knock in mice remained inefficient so far. MOG-specific Treg were shown to be expanded in the periphery and to accumulate in the CNS, but did not eliminate EAE disease. However, Treg isolated from the CNS were shown to suppress MOG-specific Tcon but proved ineffective in suppressing Tcon extracted from the CNS *in vitro*. The authors of the study found proof for the fact that this is not due to improper potential of the CNS-derived Treg but due to the CNS-derived Tcon secreting interleukin 6 (IL-6) and tumor necrosis factor (TNF), rendering the Treg ineffective [223].

This leads to the assumption that besides an EAE specificity of Treg the inflammatory potential of the tissue has to be controlled as well in order to lead to disease amelioration [223]. Therefore other aspects beside the here manifested increase in EAE specific Treg during EAE and a simultaneous pregnancy involving a modification of the local cytokine milieu are likely.

Contrary to this concept it is possible that Treg from pregnant EAE mice might still be able to control peripheral Tcon before entering the CNS at all and thus mediating protection from EAE disease.

Still another method to focus also more on the *in vivo* relevance of the observed pregnancy mediated disease protection could be the use of an adoptive transfer model, similar to work done in a rheumatoid arthritis mouse model [78]. Here CD4+ cells from virgin versus pregnant mice are isolated and transferred into CD4+ depleted mice in which an EAE is induced afterwards. This should hypothetically show that mice that receive CD4+ cell pools extracted from pregnant EAE mice and containing Treg with EAE clonotypes should be protected from EAE. Mice receiving CD4+ cells extracted from virgin EAE mice do not contain increased Treg with EAE clonotypes and thus might get a normal EAE disease. With a similar transfer model the authors of the rheumatoid arthritis work show that Treg from pregnant donors protect recipients from autoimmune arthritis [78]. An exposure of the mother to paternal transplantation antigens prior to pregnancy induces a drastic immune response against the graft. Only in the context of pregnancy this process was suppressed. The authors suggests that in their model the concentration of highly antigen-specific Treg localized in the uterus mediates suppression of the anti-fetal immune response [224].

Furthermore, outside pregnancy adoptive transfer of lymphocytes with engineered antigen-specific cells (TCR) that recognize e.g. tumor antigens have revolutionized cancer treatment. As a next generation of treatment outside cancer adoptive transfer of Treg is progressing as a treatment in autoimmune diseases like Type 1 diabetes and rheumatoid artists and graft versus host disease [225].

Adoptive transfer of polyclonal Treg makes use of these cells as a potent disease treatment to repair or replace Treg in e.g. the autoimmune disease T1D in the attempt to reverse autoimmunity and to protect the remaining insulin-producing β cells. In this study Treg are isolated and expanded from patients with T1D and are re-infused. Interestingly after stimulation with anti-CD3 and anti-CD28 the Treg retained their T cell receptor diversity and showed enhanced functional activity; they increased in numbers and remained stable for key parameters (e.g. Foxp3, CD25) over a long time in the transferred individuals [225,226].

Potentially, adoptively transferred antigen-specific Treg could also work as a treatment strategy in MS and potentially reduce lymphocyte activation and inflammation inside the CNS. In order to be able to generate effective antigen-specific Treg, pregnancy provides a small window into the body-own processes and to identify such potentially effective antigen-specific TCRs. However, plenty additional research is needed to potentially lead to such developments that are dreamed of by many. They have potential to be exploited for successful therapy development of autoimmune diseases like multiple sclerosis.

The present investigation of the mouse TCR repertoire during EAE and pregnancy could be continued for the time point after pregnancy. For an insightful understanding of the processes during pregnancy it should be vital to define pregnancy-mediated progresses via analysis before and after pregnancy. It can be anticipated that the increase of EAE-specific Treg clonotypes during EAE and pregnancy might decrease after pregnancy. However, it is also possible that EAE-specific Treg clonotypes persist in mice in numbers that are at least higher than before pregnancy and can be reactivated in subsequent pregnancies or autoimmune attacks again. However this currently remains speculative.

Overall, this thesis further suggests that amelioration of the MS mouse model EAE during pregnancy could be, at least in parts, a Treg mediated effect. By detection of an increase in EAE clonotype-specific Treg during pregnancy, a potential mechanism for pregnancy-associated protection in EAE was identified.

5. Summary

Autoimmune disease activity in multiple sclerosis (MS) and its animal model experimental autoimmune encephalomyelitis (EAE) is temporarily suppressed by pregnancy. However, after delivery women and mice develop an overshooting disease course, before returning to the pre-pregnancy level. Regulatory T cells (Treg) play a pivotal role in controlling both feto-reactive T cells during pregnancy and auto-reactive T cells in autoimmune diseases. However, it remains unknown whether the protective phenotype is predominantly mediated by Treg. And if this is the case, whether it is due to the Treg exerting increased functionality during pregnancy or whether it is due to antigen-specific regulation of disease-causing conventional T cells (Tcon) and immuno-suppressive Treg during pregnancy. Immune protection of the semi-allogenic fetus is achieved by local expansion of Treg in the reproductive tract and draining lymph tissue during pregnancy.

The aim of this work is to unravel whether increased Treg numbers during pregnancy are accompanied by enhanced Treg functionality. Therefore three main Treg functionalities were analyzed:

Suppressive capacity and metabolism were analyzed in cells extracted from virgin or pregnant mice. The suppressive capacity of bulk Treg isolated from pregnant animals was not found to be increased in comparison to Treg from non-pregnant donors.

Also immunometabolism measurements showed oxidative phosphorylation (OXPHOS) not to be increased in Treg isolated from pregnant animals, but in contrast OXPHOS as well as glycolysis was found to show a higher activity in Tcon. These assays analyzed global function of pooled Treg.

Further, systematic analyses of the clonal T cell receptor (TCR) β repertoire of Tcon and Treg in EAE and pregnancy were performed. This was conducted to understand whether antigen-specificity is a relevant driving force of pregnancy-associated protection from autoimmunity. It was shown that EAE, but not pregnancy, robustly increases the TCR repertoire clonality in both peripheral Tcon and Treg. Pregnancy is required for the expansion of Treg harboring the dominant EAE-associated TRBV chain 13.2 and increases the frequency of EAE-associated clonotypes within the Treg compartment.
Thus, pregnancy supports the expansion of Treg clonotypes that are equipped to recognize EAE-associated antigens. These Treg are thereby particularly suited to control corresponding encephalitogenic Tcon responses and likely contribute to pregnancy-associated protection in autoimmunity.

This thesis further suggests that the amelioration of the disease course of the MS mouse model EAE during pregnancy is, at least in parts, a Treg mediated effect. This work provides potent indications that the mechanism leading to changes in Treg potentially happens due to increases in EAE clonotype-specific Treg during pregnancy. Further explorations of a targeted expansion of autoreactive Treg during pregnancy are needed. They have the potential to lead to a treatment strategy in MS and other autoimmune diseases.

Zusammenfassung

Die Aktivität der Autoimmunerkrankung Multiple Sklerose (MS) und ihres Tiermodells Experimentelle autoimmune Enzephalomyelitis (EAE) wird durch eine Schwangerschaft vorübergehend vermindert. Nach der Schwangerschaft entwickeln Frauen und Mäuse jedoch einen verstärkten Krankheitsverlauf, bevor sie zu dem Level von vor der Schwangerschaft zurückkehren. Es ist bisher unverstanden, ob der protektive Phänotyp hauptsächlich durch regulatorische T Zellen (Treg) vermittelt wird. Wenn dies der Fall ist, bleibt unklar, ob dies durch eine gesteigerte Funktionalität der Treg während der Schwangerschaft geschieht oder durch eine antigen-spezifische Regulation von krankheitsvermittelnden konventionellen T Zellen (Tcon) und immun-suppressiven Treg während der Schwangerschaft. Eine Immunprotektion des semi-allogenen Fetus wird durch eine lokale Zunahme von Treg in den Reproduktionsorganen und drainierenden Lymphknoten erreicht.

Das Ziel dieser Arbeit ist es herauszufinden, ob eine höhere Zahl an Treg auch von gesteigerter Funktionalität der Treg begleitet ist. Dazu wurden drei Hauptfunktionen von Treg analysiert:

Suppressive Kapazität und Metabolismus wurden in Zellen analysiert, die von jungfräulichen oder schwangeren Mäusen entnommen wurden. Festgestellt wurde, dass die suppressive Kapazität in Treg-Massen, isoliert aus schwangeren im Vergleich zu nicht schwangeren Mäusen, nicht gesteigert ist.

Ebenfalls zeigten Messungen des Immun-Metabolismus, dass oxidative Phosphorylierung (OXPHOS) in Treg aus schwangeren Tieren nicht zugenommen hat. Stattdessen zeigen OXPHOS sowie auch Glykolyse eine gesteigerte Aktivität in Tcon. Diese Untersuchungen analysieren die Funktion von gepoolten Treg.

Weiterhin wurden klonale Analysen des T Zell Rezeptor (TCR) β Repertoires von Tcon und Treg in EAE und der Schwangerschaft durchgeführt. Dies geschah um zu verstehen, ob Antigen-Spezifität eine treibende Kraft ist hinter dem schwangerschafts-vermittelten Schutz vor Autoimmunität. Es konnte gezeigt werden, dass EAE, aber nicht Schwangerschaft, sehr robust das TCR Repertoire von peripheren Tcon und Treg steigert. Schwangerschaft ist nötig für eine Expansion von Treg, denen die EAE-assoziierte dominante TRBV Kette 13.2 eigen ist. Schwangerschaft erhöht auch die Frequenz von EAE-assoziierten Klonotypen innerhalb der Gruppe der Treg.
Daher unterstützt Schwangerschaft eine Expansion von Treg Klonotypen, die so ausgestattet sind, dass sie EAE-assoziierte Antigene erkennen können. Diese Treg sind daher besonders geeignet, um korrespondierende enzephalitogene Tcon-Antworten zu kontrollieren und sie haben höchstwahrscheinlich Teil an der schwangerschafts-vermittelten Protektion vor Autoimmunität.

Diese Arbeit weist weiter darauf hin, dass die Verminderung des Krankheitsverlaufes im MS-Mausmodell EAE während der Schwangerschaft – zumindest in Anteilen – ein Treg vermittelter Effekt ist. Sie liefert starke Anhaltspunkte dafür, dass der Mechanismus, der zu Veränderungen innerhalb der Treg führt, potentiell durch eine Zunahme von EAE klonotypen-spezifischen Treg während der Schwangerschaft passiert. Weitergehende Untersuchungen zur gezielten Expansion von autoreaktiven Treg während der Schwangerschaft sind nötig. Sie haben das Potential, zur Entwicklung von Behandlungsstrategien von MS und anderen Autoimmunerkrankungen zu führen.

6. References

1. Dendrou, C. A., Fugger, L. & Friese, M. A. Immunopathology of multiple sclerosis. *Nat. Rev. Immunol.* **15,** 545–558 (2015).

2. Confavreux, C., Hutchinson, M., Hours, M. M., Cortinovis-Tourniaire, P. & Moreau, T. Rate of Pregnancy-Related Relapse in Multiple Sclerosis. *N. Engl. J. Med.* **339,** 285–291 (1998).

3. Engler, J. B. *et al.* Glucocorticoid receptor in T cells mediates protection from autoimmunity in pregnancy. *Proc. Natl. Acad. Sci.* **114,** E181–E190 (2017).

4. Gatson, N. N. *et al.* Induction of pregnancy during established EAE halts progression of CNS autoimmune injury via pregnancy-specific serum factors. *J. Neuroimmunol.* **230,** 105–113 (2011).

5. Finkelsztejn, A., Brooks, J. B. B., Paschoal, F. M. J. & Fragoso, Y. D. What can we really tell women with multiple sclerosis regarding pregnancy? A systematic review and meta-analysis of the literature. *BJOG* **118,** 790–797 (2011).

6. Patas, K., Engler, J. B., Friese, M. A. & Gold, S. M. Pregnancy and multiple sclerosis: Feto-maternal immune cross talk and its implications for disease activity. *J. Reprod. Immunol.* **97,** 140–146 (2013).

7. Fontenot, J. D., Gavin, M. A. & Rudensky, A. Y. Foxp3 programs the development and function of CD4+CD25+ regulatory T cells. *Nat. Immunol.* **4,** 330–336 (2003).

8. Schumacher, A. & Zenclussen, A. C. Regulatory T Cells: Regulators of Life. *Am. J. Reprod. Immunol.* **72,** 158–170 (2014).

9. Tilburgs, T. *et al.* Differential distribution of CD4+CD25bright and CD8+CD28− T-cells in decidua and maternal blood during human pregnancy. *Placenta* **27,** S47–S53 (2006).

10. Aluvihare, V. R., Kallikourdis, M. & Betz, A. G. Regulatory T cells mediate maternal tolerance to the fetus. *Nat. Immunol.* **5,** 266–271 (2004).

11. Rowe, J. H., Ertelt, J. M., Xin, L. & Way, S. S. Pregnancy imprints regulatory memory that sustains anergy to fetal antigen. *Nature* **490,** 102–106 (2012).

12. Erlebacher, A. Mechanisms of T cell tolerance towards the allogeneic fetus. *Nat. Rev. Immunol.* **13,** 23–33 (2013).

13. Tsuda, S., Zhang, X., Hamana, H., Shima, T. & Ushijima, A. Clonally Expanded Decidual Effector Regulatory T Cells Increase in Late Gestation of Normal Pregnancy, but Not in Preeclampsia, in Humans. *Front. Immunol.* **9,** 1–10 (2018).

14. Kahn, D. A. & Baltimore, D. Pregnancy induces a fetal antigen-specific maternal T regulatory cell response that contributes to tolerance. *Proc. Natl. Acad. Sci. U. S. A.* **107,** 9299–9304 (2010).

15. Rowe, J. H., Ertelt, J. M., Aguilera, M. N., Farrar, M. a. & Way, S. S. Foxp3 + regulatory T cell expansion required for sustaining pregnancy compromises host defense against prenatal bacterial pathogens. *Cell Host Microbe* **10,** 54–64 (2011).

16. Charcot, J. M. Histologie de la sclérose en plaques. *Gaz. des Hop.* **41,** 554–555 (1868).

17. Atlas of MS 2013 https://www.msif.org/about-us/who-we-are-and-what-we-do/advocacy/atlas (2019-01-25) (2013).

18. Whitacre, C. C. *et al.* A gender gap in autoimmunity. *Science* **283,** 1277–1278 (1999).

19. Noseworthy, J. H., Lucchinetti, C., Rodriguez, M. & Weinshenker, B. G. Multiple Sclerosis. *N. Engl. J. Med.* **343,** 938–952 (2000).

20. Compston, A. & Coles, A. Multiple sclerosis. *Lancet* **372,** 1502–1517 (2008).

21. International Multiple Sclerosis Genetics Consortium (IMSGC) *et al.* Analysis of immune-related loci identifies 48 new susceptibility variants for multiple sclerosis. *Nat. Genet.* **45,** 1353–1360 (2013).

22. Moutsianas, L. *et al.* Class II HLA interactions modulate genetic risk for multiple sclerosis. *Nat. Genet.* **47,** 1107–1113 (2015).

23. Martin, R. HLA class I: friend and foe of multiple sclerosis. *Nat. Med.* **14,** 1150–1151 (2008).

24. Friese, M. A. *et al.* Opposing effects of HLA class I molecules in tuning autoreactive CD8+ T cells in multiple sclerosis. *Nat. Med.* **14,** 1227–1235 (2008).

25. International Multiple Sclerosis Genetics Consortium (IMSGC) *et al.* Genetic risk and a primary role for cell-mediated immune mechanisms in multiple sclerosis. *Nature* **476,** 214–219 (2011).

26. Boyman, O. & Sprent, J. The role of interleukin-2 during homeostasis and activation of the immune system. *Nat. Rev. Immunol.* **12,** 180–190 (2012).

27. Gregory, S. G. *et al.* Interleukin 7 receptor α chain (IL7R) shows allelic and functional association with multiple sclerosis. *Nat. Genet.* **39,** 1083–1091 (2007).

28. Hartmann, F. J. *et al.* Multiple sclerosis-associated IL2RA polymorphism controls GM-CSF production in human TH cells. *Nat. Commun.* **3,** 1–10 (2014).

29. Munger, K. L. *et al.* Vitamin D intake and incidence of multiple sclerosis. *Neurology* **62,** 60–65 (2004).

30. Ghareghani, M., Reiter, R. J., Zibara, K. & Farhadi, N. Latitude, Vitamin D, Melatonin, and Gut Microbiota Act in Concert to Initiate Multiple Sclerosis: A New Mechanistic Pathway. *Front. Immunol.* **9,** (2018).

31. Elian, M., Nightingale, S. & Dean, G. Multiple sclerosis among the United Kingdom-born children of immigrants from the West Indies. *J. Neurol. Neurosurg. Psychiatry* **53,** 906–911 (1990).

32. Dean, G. & Kurtzke, J. F. On the Risk of Multiple Sclerosis According to Age at Immigration to South Africa. *Br. Med. J.* **3,** 725–729 (1971).

33. Handel, A. E. *et al.* An updated meta-analysis of risk of multiple sclerosis following infectious mononucleosis. *PLoS One* **5,** e12496 (2010).

34. Marrodan, M., Alessandro, L., Farez, M. F. & Correale, J. The role of infections in multiple sclerosis. *Mult. Scler. J.* Epub ahead of print (2919-01-28) (2019).

35. Goverman, J. Autoimmune T cell responses in the central nervous system. *Nat. Rev. Immunol.* **9,** 393–407 (2009).

36. Münz, C., Lünemann, J. D., Getts, M. T., Miller, S. D. & Blink, S. E. Antiviral immune responses: triggers of or triggered by autoimmunity? *Nat. Rev. Immunol.* **9,** 246–258 (2009).

37. Sundqvist, E. *et al.* Cytomegalovirus seropositivity is negatively associated with multiple sclerosis. *Mult. Scler. J.* **20,** 165–173 (2014).

38. Ramien, C. *et al.* Sex effects on inflammatory and neurodegenerative processes in multiple sclerosis. *Neurosci. Biobehav. Rev.* **67,** 137–146 (2016).

39. Dunn, S. E., Gunde, E. & Lee, H. Sex-Based Differences in Multiple Sclerosis (MS): Part II: Rising Incidence of Multiple Sclerosis in Women and the Vulnerability of Men to Progression of this Disease. *Curr. Top. Behav. Neurosci.* **26,** 57–86 (2015).

40. Hedström, A. K. *et al.* Smoking and two human leukocyte antigen genes interact to increase the risk for multiple sclerosis. *Brain* **134,** 653–664 (2011).

41. Yatsunenko, T. *et al.* Human gut microbiome viewed across age and geography. *Nature* **486,** 222–227 (2012).

42. Bagur, M. J. *et al.* Influence of Diet in Multiple Sclerosis: A Systematic Review. *Adv. Nutr.* **8,** 463–472 (2017).

43. Chu, F. *et al.* Gut microbiota in multiple sclerosis and experimental autoimmune encephalomyelitis: current applications and future perspectives. *Mediators Inflamm.* **2018,** (2018).

44. Kolber, P. *et al.* Aktuelles zur Therapieumstellung bei Multipler Sklerose. *Nervenarzt* **86,** 1236–1247 (2015).

45. Klotz, L., Meuth, S. G. & Wiendl, H. Immune mechanisms of new therapeutic strategies in multiple sclerosis-A focus on alemtuzumab. *Clin. Immunol.* **142,** 25–30 (2012).

46. Kappos, L. *et al.* A Placebo-Controlled Trial of Oral Fingolimod in Relapsing Multiple Sclerosis. *N. Engl. J. Med.* **362,** 387–401 (2010).

47. Yednock, T. A. *et al.* Prevention of experimental autoimmune encephalomyelitis by antibodies against alpha 4 beta 1 integrin. *Nature* **356,** 63–66 (1992).

48. Hauser, S. L. *et al.* Ocrelizumab versus Interferon Beta-1a in Relapsing Multiple Sclerosis. *N. Engl. J. Med.* **376,** 221–234 (2017).

49. Haghikia, A., Hohlfeld, R., Gold, R. & Fugger, L. Therapies for multiple sclerosis: Translational achievements and outstanding needs. *Trends Mol. Med.* **19,** 309–319 (2013).

50. Kornberg, M. D. *et al.* Dimethyl fumarate targets GAPDH and aerobic glycolysis to modulate immunity. *Science* **360,** 449–453 (2018).

51. Traub, J. *et al.* Dimethyl fumarate impairs differentiated B cells and fosters central nervous system integrity in treatment of multiple sclerosis. *Brain Pathol.* Epub ahead of print (2019-03-19) (2019).

52. Gold, R. *et al.* Placebo-Controlled Phase 3 Study of Oral BG-12 for Relapsing Multiple Sclerosis. *New Engl. J. Med.* **367,** 1098–1107 (2012).

53. Aharoni, R. The mechanism of action of glatiramer acetate in multiple sclerosis and beyond. *Autoimmun. Rev.* **12,** 543–553 (2013).

54. Prinz, M. *et al.* Distinct and Nonredundant In Vivo Functions of IFNAR on Myeloid Cells Limit Autoimmunity in the Central Nervous System. *Immunity* **28,** 675–686 (2008).

55. Bruneau, J.-M. *et al.* Purification of human dihydro-orotate dehydrogenase and its inhibition by A77 1726, the active metabolite of leflunomide. *Biochem. J.* **336,** 299–303 (1998).

56. Kirk, P. & Compston, A. The effect of methylprednisolone on lymphocyte phenotype and function in patients with multiple sclerosis. *J. Neuroimmunol.* **26,** 1–8 (1990).

57. Reichardt, H. M., Gold, R. & Lühder, F. Glucocorticoids in multiplesclerosis and experimental autoimmune encephalomyelitis. *Expert Rev. Neurother.* **6,** 1657–1670 (2006).

58. Correale, J., Arias, M. & Gilmore, W. Steroid Hormone Regulation of Cytokine Secretion by Proteolipid Protein-Specific CD4+ T Cell Clones Isolated from Multiple Sclerosis Patients and Normal Control Subjects. *J. Immunol.* **15,** 183–194 (2018).

59. Kim, M. J. *et al.* Combined Treatment with Methylprednisolone and Human Bone Marrow-Derived Mesenchymal Stem Cells Ameliorate Experimental Autoimmune Encephalomyelitis. *Tissue Eng. Regen. Med.* **15,** 183–194 (2018).

60. Abbas, A. K., Lichtman, A. H. & Pillai, S. *Basic Immunology - Functions and disorders of the immune system*. 4th ed. Philadelphia: Elsevier (2014).

61. Hellings, N. *et al.* T-cell reactivity to multiple myelin antigens in multiple sclerosis patients and healthy controls. *J. Neurosci. Res.* **63,** 290–302 (2001).

62. Bielekova, B. *et al.* Expansion and Functional Relevance of High-Avidity Myelin-Specific CD4+ T Cells in Multiple Sclerosis. *J. Immunol.* **172,** 3893–3904 (2014).

63. Daneman, R. & Prat, A. The Blood-Brain Barrier. *Cold Spring Harb. Perspect. Biol.* **7,** 1–23 (2015).

64. Stuart, G. & Krikorian, K. S. The neuro-paralytic accidents of anti-rabies treatment. *Ann. Trop. Med.* **22,** 327–377 (1928).

65. Bassoe, Peter & Grinker, R. R. Human rabies and rabies vaccine encephalomyelitis. *Arch. Neurol. Psych.* **23,** 1138–1160 (1930).

66. Baxter, A. G. The origin and application of experimental autoimmune encephalomyelitis. *Nat. Rev. Immunol.* **7,** 904–912 (2007).

67. Gold, R., Linington, C. & Lassmann, H. Understanding pathogenesis and therapy of multiple sclerosis via animal models: 70 years of merits and culprits in experimental autoimmune encephalomyelitis research. *Brain* **129,** 1953–1971 (2006).

68. Stromnes, I. M. & Goverman, J. M. Active induction of experimental allergic encephalomyelitis. *Nat. Protoc.* **1,** 1810–1819 (2006).

69. Steinman, L. & Zamvil, S. S. How to successfully apply animal studies in experimental allergic encephalomyelitis to research on multiple sclerosis. *Ann. Neurol.* **60,** 12–21 (2006).

70. Lassmann, H. & Bradl, M. Multiple sclerosis: experimental models and reality. *Acta Neuropathol.* **133,** 223–244 (2017).

71. Kara, E. E. *et al.* CCR2 defines in vivo development and homing of IL-23-driven GM-CSF-producing Th17 cells. *Nat. Commun.* **6,** 1–17 (2015).

72. Krishnamoorthy, G. & Wekerle, H. EAE: An immunologist's magic eye. *Eur. J. Immunol.* **39,** 2031–2035 (2009).

73. Willmann, R. *Der Stammbaum des Lebens*. Göttingen: Planet Poster Editions (2004).

74. Arck, P. C. & Hecher, K. Fetomaternal immune cross-talk and its consequences for maternal and offspring's health. *Nat. Med.* **19,** 548–556 (2013).

75. Sakaguchi, S., Yamaguchi, T., Nomura, T. & Ono, M. Regulatory T Cells and Immune Tolerance. *Cell* **133,** 775–787 (2008).

76. Billingham, R. E., Brent, L. & Medawar, P. B. Actively acquired tolerance of foreign cells. *Nature* **172,** 603–606 (1953).

77. Trowsdale, J. & Betz, A. G. Mother's little helpers: mechanisms of maternal-fetal tolerance. *Nat. Immunol.* **7,** 241–246 (2006).

78. Munoz-Suano, A., Kallikourdis, M., Sarris, M. & Betz, A. G. Regulatory T cells protect from autoimmune arthritis during pregnancy. *J. Autoimmun.* **38,** J103–J108 (2012).

79. Robinson, D. P. & Klein, S. L. Pregnancy and pregnancy-associated hormones alter immune responses and disease pathogenesis. *Horm. Behav.* **62,** 263–271 (2012).

80. Voskuhl, R. R. & Gold, S. M. Sex-related factors in multiple sclerosis susceptibility and progression. *Nat. Rev. Neurol.* **8,** 255–263 (2012).

81. Chan, J. *et al.* Glucocorticoid-induced apoptosis in human decidua: A novel role for 11β-hydroxysteroid dehydrogenase in late gestation. *J. Endocrinol.* **195,** 7–15 (2007).

82. Kim, M. R. *et al.* Progesterone-dependent release of transforming growth factor-beta1 from epithelial cells enhances the endometrial decidualization by turning on the Smad signalling in stromal cells. *Mol. Hum. Reprod.* **11,** 801–808 (2005).

83. Voskuhl, R. R. & Gold, S. M. Sex-related Factors in Multiple Sclerosis: Genetic, Hormonal and Environmental Contributions. *Nat. Rev. Neurol.* **8,** 255–263 (2012).

84. Zenclussen, M. L. *et al.* The persistence of paternal antigens in the maternal body is involved in regulatory T-cell expansion and fetal–maternal tolerance in murine pregnancy. *Am. J. Reprod. Immunol.* **63,** 200–208 (2010).

85. Mjösberg, J., Berg, G., Jenmalm, M. C. & Ernerudh, J. FOXP3+ regulatory T cells and T helper 1, T helper 2, and T helper 17 cells in human early pregnancy decidua. *Biol. Reprod.* **82,** 698–705 (2010).

86. Zhao, J. X., Zeng, Y. Y. & Liu, Y. Fetal alloantigen is responsible for the expansion of the CD4(+)CD25(+) regulatory T cell pool during pregnancy. *J. Reprod. Immunol.* **75,** 71–81 (2007).

87. Prabhudas, M. *et al.* Immune mechanisms at the maternal-fetal interface: perspectives and challenges. *Nat. Immunol.* **16,** 328–334 (2015).

88. Collins, M. K., Tay, C.-S. & Erlebacher, A. Dendritic cell entrapment within the pregnant uterus inhibits immune surveillance of the maternal/fetal interface in mice. *J. Clin. Invest.* **119,** 2062–2073 (2009).

89. Nancy, P. *et al.* Chemokine gene silencing in decidual stromal cells limits T cell access to the maternal-fetal interface. *Science* **336,** 1317–1321 (2012).

90. Rieger, L. *et al.* Specific subsets of immune cells in human decidua differ between normal pregnancy and preeclampsia - a prospective observational study. *Reprod. Biol. Endocrinol.* **7,** 1–11 (2009).

91. Erlebacher, A. Immunology of the Maternal-Fetal Interface. *Annu. Rev. Immunol.* **31,** 387–411 (2013).

92. Aghaeepour, N. *et al.* An immune clock of human pregnancy. *Sci. Immunol.* **2,** 1–12 (2017).

93. Krause, M. L. & Makol, A. Management of rheumatoid arthritis during pregnancy: Challenges and solutions. *Open Access Rheumatol. Res. Rev.* **8,** 23–36 (2016).

94. Buchel, E., Werner, V. S., Nevens, F. & Fevery, J. Improvement of autoimmune hepatitis during pregnancy followed by flare-up after delivery. *Am. J. Gastroenterol.* **97,** 3160–3165 (2002).

95. Chiam, N. P. Y., Hall, A. J. H., Stawell, R. J., Busija, L. & Lim, L. L. P. The course of uveitis in pregnancy and postpartum. *Br. J. Ophthalmol.* **97,** 1284–1288 (2013).

96. Wetherhead, S., Robson, S. C. & Reynolds, N. J. Management of psoriasis in pregnancy. *BMJ* **334,** 1218–1220 (2007).

97. Lateef, A. & Petri, M. Managing lupus patients during pregnancy. *Best Pract. Res. Clin. Rheumatol.* **27,** 435–447 (2013).

98. Vargas, R., Repke, J. T. & Ural, S. H. Type 1 Diabetes mellitus and pregnancy. *Rev. Obstet. Gynacology* **3,** 92–100 (2010).

99. Roullet, E. *et al.* Pregnancy and multiple sclerosis: Longitudinal study of 125 remittent patients. *J. Neurol. Neurosurg. Psychiatry* **56,** 1062–1065 (1993).

100. Hutchinson, M. Pregnancy in multiple sclerosis. *J. Neurol. Neurosurg. Psychiatry* **56,** 1043–1045 (1993).

101. Voskuhl, R. R. *et al.* Estriol combined with glatiramer acetate for women with relapsing-remitting multiple sclerosis: A randomised, placebo-controlled, phase 2 trial. *Lancet Neurol.* **15,** 35–46 (2016).

102. Kipp, M. & Beyer, C. Impact of sex steroids on neuroinflammatory processes and experimental multiple sclerosis. *Front. Neuroendocrinol.* **30,** 188–200 (2009).

103. Gold, S. M. & Voskuhl, R. R. Estrogen and testosterone therapies in multiple sclerosis. *Prog. Brain Res.* **175,** 239–251 (2009).

104. Leber, A., Teles, A. & Zenclussen, A. C. Regulatory T Cells and Their Role in Pregnancy. *Am. J. Reprod. Immunol.* **63,** 445–459 (2010).

105. Shevach, E. M. Foxp3+T regulatory cells: Still many unanswered Questions-A perspective after 20 years of study. *Front. Immunol.* **9,** 1–9 (2018).

106. Sakaguchi, S., Sakaguchi, N., Asano, M., Itoh, M. & Toda, M. Immunologic self- tolerance maintained by activated T cells expressing IL-2 receptor alpha-chains (CD25). Breakdown of a single mechanism of self-tolerance causes various autoimmune diseases. *J. Immunol.* **155,** 1151–1164 (1995).

107. Sakaguchi, S. Naturally arising Foxp3-expressing CD25+CD4+ regulatory T cells in immunological tolerance to self and non-self. *Nat. Immunol.* **6,** 345–352 (2005).

108. Zenclussen, A. C. *et al.* Regulatory T cells induce a privileged tolerant microenvironment at the fetal-maternal interface. *Eur. J. Immunol.* **36,** 82–94 (2006).

109. Somerset, D. A., Zheng, Y., Kilby, M. D., Sansom, D. M. & Drayson, M. T. Normal human pregnancy is associated with an elevation in the immune suppressive CD25+ CD4+ regulatory T-cell subset. *Immunology* **112,** 38–43 (2004).

110. Heikkinen, J., Möttönen, M., Alanen, A. & Lassila, O. Phenotypic characterization of regulatory T cells in the human decidua. *Clin. Exp. Immunol.* **136,** 373–378 (2004).

111. Sánchez-Ramón, S. & Al., E. Pregnancy-induced expansion of regulatory T- lymphocytes may mediate protection to multiple sclerosis activity. *Immunol. Lett.* **96,** 195–201 (2005).

112. Samstein, R. M., Josefowicz, S. Z., Arvey, A., Treuting, P. M. & Rudensky, A. Y. Extrathymic generation of regulatory T cells in placental mammals mitigates maternal-fetal conflict. *Cell* **150,** 29–38 (2012).

113. Josefowicz, S. Z., Lu, L. F. & Rudensky, A. Y. Regulatory T cells: mechanisms of differentiation and function. *Annu. Rev. Immunol.* **30,** 531–564 (2012).

114. Floess, S. *et al.* Epigenetic control of the foxp3 locus in regulatory T cells. *PLoS Biol.* **5,** e38 (2007).

115. Kim, Y. C. *et al.* Engineered MBP-specific human Tregs ameliorate MOG-induced EAE through IL-2-triggered inhibition of effector T cells. *J. Autoimmun.* **92,** 77–86 (2018).

116. Gagliani, N. *et al.* Th17 cells transdifferentiate into regulatory T cells during resolution of inflammation. *Nature* **523,** 221–225 (2015).

117. Wing, K. & Sakaguchi, S. Regulatory T cells exert checks and balances on self tolerance and autoimmunity. *Nat. Immunol.* **11,** 7–13 (2010).

118. Nguyen, P. *et al.* Discrete TCR repertoires and CDR3 features distinguish effector and Foxp3+ regulatory T lymphocytes in MOG-EAE. *J. Immunol.* **185,** 3895–3904 (2010).

119. Owen, J. A., Punt, J., Stranford, S. A. & Jones, P. P. *Kuby Immunology*. 7th ed. New York: W. H. Freemann (2013).

120. Rudensky, A. Y. Regulatory T Cells and Foxp3. *Immunol. Rev.* **241,** 260–268 (2011).

121. Yu, N. *et al.* CD4(+)CD25 (+)CD127 (low/-) T cells: a more specific Treg population in human peripheral blood. *Inflammation* **35,** 1773–80 (2012).

122. Rouse, B. T. Regulatory T cells in health and disease. *J. Intern. Med.* **262,** 78–95 (2007).

123. Bennett, C. L. *et al.* The immune dysregulation, polyendocrinopathy, enteropathy, X-linked syndrome (IPEX) is caused by mutations of FOXP3. *Nat. Genet.* **27,** 20–21 (2001).

124. Blois, S. M. *et al.* A pivotal role for galectin-1 in fetomaternal tolerance. *Nat. Med.* **13,** 1450–1457 (2007).

125. Wildin, R. S. *et al.* X-linked neonatal diabetes mellitus, enteropathy and endocrinopathy syndrome is the human equivalent of mouse scurfy. *Nat. Genet.* **27,** 18–20 (2001).

126. Huan, J. *et al.* Decreased FOXP3 levels in multiple sclerosis patients. *J. Neurosci. Res.* **81,** 45–52 (2005).

127. Venken, K. *et al.* Compromised CD4+ CD25high regulatory T-cell function in patients with relapsing-remitting multiple sclerosis is correlated with a reduced frequency of FOXP3-positive cells and reduced FOXP3 expression at the single-cell level. *Immunology* **123,** 79–89 (2007).

128. Nie, H. Phosphorylation of FOXP3 controls regulatory T cell function and is inhibited by TNF-α in rheumatoid arthritis. *Nat. Med.* **19,** 322–328 (2013).

129. De Man, Y. A., Dolhain, R. J. E. M., Van De Geijn, F. E., Willemsen, S. P. & Hazes, J. M. W. Disease activity of rheumatoid arthritis during pregnancy: Results from a nationwide prospective study. *Arthritis Care Res.* **59,** 1241–1248 (2008).

130. Förger, F. *et al.* Pregnancy induces numerical and functional changes of CD4+CD25 high regulatory T cells in patients with rheumatoid arthritis. *Ann. Rheum. Dis.* **67,** 984–990 (2008).

131. Humrich, J. Y. *et al.* Homeostatic imbalance of regulatory and effector T cells due to IL-2 deprivation amplifies murine lupus. *Proc. Natl. Acad. Sci. U. S. A.* **107,** 204–209 (2010).

132. Engler, J. B. *et al.* Unmasking of autoreactive CD4 T cells by depletion of CD25 regulatory T cells in systemic lupus erythematosus. *Ann. Rheum. Dis.* **70,** 2176–2183 (2011).

133. Baca Jones, C. *et al.* Regulatory T cells control diabetes without compromising acute anti-viral defense. *Clin. Immunol.* **153,** 298–307 (2014).

134. Vukusic, S. *et al.* Pregnancy and multiple sclerosis (the PRIMS study): Clinical predictors of post-partum relapse. *Brain* **127,** 1353–1360 (2004).

135. Viglietta, V., Baecher-Allan, C., Weiner, H. L. & Hafler, D. A. Loss of Functional Suppression by CD4+ CD25+ Regulatory T Cells in Patients with Multiple Sclerosis. *J. Exp. Med.* **199,** 971–979 (2004).

136. Carbone, F. *et al.* Regulatory T cell proliferative potential is impaired in human autoimmune disease. *Nat. Med.* **20,** 69–74 (2014).

137. Sellebjerg, F., Krakauer, M., Khademi, M., Olsson, T. & Sørensen, P. S. FOXP3, CBLB and ITCH gene expression and cytotoxic T lymphocyte antigen 4 expression on CD4+CD25high T cells in multiple sclerosis. *Clin. Exp. Immunol.* **170,** 149–155 (2012).

138. Kleinewietfeld, M. & Hafler, D. A. Regulatory T cells in autoimmune neuroinflammation. *Immunol. Rev.* **259,** 231–244 (2014).

139. Rakebrandt, N., Littringer, K. & Joller, N. Regulatory T cells: balancing protection versus pathology. *Swiss Med. Wkly.* **146,** w14343 (2016).

140. Tanchot, C., Vasseur, F., Pontoux, C., Garcia, C. & Sarukhan, A. Immune regulation by self-reactive T cells is antigen specific. *J.Immunol.* **172,** 4285–4291 (2004).

141. Long, S. A. & Buckner, J. H. CD4+FOXP3+ Treg in human autoimmunity: more than a numbers game. *J. Immunol.* **187,** 2061–2066 (2011).

142. Gondek, D. C., Noelle, R. J., Quezada, S. A., Sakaguchi, S. & Lu, L.-F. Cutting Edge: Contact-Mediated Suppression by CD4+CD25+ Regulatory Cells Involves a Granzyme B-Dependent, Perforin-Independent Mechanism. *J. Immunol.* **174,** 1783–1786 (2014).

143. Zhao, D. M., Thornton, A. M., DiPaolo, R. J. & Shevach, E. M. Activated CD4+CD25+ T cells selectively kill B lymphocytes. *Blood* **107,** 3925–3932 (2006).

144. P. Pandiyan, Zheng, L., Ishihara, S., Reed, J. & Lenardo, M. J. CD4+CD25+Foxp3+ regulatory T cells induce cytokine deprivation–mediated apoptosis of effector CD4+ T cells. *Nat. Immunol.* **8,** 1353–1362 (2007).

145. Gerdes, L. A. *et al.* CTLA4 as Immunological Checkpoint in the Development of Multiple Sclerosis. *Ann. Neurol.* **80,** 294–300 (2016).

146. Qureshi, O. S. *et al.* Trans-endocytosis of CD80 and CD86: a molecular basis for the cell extrinsic function of CTLA-4. *Science* **332,** 600–603 (2011).

147. Khailaie, S. *et al.* Characterization of CTLA4 Trafficking and Implications for Its Function. *Biophys. J.* **115,** 1330–1343 (2018).

148. Walker, L. S. K. EFIS Lecture: Understanding the CTLA-4 checkpoint in the maintenance of immune homeostasis. *Immunol. Lett.* **184,** 43–50 (2017).

149. Bopp, T. *et al.* Cyclic adenosine monophosphate is a key component of regulatory T cell–mediated suppression. *J. Exp. Med.* **204,** 1303–1310 (2007).

150. Ito, T. *et al.* Two functional subsets of Foxp3+ regulatory T cells in human thymus and periphery. *Immunity* **28,** 870–880 (2008).

151. Liang, B. *et al.* Regulatory T Cells Inhibit Dendritic Cells by Lymphocyte Activation Gene-3 Engagement of MHC Class II. *J. Immunol.* **180,** 5916–5926 (2008).

152. Lindsay, K. L. *et al.* Longitudinal metabolomic profiling of amino acids and lipids across healthy pregnancy. *PLoS One* **10,** 1–19 (2015).

153. Koletzko, B. *et al.* Ernährung in der Schwangerschaft – Handlungsempfehlungen des Netzwerks „Gesund ins Leben – Netzwerk Junge Familie“ Nutrition in Pregnancy – Practice Recommendations of the Network „Healthy Start – Young Family Network". *Aktuel. Ernährungsmed.* **40,** 360–367 (2015).

154. Michalek, R. D. *et al.* Cutting Edge: Distinct Glycolytic and Lipid Oxidative Metabolic Programs Are Essential for Effector and Regulatory CD4+ T Cell Subsets. *J. Immunol.* **186,** 3299–3303 (2011).

155. Buck, M. D., O’Sullivan, D. & Pearce, E. L. T cell metabolism drives immunity. *J. Exp. Med.* **212,** 1345–1360 (2015).

156. Procaccini, C. *et al.* The Proteomic Landscape of Human Ex Vivo Regulatory and Conventional T Cells Reveals Specific Metabolic Requirements. *Immunity* **44,** 406–421 (2016).

157. Angelin, A. *et al.* Foxp3 Reprograms T Cell Metabolism to Function in Low-Glucose, High-Lactate Environments. *Cell Metab.* **25,** 1282–1293.e7 (2017).

158. Rubtsov, Y. P. *et al.* Stability of the Regulatory T Cell. *Science* **329,** 1667–1671 (2010).

159. Pearce, E. L. *et al.* Enhancing CD8 T-cell memory by modulating fatty acid metabolism. *Nature* **460,** 103–107 (2009).

160. Araki, K. *et al.* mTOR regulates memory CD8 T cell differentiation. *Nature* **460,** 108–112 (2010).

161. MacIver, N. J., Michalek, R. D. & Rathmell, J. C. Metabolic Regulation of T Lymphocytes. *Annu. Rev. Immunol.* **31,** 259–283 (2013).

162. Koolman, J. & Röhm, K.-H. *Taschenatlas der Biochemie*. 3rd ed. Stuttgart: Georg Thieme (2003).

163. Heiden, M. G. Vander, Cantley, L. C. & Thompson, C. B. Understanding the Warburg Effect: The Metabolic Requirements of Cell Proliferation. *Science* **324,** 1029–1033 (2009).

164. Buck, M. D. *et al.* Mitochondrial Dynamics Controls T Cell Fate through Metabolic Programming. *Cell* **166,** 1–14 (2016).

165. van der Windt, G. J. W. *et al.* Mitochondrial Respiratory Capacity Is a Critical Regulator of CD8+ T Cell Memory Development. *Immunity* **36,** 68–78 (2012).

166. van der Windt, G. J. W., Chang, C.-H. & Pearce, E. L. Measuring bioenergetics in T cells using a seahorse extracellular flux analyzer. *Curr. Protoc. Immunol.* **113,** 3.16B.1-3.16B.14 (2016).

167. Berod, L. *et al.* De novo fatty acid synthesis controls the fate between regulatory T and T helper 17 cells. *Nat. Med.* **20,** 1327–1333 (2014).

168. La Rocca, C. *et al.* Immunometabolic profiling of T cells from patients with relapsing-remitting multiple sclerosis reveals an impairment in glycolysis and mitochondrial respiration. *Metabolism.* **77,** 39–46 (2017).

169. Choi, I. Y., Piccio, L., Childress, P., Bollman, B. & Ghosh, A. Diet mimicking fasting promotes regeneration and reduces autoimmunity and multiple sclerosis symptoms. *Cell Rep.* **15,** 2136–2146 (2016).

170. Feinstein, D. L. *et al.* Peroxisome proliferator-activated receptor-gamma agonists prevent experimental autoimmune encephalomyelitis. *Ann. Neurol.* **51,** 694–702 (2002).

171. Newton, R., Priyadharshini, B. & Turka, L. A. Immunometabolism of regulatory T cells. *Nat. Immunol.* **17,** 618–625 (2016).

172. Adaptive Biotechnologies. Understanding the immunoSEQ Assay: From Inquiry to Insights (2019-01-31). *User Man.* (2017).

173. Turner, S. J., Doherty, P. C., McCluskey, J. & Rossjohn, J. Structural determinants of T-cell receptor bias in immunity. *Nat. Rev. Immunol.* **6,** 883–894 (2006).

174. commons.wikimedia.org/wiki/File:2215_Alpha-Beta_T_Cell_Receptor.jpg (2019-02-7) (2019).

175. www.takarabio.com/areas-of-interest/immunotherapy-research/t-cell-receptor-profiling (2019-01-25) (2018).

176. LaMothe, R. A. *et al.* Tolerogenic nanoparticles induce antigen-specific regulatory T cells and provide therapeutic efficacy and transferrable tolerance against experimental autoimmune encephalomyelitis. *Front. Immunol.* **9,** 1–11 (2018).

177. Spence, A. *et al.* Revealing the specificity of regulatory T cells in murine autoimmune diabetes. *Proc. Natl. Acad. Sci. U. S. A.* **115,** 5265–5270 (2018).

178. Vanderlugt, C. L. & Miller, S. D. Epitope Spreading in Immune-mediated Diseases: Implications for Immunotherapy. *Nat. Rev. Immunol.* **2,** 85–95 (2002).

179. Corthay, A. How do regulatory t cells work? *Scand. J. Immunol.* **70,** 326–336 (2009).

180. Hsieh, C.-S. *et al.* Recognition of Peripheral Self by Naturally Arising CD25+ CD4+ T cell Receptors. *Immunity* **21,** 267–277 (2004).

181. Pacholczyk, R., Ignatowicz, H., Kraj, P. & Ignatowicz, L. Origin and T Cell Receptor Diversity of Foxp3+CD4+CD25+T Cells. *Immunity* **25,** 249–259 (2006).

182. Pacholczyk, R. *et al.* Non-self antigens are the cognate specificities of Foxp3+ regulatory T cells. *Immunity* **27,** 493–504 (2007).

183. Wong, J. *et al.* Adaptation of TCR Repertoires to Self-Peptides in Regulatory and Nonregulatory CD4+ T Cells. *J. Immunol.* **178,** 7032–7041 (2007).

184. Zhao, Y. *et al.* Preferential Use of Public TCR during Autoimmune Encephalomyelitis. *J. Immunol.* **196,** 4905–4914 (2016).

185. Mendel, I., Kerlero de Rosbo, N. & Ben-Nun, A. Delineation of the minimal encephalitogenic epitope within the immunodominant region of myelin oligodendrocyte glycoprotein: diverse Vβ gene usage by T cells recognizing the core epitope encephalitogenic for T cell receptor Vβb and T cell receptor Vβa H-2. *Eur. J. Immunol.* **26,** 2470–2479 (1996).

186. Mendel, I., Kerlero de Rosbo, N. & Ben-Nun, A. A myelin oligodendrocyte glycoprotein peptide induces typical chronic experimental autoimmune encephalomyelitis in H-2b mice: fine specificity and T cell receptor Vβ expression of encephalitogenic T cells. *Eur. J. Immunol.* **25,** 1951–1959 (1995).

187. Zamvil, S. S. *et al.* Predominant expression of a T cell receptor V beta gene subfamily in autoimmune encephalomyelitis. *J. Exp. Med.* **167,** 1586–1596 (1988).

188. Lahl, K. *et al.* Selective depletion of Foxp3 + regulatory T cells induces a scurfy-like disease. *J. Exp. Med.* **204,** 57–63 (2007).

189. www.miltenyibiotec.com/DE-en/products/macs-cell-separation/basic-principle-of-magnetic-cell-separation.html (2019-02-11) (2019).

190. Gagliani, N. *et al.* Coexpression of CD49b and LAG-3 identifies human and mouse T regulatory type 1 cells. *Nat. Med.* **19,** 739–746 (2013).

191. Kruisbeek, A. M., Shevach, E. & Thornton, A. M. Proliferative Assays for T Cell Function. *Curr. Protoc. Immunol.* **3,** (2004).

192. bio-protocol.org/e2850 (2019-01-29) (2019).

193. www.agilent.com (2019-01-21) (2019).

194. Seitz, V. *et al.* A new method to prevent carry-over contaminations in two-step PCR NGS library preparations. *Nucleic Acids Res.* **43,** (2015).

195. Bolotin, D. A. *et al.* MiXCR: Software for comprehensive adaptive immunity profiling. *Nat. Methods* **12,** 380–381 (2015).

196. Shugay, M. *et al.* VDJtools: Unifying Post-analysis of T Cell Receptor Repertoires. *PLoS Comput. Biol.* **11,** 1–16 (2015).

197. www.ncbi.nlm.nih.gov/geo (2018-12-18) (2018).

198. Döbbeling, U. The influence of Il-7 on V(D)J recombination. *Immunology* **89,** 569–572 (1996).

199. Roussel-Gervais, A. *et al.* The cables1 gene in glucocorticoid regulation of pituitary corticotrope growth and cushing disease. *J. Clin. Endocrinol. Metab.* **101,** 513–522 (2016).

200. DeBerardinis, R. J., Lum, J. J. & Thompson, C. B. Phosphatidylinositol 3-kinase-dependent modulation of carnitine palmitoyltransferase 1A expression regulates lipid metabolism during hematopoietic cell growth. *J. Biol. Chem.* **281,** 37372–37380 (2006).

201. O'Connor, R. A., Malpass, K. H. & Anderton, S. M. The Inflamed Central Nervous System Drives the Activation and Rapid Proliferation of Foxp3+ Regulatory T Cells. *J. Immunol.* **179,** 958–966 (2007).

202. Kivisakk, P. *et al.* Localizing central nervous system immune surveillance: Meningeal antigen-presenting cells activate T cells during experimental autoimmune encephalomyelitis. *Ann. Neurol.* **65,** 457–469 (2009).

203. Korn, T. & Kallies, A. T cell responses in the central nervous system. *Nat. Rev. Immunol.* **17,** 179–194 (2017).

204. Brown, D. A. & Sawchenko, P. E. Time course and distribution of inflammatory and neurodegenerative events suggest structural bases for the pathogenesis of experimental autoimmune encephalomyelitis. *J. Comp. Neurol.* **502,** 236–260 (2007).

205. Pozzilli, C. *et al.* Oral contraceptives combined with interferon β in multiple sclerosis. *Neurol. Neuroimmunol. Neuroinflammation* **2,** e120 (2015).

206. Piédavent-Salomon, M. *et al.* Multiple sclerosis associated genetic variants of CD226 impair regulatory T cell function. *Brain* **138,** 3263–3274 (2015).

207. Bao, S. H. *et al.* Decidual CD4+CD25+CD127dim/- regulatory T cells in patients with unexplained recurrent spontaneous miscarriage. *Eur. J. Gynecol. Reprod. Biol.* **155,** 94–98 (2011).

208. Liu, S. *et al.* The role of decidual immune cells on human pregnancy. *J. Reprod. Immunol.* **124,** 44–53 (2017).

209. Trinschek, B., Luessi, F., Gross, C. C., Wiendl, H. & Jonuleit, H. Interferon-beta therapy of multiple sclerosis patients improves the responsiveness of t cells for immune suppression by regulatory T cells. *Int. J. Mol. Sci.* **16,** 16330–16346 (2015).

210. Sindram-Trujillo, A., Scherjon, S., Kanhai, H., Roelen, D. & Claas, F. Increased T-Cell Activation in Decidua Parietalis Compared to Decidua Basalis in Uncomplicated Human Term Pregnancy. *Am. J. Reprod. Immunol.* **49,** 261–268 (2003).

211. Polanczyk, M. J., Hopke, C., Huan, J., Vandenbark, A. A. & Offner, H. Enhanced FoxP3 expression and Treg cell function in pregnant and estrogen-treated mice. *J. Neuroimmunol.* **170,** 85–92 (2005).

212. Mjösberg, J. *et al.* Systemic Reduction of Functionally Suppressive CD4dimCD25highFoxp3+ Tregs in Human Second Trimester Pregnancy Is Induced by Progesterone and 17β-Estradiol. *J. Immunol.* **183,** 759–769 (2009).

213. De Rosa, V. *et al.* Glycolysis controls the induction of human regulatory T cells by modulating the expression of FOXP3 exon 2 splicing variants. *Nat. Immunol.* **16,** 1174–84 (2015).

214. Gerriets, V. A. *et al.* Metabolic programming and PDHK1 control CD4+ T cell subsets and inflammation. *J. Clin. Invest.* **125,** 194–207 (2015).

215. Thiele, K., Diao, L. & Arck, P. C. Immunometabolism, pregnancy, and nutrition. *Semin. Immunopathol.* **40,** 157–174 (2018).

216. Ohkura, N., Kitagawa, Y. & Sakaguchi, S. Development and Maintenance of Regulatory T cells. *Immunity* **38,** 414–423 (2013).

217. Kalekar, L. A. & Mueller, D. L. Relationship between CD4 Tregs and anergy in vivo. *J. Immunol.* **198,** 2527–2533 (2018).

218. Duurland, C. L., Brown, C. C., O'Shaughnessy, R. F. L. & Wedderburn, L. R. CD161+Tconv and CD161+treg share a transcriptional and functional phenotype despite limited overlap in TCRβ repertoire. *Front. Immunol.* **8,** 1–18 (2017).

219. Li, M. O. & Rudensky, A. Y. T cell receptor signalling in the control of regulatory T cell differentiation and function. *Nat. Rev. Immunol.* **16,** 220–233 (2016).

220. Howie, B. *et al.* High-throughput pairing of T cell receptor alpha and beta sequences. *Sci. Transl. Med.* **7,** 301ra131 (2015).

221. tetramer.yerkes.emory.edu/tetramer-science/why-tetramers (2019-02-11) (2010).

222. tetramer.yerkes.emory.edu/reagents/3828 (2019-02-06) (2010).

223. Korn, T. *et al.* Myelin-specific regulatory T cells accumulate in the CNS but fail to control autoimmune inflammation. *Nat. Med.* **13,** 423–431 (2007).

224. Tafuri A, Alferink J, Moller P, Hammerling GJ, A. B. T cell awareness of paternal alloantigens during pregnancy. *Science* **270,** 630–633 (1995).

225. Bluestone, J. A. & Tang, Q. Treg cells—the next frontier of cell therapy. *Science* **362,** 154–156 (2018).

226. Bluestone, J. A. *et al.* Type 1 diabetes immunotherapy using polyclonal regulatory T cells. *Sci. Transl. Med.* **7,** 1–34 (2015).

Currently a manuscript on parts of this thesis is submitted.

Title: Pregnancy enables expansion of autoreactive regulatory T cells in an animal model of multiple sclerosis

Authors: Jan Broder Engler[1,*], Nina F. Heckmann[1,*], Jan Jäger[1], Stefan M. Gold[1,2] and Manuel A. Friese[1]

Affiliations:

[1]Institut für Neuroimmunologie und Multiple Sklerose, Zentrum für Molekulare Neurobiologie Hamburg, Universitätsklinikum Hamburg-Eppendorf, 20251 Hamburg, Germany

[2]Charité - Universitätsmedizin Berlin, Klinik für Psychiatrie & Medizinische Klinik m.S. Psychosomatik, Campus Benjamin Franklin, Hindenburgdamm 30, 12203 Berlin, Germany.

* J.B.E. and N.F.H. contributed equally to this work.

Eidesstattliche Erklärung - Statement of authorship

Ich versichere an Eides statt, die vorliegende Dissertation selbst verfasst und keine anderen als die angegebenen Hilfsmittel benutzt zu haben.

I declare upon oath that I have written this dissertation independently and have not used any further recourses and aids than those stated in the dissertation.

Hamburg, 02.04.2019 Nina Heckmann

Acknowledgements

I would like to thank Prof. Dr. Manuel Friese for giving me the opportunity to work on this exciting project at the INIMS, for his supervision, valuable support and insightful discussions of data and the opportunity to take part at scientific congresses.

Moreover, I am grateful to all members of my ZMNH PhD program thesis committee, namely Prof. Dr. Petra Arck and Prof. Dr. Hans-Willi Mittrücker, Dr. Anne Willing, Dr. Guido Hermey, Dr. Sabine Fleischer, Dr. Irm Hermanns-Borgmeyer for sharing their scientific experience and letting me benefit from their helpful questions.

In addition, I would like to thank Prof. Dr. Tim Gilberger for evaluation of this thesis.

I am grateful to the members of the KFO 296 of Feto-Maternal Immune Cross Talk Community for providing the opportunity to continuously present my work in internal seminars and to benefit from their experience and critical questions.

I am very grateful to and would like to address special thanks to Dr. Dr. Jan Broder Engler for his empathy, excellent supervision of the project, fruitful scientific discussions, technical assistance and his bioinformatical participation in this work.

I would also like to thank Dr. Jan Jäger for his contribution and all my current and former colleagues at the INIMS for all kinds of support and pleasant working days in the lab.

I would also like to thank Stephanie Snelson for proofreading this thesis.

Finally, I am truly thankful to my partner, family and friends for their love, encouragement and unconditional support.